2014

Development of an optical sensor for real-time weed detection using laser based spectroscopy

Arie Jacobus Paap
Edith Cowan University

Development of an optical sensor for real-time weed detection using laser based spectroscopy

Arie Jacobus Paap
Edith Cowan University, apaap@our.ecu.edu.au

Edith Cowan University

Copyright Warning

DEVELOPMENT OF AN OPTICAL SENSOR FOR REAL-TIME WEED DETECTION USING LASER BASED SPECTROSCOPY

by

Arie Jacobus Paap, BSc (hons)

This thesis is presented in fulfilment of the requirements for the degree of

Doctor of Philosophy

at

Electron Science Research Institute

Faculty of Computing, Health and Science

Edith Cowan University

Principal Supervisor:	Prof. Kamal Alameh, Edith Cowan University
Co-supervisor:	Dr Sreten Askraba, Edith Cowan University
Associate Supervisors:	Dr Mikhail Vasiliev and Dr Geoff Swan, Edith Cowan University

March 2014

USE OF THESIS

The Use of Thesis statement is not included in this version of the thesis.

Abstract

The management of weeds in agriculture is a time consuming and expensive activity, including in Australia where the predominant strategy is blanket spraying of herbicides. This approach wastes herbicide by applying it in areas where there are no weeds. Discrimination of different plant species can be performed based on the spectral reflectance of the leaves. This thesis describes the development of a sensor for automatic spot spraying of weeds within crop rows. The sensor records the relative intensity of reflected light in three narrow wavebands using lasers as an illumination source.

A prototype weed sensor which had been previously developed was evaluated and redesigned to improve its plant discrimination performance. A line scan image sensor replacement was chosen which reduced the noise in the recorded spectral reflectance properties. The switching speed of the laser sources was increased by replacing the laser drivers. The optical properties of the light source were improved to provide a more uniform illumination across the viewing area of the sensor. A new opto-mechanical system was designed and constructed with the required robustness to operate the weed sensor in outdoor conditions. Independent operation of the sensor was made possible by the development of hardware and software for an embedded controller which operated the opto-electronic components and performed plant discrimination.

The first revised prototype was capable of detecting plants at a speed of 10 km/h in outdoor conditions with the sensor attached to a quad bike. However, it was not capable of discriminating different plants. The final prototype included a line scan sensor with increased dynamic range and pixel resolution as well as improved stability of the output laser power. These changes improved the measurement of spectral reflectance properties of plants and provided reliable discrimination of three different broadleaved plants using only three narrow wavelength bands. A field trial with the final prototype

demonstrated successful discrimination of these three different plants at 5 km/h when a shroud was used to block ambient light.

A survey of spectral reflectance of four crops (sugarcane, cotton, wheat and sorghum) and the weeds growing amongst these crops was conducted to determine the potential for use of the prototype weed sensor to control spot-spraying of herbicides. Visible reflectance spectra were recorded from individual leaves using a fibre spectrometer throughout the growing season for each crop. A discriminant analysis was conducted based on six narrow wavebands extracted from leaf level spectral reflectance measured with a spectrometer. The analysis showed the potential to discriminate cotton and sugarcane from important weeds growing amongst those crops with 85-95% accuracy.

Declaration

I certify that this thesis does not to the best of my knowledge and belief:

i. *incorporate without acknowledgement any material previously submitted for a degree or diploma in any institution of higher education*

ii. *contain any material previously published or written by another person except where due reference is made in the text; or*

iii. *contain any defamatory material.*

I also grant permission for the Library at Edith Cowan University to make duplicate copies of my thesis as required.

Signature: .....

Date: 30/7/2014

Acknowledgements

I would like to thank my supervisors for their continued support throughout my Ph. D. programme. My principal supervisor Prof. Kamal Alameh has guided me through my research. I appreciate his expertise, ideas, enthusiasm and optimism which all helped me to complete this work. I would like to thank Dr Sreten Askraba for his guidance and our many lively discussions. I would like to thank Dr Mikhail Vasiliev and Dr Geoff Swan for their encouragement and many helpful discussions.

I would like to acknowledge the financial support for this research project provided by Photonic Detection Systems Pty Ltd, by the Australian Research Council via two Linkage Project grants and by Edith Cowan University. I would also like to acknowledge the assistance I received from Dr Hoang Nguyen, Steven Silva, Robert Shaw and Electro Design Pty Ltd in design and manufacture of the electronic circuit boards. Thank you to Glenn of Arrawatta farm in Dalby, Queensland and Mike Smith of Bundaberg Sugar in Bundaberg, Queensland for allowing me to conduct fieldwork on their properties.

My greatest thanks go to my family for their loving support, especial to Michelle and Xavier for helping me see this thesis through to the end. Thank you to Val for countless hours helping me turn ideas into words on a page. Thank you all for believing in me.

Table of Contents

List of Figures

List of Tables

List of Publications

Journal Articles

Askraba, S., A. Paap, K. Alameh, J. Rowe and C. Miller (2013). "Optimization of an Optoelectronics-Based Plant Real-Time Discrimination Sensor for Precision Agriculture," *Journal of Lightwave Technology* **31**(5): 822-829.

Paap, A., S. Askraba, K. Alameh and J. Rowe (2008). "Photonic-based spectral reflectance sensor for ground-based plant detection and weed discrimination," *Optics Express* **16**(2): 1051-1055.

Conference Papers

Askraba, S., A. Paap, K. Alameh and J. Rowe (2011). "Design of laser multi-beam generator for plant discrimination," in *High Capacity Optical Networks and Enabling Technologies (HONET), 2011*, Riyadh, Saudi Arabia

Paap, A., S. Askraba, K. Alameh and J. Rowe (2008). "Evaluation of an optical image sensor for use in the micro-photonic real-time vegetation discrimination system," in *Opto-Electronics and Communications Conference, 2008 and the 2008 Australian Conference on Optical Fibre Technology. OECC/ACOFT 2008. Joint conference of the*, Sydney, Australia.

Paap, A., S. Askraba, K. Alameh and J. Rowe (2008). "Photonic-based spectral reflectance sensor for ground-based plant detection and weed discrimination," in *19th International Conference on Optical Fibre Sensors*, Perth, Australia.

Chapter 1

Introduction

1.1 Background

Agriculture plays an important role in the economies and health of our world. Wherever land is put to agricultural use, weeds will grow. The Australian Weeds Strategy considers a weed to be a plant "*that requires some form of action to reduce its harmful effects on the economy, the environment, human health and amenity*" [1]. Weeds have significant environmental as well as socio-economic impacts, causing damage to natural landscapes, agricultural lands, waterways and coastal areas, interfering with recreational activities on the water and in the bush, competing with production (leading to low yields), contaminating produce and poisoning livestock. In addition, some weeds affect human and animal health, causing allergies and respiratory problems, as well as poisoning, thus increasing health-care costs. Furthermore, weeds can provide high fuel loads that increase bushfire intensity, resulting in increased losses of properties, rural infrastructure and biodiversity.

In Australia, agricultural businesses occupy approximately 425 million ha which covers 55% of Australia's land area. These businesses range from large pastoral holdings occupying millions of hectares to small market gardens and undercover agriculture industries occupying less than 1 hectare [2]. The value of agricultural production contributes around $36 billion to Australia's economy [3]. Australia spends considerable time and money each year in combating weed problems and protecting ecosystems and primary production on private and public land. The total economic cost of weeds to agriculture in

Australia, including lost production and opportunity costs, is around $4 billion per annum [2, 4].

Of the 2700 species of introduced plants now established in Australia, 429 have been declared noxious or are under some form of legislative control in Australia, and pose ongoing challenges to the government, the industry and the country, resulting from (i) the introduction of exotic plants and (ii) movement by native species into new areas in response to changed land and water use and management practices. Even with the strongest quarantine procedures and excellent weed management programs, new weed invasions and weed problems continue to occur in Australia. For example, in Victoria more than 200 species have naturalised outside their native range, while in Western Australia 90 species are similarly recorded.

Many industries, such as agriculture, livestock, forestry, horticulture, nursery, landscaping, fishing, aquaculture, transport and tourism, are now promoting policies, guidelines, standards and activities to manage and control the spread of weeds, and understand the weed problem in order to reduce the weed-related costs and enhance their profitability and sustainability. Therefore, innovative research and development of advanced weed sensors that can identify plants and discriminate weeds from crops would benefit the Australian government and many Australian industries and put Australia at the forefront of weed control and management and strengthen collaborative research and development capabilities that address weed problems and threats around the globe.

1.2 The Impact of Weeds on Agriculture

Weed problems are complex, with multiple causes, and in order to reduce their impacts, efforts must be coordinated across all layers of a nation, to ensure that priorities are identified and consistent guidance is established for the management of existing weeds and prevention of the development of new weeds. The presence of weeds in agriculture not only affects the production and quality of crops but also harms the health of livestock. In agricultural crops, weeds compete with crops for water, light and the nutrients in the soil. Competition from weeds reduces the quantity of the harvested crop and can

affect quality through contamination. The presence of weed material that harbours pests and diseases may also adversely affect the crop. Management of agricultural weeds increases the production cost of crops by the investment in machinery and expenditure on labour and herbicides.

1.2.1 Current Weed Management Practices

Most weed control in Australian agriculture is mechanised through either cultivation or application of herbicides. For reasons of land and soil conservation, Australian agriculture has shifted from cultivation to minimum tillage with a greater reliance on herbicides [5]. The adaptability of weed populations to herbicides and the changing populations of weeds are constant challenges to agricultural productivity. These challenges have brought about a need to combine weed management techniques with scientific and technological knowledge that is economically and environmentally sustainable.

Weed management practices used in Australia include cultivation of the soil, herbicide application to directly kill weeds, biological control of weeds using insects, fungi and bacteria, and crop selection including the use of cover crops to smother weed growth through competition [6]. The use of each of these techniques has an immediate weed control effect and also a long-term impact on weed populations and farm productivity. Integrated weed management (IWM) is a "*sustainable management system that combines all appropriate weed control options*" [5]. IWM targets all weeds at some phase of the cropping cycle, with the aim to reduce the weed seed bank and decrease the impact of weeds on the crop.

Research and development into new technology for agriculture can support IWM by providing new weed control techniques and improved data collection and management. Detailed information about the variability of soil conditions, crop health and weed density allows site-specific crop management to be undertaken. This modern return to localised decision making combines the benefits of traditional small-scale agriculture with the productivity of modern agriculture. The use of this technology in farming is known as precision agriculture (PA). As with integrated weed management, PA is a whole of farm

management system which considers the impact of crop management decisions on the productivity and profitability of the farm [7].

1.2.2 Site specific weed management

The only commercially available sensor for variable-rate herbicide application is the WeedSeeker® by NTech Pty Ltd. The WeedSeeker is a spectral reflectance sensor which uses red and near infra-red LEDs for illumination and a photodiode to detect the intensity of reflected light [8]. This system is designed for discrimination of green vegetation from soil and has seen adoption for use in fallow (no crop) and with hooded sprayers for between row herbicide spraying.

The maximum benefit from reduction of herbicide use requires reliable information on weed abundance and distribution. Weed mapping is one approach which involves the production of a detailed weed map, combined with other data to determine a variable rate treatment map. Mapping relies on human observation, which is time consuming, expensive and inefficient, or remote sensing. Remote sensing can produce weed maps where patches of weeds are of sufficient size, but provides limited spatial resolution while requiring considerable time and expense for image acquisition and processing [9].

Proximate sensing can use either imaging or non-imaging sensors, and provides resolution below the size of individual leaves. It is an alternative to remote sensing which offers the potential for real-time detection and spot spraying of weeds. Several advantages over remote sensing include high spatial resolution and the ability to use artificial lighting to illuminate the ground. Such a sensor may operate on a similar principle to the WeedSeeker to determine spectral properties of the crop and weeds, or use an imaging sensor and apply machine vision techniques to classify crop and weeds based on leaf size and shape, colour, and/or texture. The potential of these technologies to target spray weeds is promising and would reduce the cost and volume of herbicide used, the associated labour costs, environmental impacts and provide greater opportunity to implement site specific weed management.

1.3 Previous weed sensor development

In 2002, Photonic Detection Systems (PDS, then known as Weed Control Australia) developed a series of weed sensor prototypes consisting of sensor modules mounted on agricultural spray equipment less than 1 m above ground. The sensor had multiple groups of red and infrared lasers combined with a photodetector. Eight groups of lasers and photodiode were spaced 60 mm apart in a 0.5 m box as shown in Figure 1.1. The laser output beams and photodetector were aligned to detect plant leaves at a specified height above the ground and several boxes were mounted on a boom. This weed sensor prototype only used two wavelengths and had the capacity to differentiate green plants from soil or stubble, based on the spectral response. As with the WeedSeeker, this allowed precise spraying of green plants only – "green from brown" as opposed to blanket spraying. Differentiation between green plants was not reliable with only two wavelengths.

Figure 1.1. Prototype weed sensor developed by Photonic Detection Systems with 8 modules consisting of two lasers and a photodiode.

Using information about the speed of the sensor while scanning over the ground, it was possible to estimate the leaf size. Determination of the leaf size combined with the spectral reflectance ratio allowed differentiation of dissimilar sized plants, however similar sized plants could not be accurately differentiated with this sensor design. Additionally, small plants were only detected if they passed under one of the laser/photodiode groups and only if they were at the correct distance from the sensor.

In 2005, PDS approached The WA Centre of Excellence for MicroPhotonic Systems (COMPS) at Edith Cowan University (ECU) seeking assistance with

the development of their weed sensor design. Based on the requirement of discriminating “green from green” using the reflected intensity of multiple (3 or more) lasers and operating at a vehicle speed of 15 km/h, COMPS designed a prototype spectral reflectance based weed sensor. The device, presented by Sahba *et al*. [10] and discussed in detail in Chapters 2 and 4, uses a laser combiner module to combine the output laser beams. This combiner was designed to align the three lasers along one direction, maintaining beam overlap over a long working distance. The beam combiner was used in conjunction with a novel optical cavity to generate an array of laser beams. The reflected light from all beams was captured by a line scan sensor in the centre of the device. Only two sets of lasers were used, reducing the cost of the device while increasing the spatial resolution compared to the original PDS design.

1.4 Scope of Study

The purpose of this project was to further develop the prototype weed sensor with a goal of meeting the following objectives:

- Real-time operation – the sensor should operate at a typical speed of farm vehicles used for herbicide application (>15 km/hr);
- Robustness to variations in terrain – detection of plants and crop/weed classification should not be hampered by changes in sensor height;
- “Green from Green” discrimination – improve the plant discrimination capability such that discrimination of green plants in a controlled outdoor environment is possible at 15 km/hr
- Assess required wavelengths – based on analysis of spectral reflectance of a crop and weeds, what are the most suitable wavelengths to use?
- Determine limitations of the sensor – is the weed sensor design able to discriminate between crops and weeds?

1.5 Thesis Outline

Chapter 2 reviews previous research to provide an overview of management of agricultural weeds. The impact of weeds on Australian agriculture and the economy will be discussed along with current weed management techniques.

The potential for use of new weed management technology in cotton and sugarcane is considered as well as management of noxious weeds. The previous research on weed mapping including remote sensing is considered followed by a review of previous research on real-time sensors for crop/weed classification.

Chapter 3 provides further detail of the initial prototype weed sensor's design and describes the use of a fibre spectrometer to record spectral reflectance data. The components which make up the weed sensor are described and characterised followed by detailed description of the improvements required to improve the performance of the weed sensor.

Chapter 4 will describe the initial prototype weed sensor and the further development of two revised models culminating in a working field prototype. For each revision of the weed sensor a description of the design and function will be given with reference to the components described in Chapter 3.

Chapter 5 presents results of the spectral reflectance data recorded from a cotton farm and a sugarcane farm. At each stage of the weed sensor's development, its ability to detect and discriminate between different plants was assessed. The results of this assessment carried out under various conditions in the laboratory and on an outdoor testing ground are presented.

Chapter 6 draws conclusions on the performance of the prototype weed sensor and the potential for its use in the sugarcane, cotton and other agricultural industries. Lastly, some ideas for improvement of the sensor performance are provided.

Chapter 2

Literature Review

2.1 Introduction

This chapter outlines previous research and development to provide an overview of management of agricultural weeds. The impact of weeds on Australian agriculture and the economy will be reviewed. The current management techniques will be introduced, including an overview of Integrated Weed Management. The adoption of Precision Agriculture to manage the variability on farms through the use of spatial and monitoring technology is explored and provides and insight into the missing pieces of agricultural technology. The potential for use of new weed management technology in cotton and sugarcane is considered along with the current methods of plant recognition which are available.

The available methods for detecting weeds amongst a crop include weed mapping using remote sensing and real time detection with proximate sensing. Remote sensing typically involves spectral reflectance imaging whereas proximate sensing uses either machine vision or non-imaging sensors based on spectral reflectance. Previous studies of past work covering a range of spatial resolution from 1 m down to 1 mm using these techniques will be reviewed. The spectral reflectance of plants is determined by their physiological characteristics and is determined by a wide range of factors and requires methods of extracting the desired characteristics such as species. A range of previous implementations of weed sensing technology will be reviewed. This review informs the design of an optical weed sensor that is capable of discriminating

between different plant types in an agricultural cropping environment in order to spot spray weeds.

2.2 Weeds in Australia

Weeds have major economic, environmental and social impacts in Australia, with detrimental effects on agricultural land, natural landscapes, parks and gardens, waterways and coastal areas. They are dispersed through a range of processes that move plants to new areas where the environment is suitable for their growth and spread. Many weeds are introduced plants which were intended to provide food crops, pasture for grazing, shelter, medicines, or enjoyment in gardens and parklands. Unintentional weed introduction has occurred with human travel and the movement of plant material as contaminants in seed, soil, fleece or bedding and fodder [11].

Examining the non-economic impacts of weeds, Sinden equates the well-being of the whole community to the sum of the producers' surplus and the amount the consumer has to pay in the market place [4]. The economic impacts of weeds primarily originate in Australia's large agricultural sector and are examined in detail in Section 2.2.1. In order to manage the impact of weeds, the agriculture industry has developed many different strategies. Integrated weed management (IWM) is a method of farm management which considers the long-term effects of any weed control action. In parallel with IWM has come the development of precision agriculture technology, allowing farmers to manage their crops according to local requirements and increase their farm productivity. Integrated weed management and precision agriculture are explored in Sections 2.2.2 and 2.2.3.

2.2.1 Impact of Weeds on Agriculture

The presence of weeds has a significant impact on the Australian economy and the environment. Weeds impact on our ability to grow and produce food. To maintain a level of agricultural production that is economically viable, the technological development in agricultural tools, and farming practices in response to this challenge and to the suppression of weeds will be described.

The Australian Bureau of Statistics reported the total value of agricultural produce in 2006-07 to be $36 billion [3]. In the same year $1.6 billion was spent by producers on weed management [2]. Australia is a strong competitor in the world market with approximately two thirds of total agriculture produce exported. Exports of Australian agricultural produce in 2006-07 accounted for 18% of Australian merchandise exports [12]. The agricultural industry has a need to maintain high levels of production, to adapt to environmental changes, market pressure and to reduce financial inputs. Weeds reduce the quality and quantity of product from the agricultural, horticultural and forestry sectors, improved technological advances will help reduce these impacts.

Crop productivity is determined by the crop's access to nutrients (nitrogen, phosphorous and potassium), water and light. Weeds compete with the crop for these resources and are often more successful in obtaining them. Agriculture production costs are increased by a need to manage weeds before emergence of the crop and post-emergent when there are weed germination events such as rainfall. The germination of crop and weed seeds differs in time, with evidence that weeds which emerge before or with the crop causes the greatest yield losses. The length of time the crop is required to be kept weed free in order to prevent yield loss depends on the crop, the weed species and on the farm location and conditions [13, p. 172].

Climate change is anticipated to have a significant impact on agriculture in Australia and worldwide as changes occur in rainfall, water quality, temperature, distribution of pests and diseases. These factors increase the competition between weeds and crop and make the crop more vulnerable. The projected higher temperatures and lower rainfall would result in a positive carbon fertilisation effect for some plants. However, climate change projections indicate that that crop quality would be reduced, and these impacts would decrease agricultural productivity in Australia and throughout the world. [14].

Advances in Australian agricultural practice over the last decade has seen a greater reliance on herbicide application for weed control and a shift to minimum tillage with a greater reliance on herbicides for weed management [15]. An ABS survey of Australian agricultural land management practices reported that 53% of agricultural businesses growing crops and pastures

throughout the country preferred to use minimum tillage or zero tillage [16]. There are about 30 herbicides in common use in WA. Herbicides differ in their mode of action and in the method of application. They may be applied to the foliage, rely on uptake through roots or both. Residual herbicides remain active in the soil and control weed seedlings as they germinate. Herbicides may be selective, affecting only some species of plants whilst knock-down herbicides affect all plants they contact [11].

2.2.1.1 Economic Impact

In 2006 the Australian Bureau of Statistics conducted a national agricultural census. Of the 20,000 Australian agricultural businesses surveyed more than 94% reported undertaking natural resource management activities to manage weeds, pests, land and soil. In total, undertaking these activities cost almost $3 billion. Of this $3 billion spent, $1.6 billion was spent on managing weeds including $982 million spent for herbicides [2]. In addition to weed control costs, the Cooperative Research Centre for Australian Weed Management estimated that in 2001 weeds caused production losses of between $2 billion and $2.5 billion per annum [4].

To reduce agricultural production costs farmers need effective weed management tools that will reduce the use of the chemicals and the cost associated with application of herbicides. A real-time optical weed sensor that can deliver herbicide with precision to weeds at the most suitable dosage would provide effective weed control and economic benefits. It would be an important part of sustainable agricultural practices that increase productivity while minimising degradation of the environment.

2.2.2 Integrated Weed Management

The widespread use of chemicals in agriculture developed after field trials with 2,4-D in 1945 as a selective herbicide. Other herbicides were developed over the following decades and their adoption resulted in a reduction in labour, greater mechanisation of farming and improvement in crop quality and production [13]. Selective herbicides began to replace the traditional means of weed control using tillage, mulching, hoeing, flooding, burning, mowing and

collecting weed seed in the harvester's "seconds box" [17]. Over time, problems have emerged with the ongoing use of herbicides, particularly in minimum and no-till farming systems where herbicide resistance is greatest.

Resistance to herbicides occurs when a small number of plants survive herbicide application and the genetic adaptation leads to an emerging herbicide tolerant weed becoming dominant. Herbicide resistance was first reported in Australia in the 1980's. In 2006 there were 25 weed species with herbicide-resistant populations recorded in Australia [18].

Species shift occurs when the population distribution of weed species changes over time. This change can occur as a result of cultivation, use of different or selective herbicides or environmental impacts such as fire, flood and drought. As weeds recover from these incidents at different rates, a previously small weed species population can rapidly expand in the changed environment and become the dominant weed [19]. Species shift and the development of herbicide resistance can both be effectively managed using Integrated Weed Management (IWM).

Integrated Weed Management is a systemized approach to weed management which is modelled on Integrated Pest Management (IPM), a management technique in development since the 1950's. IPM, and hence IWM, emphasise the use of a wide range of techniques to control pests and weeds with consideration of the long-term effects of any control action. IWM practice uses a combination of preventative, cultural, mechanical and chemical control practices as the basis for a weed management program. A range of different agronomic practices should be combined to keep weeds "off balance" and less able to adapt to a constantly changing system that uses many different control practices [5]. IWM aims to maintain weed densities at manageable levels while preventing shifts in weed populations to more difficult-to-control weeds. In practice these strategies prevent weed seed production, reducing weed emergence and minimises crop competition. Whilst IWM does not completely control weeds, it assists the decisions being made about crop/weed management to reduce the impact of weeds while reducing the risk of new weed problems emerging [20].

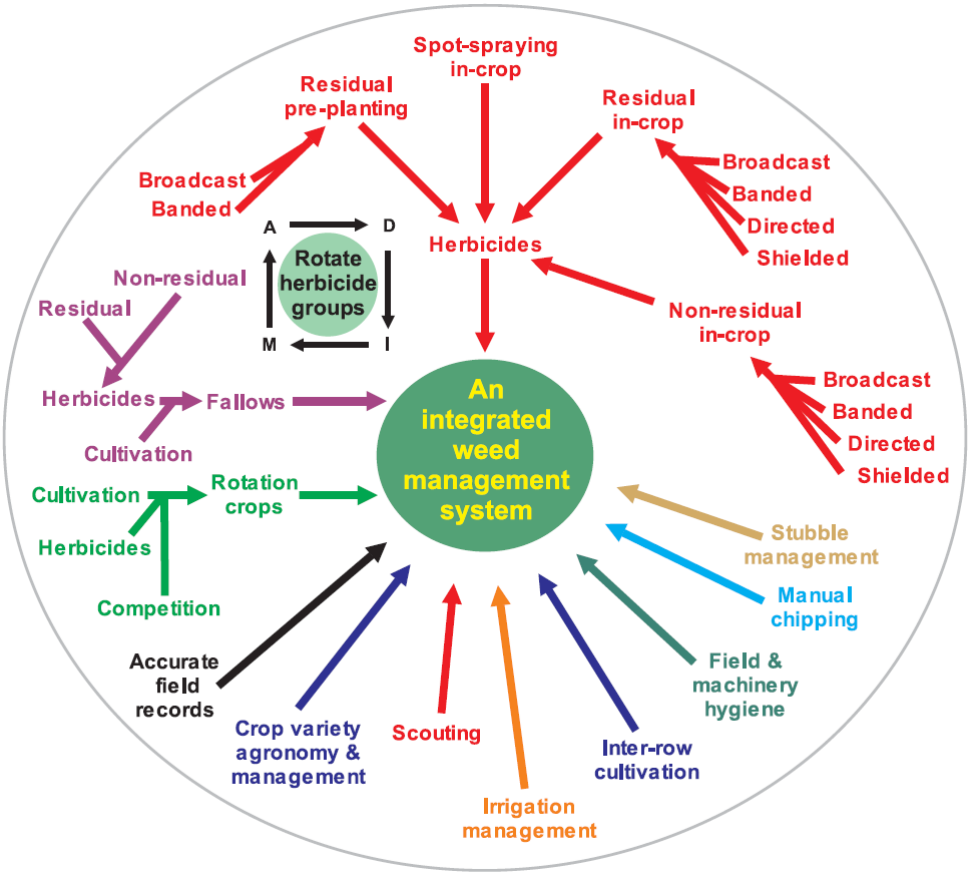

Figure 2.1. The many aspects of integrated weed management combine to give an effective weed management strategy. (Source: [21])

Weed management techniques in Australia include the cultivation of the soil, herbicide application to directly kill weeds, biological control of weeds using insects, fungi and bacteria, and crop selection, including the use of cover crops to smother weed growth through competition [6]. Each of these practices has costs and risks associated with the financial benefit attainable. The chosen strategies for weed management and the choice of which crop to grow depend on many external factors including demand for and the price of the crop, the climate and weather, and the availability and cost of inputs such as fertiliser, water and labour. The best decisions can be made by considering all these factors, combined with the local conditions specific to each farm and each field within the farm. This site specific data is used in models of crop yield which guide crop management, including an integrated approach to weed management [22].

2.2.3 Precision Agriculture

The development of spatial information technology which provide localised crop and paddock information allows site specific crop management. Known as precision agriculture (PA), this technology gives farmers the capacity to increase farm productivity while considering environmental impacts. PA recognises that the potential productivity of agricultural land can vary considerably, even over very short distances (a few metres). The fundamental technology utilised by precision agriculture are the Global Positioning System (GPS) to provide location information and geographic information systems (GIS) to make precise management decisions based on the farm data provided by tools such as yield monitoring and soil sampling and remote sensing [23].

The United States, Canada and Australia were the pioneering nations that developed precision agriculture. Broad-acre farming made it more difficult for growers to understand the variability within fields to optimise crop productivity with appropriate and timely adjustment to farm inputs [22]. By the end of the 1980s the practice of grid sampling resulted in the first practical field maps for fertilizer and pH corrections. Further soil chemical sampling was then used in the US to determine the application rate of chemical fertilisers [22]. In Australia, steering guidance, steering assist and auto steering in agricultural vehicles have minimised soil compaction, allowing inter-row sowing, and cultivation as well as improving soil moisture management and reducing labour inputs.

To utilise the PA and SSCM tools for fields and crop, farmers need the agronomic history of yield as well as soil analysis and topography to better understand of the causes of yield variability. Information about soil ph and sodicity/salinity issues, the effectiveness of weed control, and elevation mapping to help with water management, provide the background information for crop management and decision-making. These steps along with vehicle navigation aids contribute to managing inter-field and across-farms variability for the input of fertilisers, pesticides, fungicides and soil ameliorants to better match the specific conditions of the site [7].

2.2.3.1 Economic benefits

Australian farmers have adopted precision agriculture practices, particularly vehicle navigation and variable rate technology (VRT) for application of fertiliser based on yield maps and soil sampling. A whole farm economic analysis of six farms in NSW and WA estimated the economic benefit of PA technologies being used on those farms. The technology being used on these farms included vehicle navigation, auto-steer, NDVI monitoring, VRT for fertiliser application and in one case VRT for insecticide application. Across the six farms the capital investment amounted to $14-44/ha while the annual benefit ranged from $14-30/ha. Analysis showed that the capital outlay was recovered in 2-5 years [24].

The use of site specific weed management has been adopted on some farms in America and Australia. The methods used range from weed mapping using remotely sensed data and sensor based spot spraying (for weed control in fallow or between rows with hooded sprayers). Variable rate herbicide application has been reported to provide equivalent weed control to conventional spraying and offer reductions in herbicide use from 15-95%, which is largely dependent on the weed density present [25-27]. The net economic benefit is not as clear as in some cases the increased application costs erode the savings from reduced herbicide application [26]. This highlights the need to consider the adoption of technology based on a whole of farm analysis and consider new opportunities afforded by the use of this technology. Swinton [9] argues that the greatest benefit of adoption of site-specific weed management will come from production of value added products and benefit from reduced environmental impact. Improved management of herbicide resistant weeds is another opportunity not directly related to herbicide savings [28].

Australian farmers spend over $3 billion annually on herbicides, pesticides, fertilisers and soil conditioners. Precision application of these agrochemicals to crops is necessary to maximise the benefit from their application. Precision agriculture provides both economic and environmental benefits which will keep Australian farms competitive.

2.3 Industry applications of weed discrimination

The agriculture sector has benefited from the advances in technology that utilise data collected from yield mapping, soil analysis, and the use of GPS and GIS to assist with traffic management and the variable rate of application of fertiliser and soil conditioners. The cotton industry as an example has developed both biological and precision technologies that have increased its profitability and productivity. Similarly, the sugar industry has been developing PA tools to remain competitive in the world market. Both industries also need to manage weed populations within the crop to maintain productivity. Governments in support of the agriculture industry can have a focus on eradication and control of weed infestations that threaten the large cropping regions. Skeleton weed is one such weed that is seen as a real threat to cereal producers and was subject to an eradication program in Western Australia for three and a half decades.

Site specific weed management is a minimally practised management tool on large farms. Manual weed removal and spot spraying are effective on small scales but labour intensive and costly. In many cases this may be the only option if targeted treatment is required. Physical devices such as “weed wipers” can apply herbicide to weeds which are taller than the crop using a roller, but they cover only a narrow swath and their scope of application is limited. Weed mapping allows the creation of a digital variable rate treatment map which is subsequently used to apply the required herbicide rate. Such maps can be produced by scouting [25] or from remotely sensed data [29]. However, use of such maps comes with high cost for surveying or data acquisition and data processing as well as a lag time between collection of data and use of the map. Sensor based systems are currently used in fallow weed control [27] or in-between row spraying and have shown efficient reduction in herbicide use, but there is currently no sensor based system to detect weeds growing amongst the crop.

2.3.1 Cotton in Australia

Australia’s cotton industry is comparatively small but is the world’s third largest exporter in the world, generating revenue of $1 billion per year. Cotton is grown in central and north-western NSW and central and southern Queensland

encompassing around 500,000 hectares. These farms are heavily mechanised and technologically sophisticated in order to manage large areas under crop, 84% of which are irrigated.

Over the last two decades, Australian cotton production has undergone a series of changes driven by the adoption of genetically modified (transgenic) cotton varieties. Since 2004 over 95% of Australian cotton growers have planted transgenic cotton. The most widely used transgenic varieties are herbicide resistant varieties such as Roundup Ready Flex® and varieties which are toxic to one of the main cotton insect pests, the *Helicoverpa* caterpillar, such as Bolgard II® [30].

The cotton industry in Australia is heavily reliant upon glyphosate used with farming strategies that include reduced tillage and ‘over the top’ spraying of glyphosate on genetically modified glyphosate tolerant cotton varieties. The increased reliance on glyphosate has altered the weed spectrum with a shift towards naturally tolerant weed species. An integrated management approach focuses on diminishing the weed seed bank to ensure that glyphosate is of value to the industry for the future [31].

2.3.2 Sugarcane in Australia

The sugarcane industry in Australia covers 390,000 ha along the eastern Queensland and northern New South Wales coast. It produces 32-35 million tonnes of cane per year, which is processed in Australian mills located within the growing regions [32]. Of the 4.5-5 million tonnes of sugar produced about 80% is exported and 20% refined for the domestic market. The value of production is between $1.5-2.5 billion annually depending on production and global price [33]. The average sugarcane farm size in Australia is 100 ha which is considerably smaller than the average farm size for cereal and cotton growers. The average farm size has been steadily growing each year as cane farmers have adopted new technology allowing them to expand their business. The Australian sugarcane industry is focussing its research effort on reduction of the cost of farming as it faces a reduction in the value of production and increasing input costs. To offset some of these costs, the industry is moving towards a minimum tillage farming system and a reliance on herbicides for

weed management. The use of GPS for guidance and auto steer has seen demonstrated benefits in more even row spacing, reduced overlap of fertilizer and herbicides, increasing machine efficiency and reduced driver fatigue whilst maintaining the capacity to operate at night [34].

Remote sensing provides an estimate of the size of the crop to the management of harvesting and milling operations and marketing the end product. There have been a number of attempts to monitor yield within a block to offset concerns of sugar loss that in some cases, is estimated to exceed 20%. The development of a reliable yield monitor for the sugarcane industry has been slow and at this point in time there is no commercially available monitor. A prototype yield monitor developed by the University of South Queensland was used in combination with soil sampling for a case study on a 100 ha farm Burdekin, Queensland. A variable rate of gypsum was applied to ameliorate the soil sodicity. This study showed a $563 per ha benefit over 5 years when compared to standard input application [35].

Weeds which are particularly difficult to control in sugar cane are mostly perennial grasses such as guinea grass, green panic and Johnson grass. These grasses have similar leaf shape, texture and colour to sugarcane. The spatial similarity amongst different species presents challenges to the development of a ground-based optical weed sensor for the industry. The sugarcane industry would benefit from precision spray technologies that target weeds in crop. This development would have the potential to contribute to greater productivity and a reduction of herbicide use.

2.3.3 Surveying for Skeleton Weed Eradication

Skeleton weed (*Chondrilla juncea* L.) is an herbaceous perennial weed of Eurasian and North African origin that became established in south-eastern Australia early this century. Skeleton weed is found throughout New South Wales, South Australia, Victoria and in the wheat belt of Western Australia. Although a long established, widespread weed in south-eastern Australia, skeleton weed was not detected in Western Australia until 1963 and is a Declared Plant in Western Australia under the Agriculture and Related Resources Act 1976 [36].

Since 1974 it was the subject of an eradication program in Western Australia, costing between $3 million and $4 million per annum, funded from a levy on all Western Australian grain growers [37]. This program significantly limited the weed's impact and rate of spread [36]. In 2008 a review of the Skeleton Weed Committee's operation recommended that the focus be revised from eradication to monitoring and management, however in areas where plant density is low eradication continues to be a goal [37].

The skeleton weed eradication program was both labour intensive and costly. Dodd considered a range of plant species which have been the target of eradication programs from among approximately 200 species declared noxious and the subject of eradication programs [38]. Very few species have been successfully eradicated, and those which have were only present in a limited and known range or eradicated from a part of their previous distribution. Dodd promotes the use of ecological studies in assessing both the need for eradication and the potential for success thereof [38]. An important aspect of any successful eradication programme would be knowledge of where individual plants and patches of the target species are. Automated recognition of plant species could become an important part of such a programme.

2.4 Spectral reflectance of plants

The spectral reflectance of plants is determined by the cellular and biochemical structure of the leaves and the structure of the leaf canopy. Figure 2.2 shows the reflectance and transmittance spectra of a single leaf. The difference between the reflectance and transmittance spectra is the due to absorption. Within the visible spectrum (400-700 nm) the spectra are dominated by absorption due to various pigments, primarily chlorophylls. In the very near infra-red region of the spectrum the reflectance is high (close to 50%) and flat. Above 1300 nm, reflectance decreases again due to absorption by water present in the leaf structure.

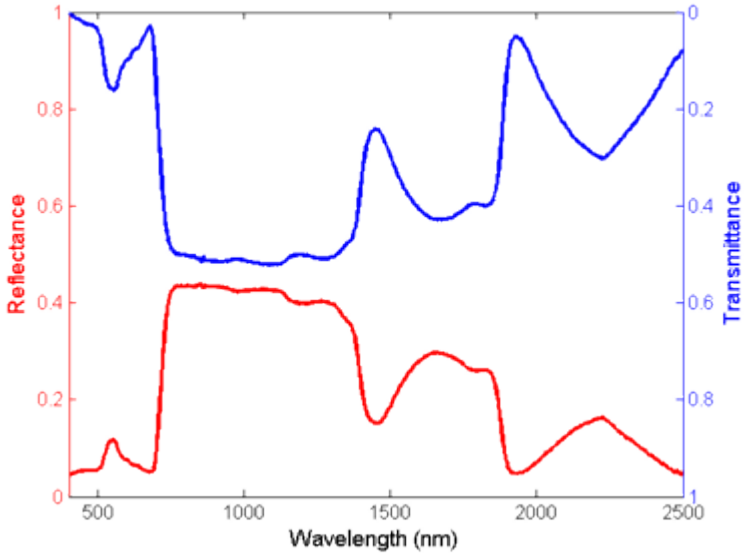

Figure 2.2. Typical reflectance (below) and transmittance (above) spectrum of a green leaf (source: [39]).

2.4.1 Leaf structure and biochemistry

The characteristic green colour of plant leaves is due to the chemicals used for photosynthesis. Through photosynthesis, plants convert carbon dioxide and water into organic compounds using energy from light ($CO_2 + H_2O$ photons $\rightarrow CH_2O + O_2$). Plants use a range of chemicals for this purpose, primarily chlorophylls, specifically “chlorophyll a” and “chlorophyll b”, which are contained in chloroplasts within the mesophyll cells. Each of the chlorophylls absorbs light in a fairly narrow band of both the red and blue ends of the visible spectrum. Plants also contain other pigments, including carotenoids and xanthophylls, which absorb light and aid photosynthesis, however at a lower efficiency than that of the chlorophylls. Figure 2.3 shows the absorption spectrum of the two chlorophylls, the carotenoids and also of water and cellulose.

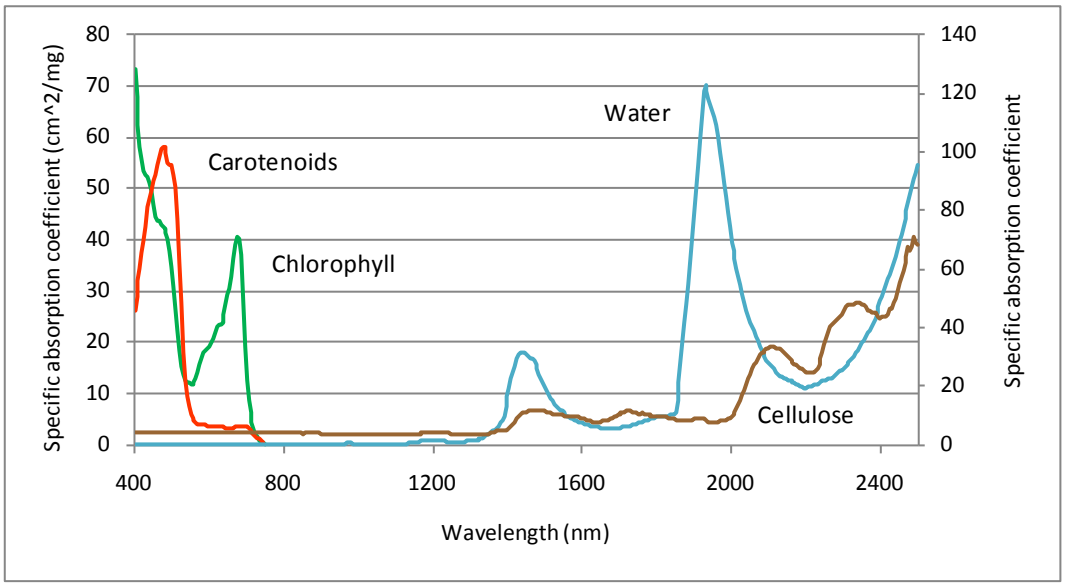

Figure 2.3. Specific absorption coefficient of chlorophyll a+b and carotenoids (cm^2/mg) on the left axis; and of water (/cm) and cellulose (cm^2/g) on the right axis (data source: [40]).

The absorption spectrum of water starts at wavelengths longer than 950 nm but has little effect below 1200 nm. There are three main absorption peaks at 1450, 1940 and 2500 nm as shown in Figure 2.3. The absorption spectrum of leaf dry matter is very low in the visible and near-infrared, and stronger at wavelengths longer than 1200 nm. None of these compounds absorbs much energy in the region between 750 nm and 1250 nm, which explains why leaf reflectance and transmittance are high in this region. The high reflectance in the NIR plateau is determined by multiple scattering of light from interfaces between the cell walls and air gaps, particularly in the palisade mesophyll, as shown in Figure 2.4. [39, 41].

The variation in reflectance spectra of plants can be explained by variation of pigment concentrations and cell structure within the leaves of different plants. Within a single species and individual plant these properties are affected by a range of factors, including the age and growth stage of the plant, water stress, nutrient deficiency and disease.

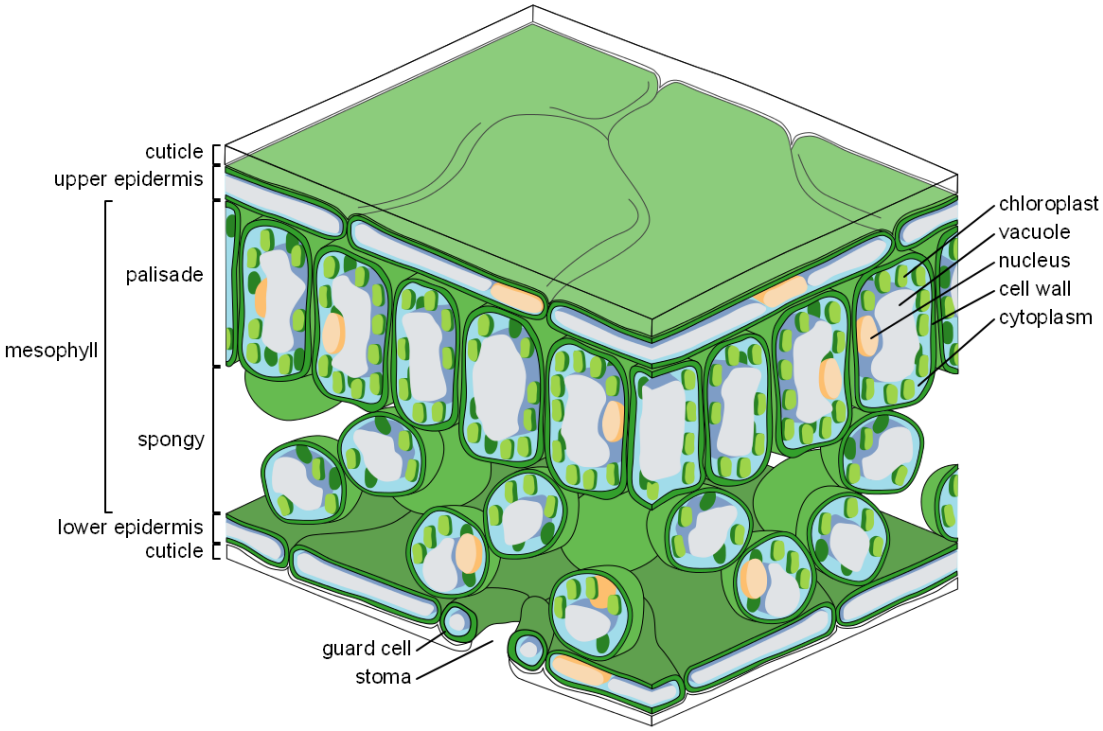

Figure 2.4. Diagram of leaf structure showing layers within the leaf and cell structure (source: [42]).

When observing the reflectance spectra from a distance, as with remote sensing, the plant organisation also affects the observed spectra. The canopy reflectance is primarily determined by the leaf level reflectance but also affected by the leaf orientation and angle of incidence of light, the distribution of leaf angles and the multiple reflections of light from different leaves above and below each other. Many different models have been put forward to describe the interaction of light with leaves (both for single leaves and leaf canopies). The most widely tested and used is PROSAIL: a combination of PROSPECT for leaf reflectance modelling and SAILH, a bidirectional model of canopy reflectance [39].

SAILH (Scattering Arbitrary Inclined Leaves) is a one dimensional model of canopy reflectance which solves the scattering and absorption of specular and diffuse light incident on a leaf canopy (and the ground below). The model input is wavelength dependent transmittance and reflectance of the leaves and the reflectance of the soil. PROSPECT (Leaf Optical Properties Spectra) models the leaf as a stack of several plates with partially isotropic light source to model the surface roughness. The optical properties of, and the number of, plates are

determined by input parameters which describe the leaf structure, the average number of cell wall/air interfaces, the equivalent water thickness, the total chlorophyll content, the total carotenoid content and the dry matter (cellulose, lignin and protein) content. The radiative transfer is then calculated based on summing all the partial reflected and transmitted components of the incident light at each interface of the model [43]. These two models combined as PROSAIL can be used to estimate the leaf biophysical parameters which produced a measured reflectance spectra.

2.4.2 Use of hyperspectral reflectance in remote sensing

The relationship between plant physical properties and their reflectance spectra has been utilised by remote sensing in order to determine many different characteristics of plants from their reflectance spectra. The range of plant properties which have been examined in relation to their multi-spectral and hyperspectral reflectance data includes: vegetation type [44, 45], leaf cover and wet biomass [46, 47], plant health [48], nitrogen status and requirements of a crop [49], chlorophyll and other pigment concentrations [50], the relationship of chlorophyll concentration to stress [48], plant uptake of heavy metals [51], as well as the presence of weeds [52]. Many other studies have also looked at the relationship between plant biophysical properties and the reflectance spectra observed either at the leaf level, canopy level or from remote sensing and found correlations between them. The goal with most such studies is to find a relationship between one or more of these inter-related factors and the resulting spectra which can be used to make predictions about the biophysical parameter across a broad range of species and environmental conditions.

Remote sensing with hyperspectral reflectance data usually provides a large volume of data related to the properties of plants of which a large fraction is redundant or not related to the plant characteristics of interest. There are broadly two different approaches to dealing with this volume of data for the purpose of determining the properties of plants. The first is to use all of the data available in the spectrum and to use a model such as PROSAIL to determine the biophysical parameters which best match the measured spectra. This is a computationally intensive approach; however it does give the most reliable results. The second approach is to determine which part of the spectrum is

most highly correlated with the plant properties of interest and derive an empirical relationship between those properties and an index made up of some combination of reflectance values at given wavelengths. Hatfield *et al*. provided a comprehensive review of such indices relevant to agriculture [53].

2.4.2.1 Methods of optimal waveband determination

A range of techniques have been used to determine the optimal wavebands for estimation of biophysical parameters and also for plant classification. Selecting wavebands with a high correlation between the parameter of interest and the reflectance in that waveband is frequently used to find one or a few wavebands which can be used to form a predictive index e.g. Zhao*, et al.* found optimum reflectance ratios to estimate nitrogen content in cotton leaves via linear regression analysis of reflectance and leaf nitrogen content [54]. A similar exploratory technique was used by Gitelson *et al*. to find features in spectral reflectance with a high correlation to carotenoid content [55]. In the domain of classification, a broader range of techniques have been used. This may be classification into species or other classes such as healthy/diseased or crop/weed. Thenkabail *et al.* reported a study of hyperspectral reflectance data for plant discrimination with a range of crops, weeds and shrubs [56]. The study explored techniques to identify and discard redundant information in the spectral data and stepwise discriminant analyses to identify optimal wavebands for plant classification. A lambda-lambda R^2 model determined cross-correlation between two wavebands (λ_i, λ_j) for all pair of wavebands. Pairs of wavebands with a high correlation were associated with redundant information. Low correlation indicated unique information about the plant species. This test was best suited to individual species where the spectra were mostly similar.

Two other techniques assessed by Thenkabail *et al.* were principle component analysis and stepwise discriminant analysis [56]. Both these techniques have been used broadly for the determination of optimal wavebands or formulation of new indices. A discriminant analysis determines a function of variables which is able to separate observations into classes. This function is often a linear combination but many other functions have been used. For spectral reflectance data a stepwise method is used where wavebands which improve the classification are retained and wavebands which inhibit classification are

rejected [56-58]. Principal component analysis (PCA) transforms a set of observations (in this case the reflectance at each waveband) into a linear combination of principle components. The principle components are linearly independent eigenvectors calculated to have decreasing magnitude, i.e. the first principle component accounts for as much of the variability in the data as possible and each successive component accounts for as much of the variability as possible while being linearly independent of the previous components. Principle component analysis of hyperspectral data using only two components (followed by discriminant analysis) was used by Castro-Esau *et al.* to classify 12 species of lianas (woody vines) and 5 species of tree into two classes [44]. An alternative to principle component analysis is wavelet analysis; see for example Okamoto *et al*., where wavelet analysis was used to classify sugarbeet and weeds with hyperspectral reflectance data [59].

2.5 Weed detection for site specific weed management

Reliable information on weed abundance, distribution, and change over time is essential to evaluate control strategies, prevent spread to clean areas and improve weed management. Weed mapping which relies on human observation is time consuming, expensive and inefficient, especially when the target weeds cover a wide area. Several attempts have been made to discriminate plants with optical and near-infrared images using either multispectral or hyperspectral imagery. These images may be captured from aerial or satellite platforms as well as proximate sensing from vehicle mounted devices. Remote sensing is limited to imaging and has lower resolution – generally at the scale of whole plants or larger. Proximate sensing can use either imaging or non-imaging sensors, and provides resolution below the size of individual leaves. A selection of previous studies using these techniques is presented here.

2.5.1 Weed mapping

Weed detection on a large (whole field) scale gives a weed map for the field. This weed map can be integrated with other available information when making decisions about weed control strategies to increase crop yield and quality. Timmermann *et al.* conducted a four year long study on the effect of site

specific weed management in four crops [25]. Weed maps were created from manual sampling of weed density on a grid with a spacing of 7.5-15 m and linear triangular interpolation between the sampling points. Significant herbicide savings (on average 54%) were attained for all crops over the four year period from this very labour intensive process. While such study does not present an economically viable method of site-specific weed management, it does show what benefits might be afforded from weed maps which are produced from remotely sensed data.

Remote sensing with multispectral or hyperspectral imaging has been investigated for determination of crop type and for weed presence. Thenkabail used hyperspectral data from Hyperion with a spatial resolution of 30 m and multispectral data from IKONOS with a spatial resolution of 4 m to estimate biomass and classify African forests into different classes [45]. An accurate classification rate of 96% was achieved in this study with the hyperspectral data, but the multispectral data showed poor performance. Even with a similar accuracy for weed classification in crop, the 30 m resolution is not sufficient to manage small patches of weeds which frequently occur. Aerial imagery has higher spatial resolution, such as the multispectral imagery with a spatial resolution of 1 m collected by Goel *et al*. [52]. This study attempted to detect weeds in corn and soybean at a density above a predetermined economic threshold with success for some weeds but was not able to detect grasses in either corn or soybean.

Hyperspectral reflectance data has also been collected from a few meters above the canopy [56, 60] and from leaf level [57, 58]. Okamoto *et al*. used a hyperspectral camera to record images with high spectral and spatial resolution of sugarbeet and weeds [59]. Rather than selecting specific wavebands a wavelet analysis of the resulting spectra was used and better than 80% accuracy in identifying sugarbeet and weeds was reported.

An interesting outcome from the remote sensing studies, which is confirmed by the leaf level hyperspectral reflectance sensing, is that narrow wavebands generally provide improved classification over broad wavebands. Where classification of weeds is successful, the number of wavebands required ranges from 5-22, depending on the number of species, their similarity and the

environmental conditions. In all such cases addition of further wavebands does not improve the classification which confirms that there is much redundant information in the reflectance spectra. Careful selection of the wavebands used is required which considers the range of environmental conditions to be experienced.

The ability to combine weed maps with previous field data to produce a treatment map prior to application is an advantage over real-time mapping. However; the limited spatial resolution, the time delay and the cost of data collection and analysis have so far seemed to prevent this method from becoming economically viable [9].

2.5.2 Real-time weed detection

Proximate or on the ground sensors which are mounted to a vehicle or a spray boom allow real-time detection and immediate treatment of weeds in a crop field. Interpretation of this information in real time is required to automate herbicide spraying as the machinery passes over the crop. Real time methods can be performed at an individual plant scale allowing spot spraying in place of uniform treatments over large areas.

Ground based sensing can provide resolution at the single leaf scale or smaller which allows a range of different techniques to be used for plant classification. Small weeds can also be detected which can be important to prevent a single successful weed from leading to future problems. There is a greater degree of control available on the ground with the potential for use of artificial lighting, control of ambient lighting and multiple viewing angles. Artificial lighting also allows the use of fluorescence spectroscopy which may aid in discrimination of weeds from crops [61].

2.5.2.1 Non-imaging sensors based on spectral reflectance

Several multiple narrow spectral band sensors have been developed which capture light using a single sensor. The field of view of these sensors is still larger than individual plants but they have been successful detecting small plants including patches of seedlings. They have been successful in detecting

green plants against a soil background (Green-from-Brown) but not discriminating different plants.

Felton *et al*. developed an optical sensor based on the ratio of reflectance between red and near infra-red wavebands [62]. Two photodetectors fitted with appropriate filters recorded the reflected light which was adjusted for incident solar radiation by two corresponding photodiodes which were directed upwards. The device was commercially available as the DetectSpray® system for a period of time, but is no longer available. Its use in fallow weed control was reported by Blackshaw *et al*. along with limitations on size of plants detectable and the daytime operation [63].

NTech Industries manufactures weed detection equipment called WeedSeeker®, which is a commercially available sensor for Green-from-Brown detection. This device uses two red and infrared light emitting diodes to illuminate the ground and a photodetector to record the reflected light. It is used in fallow weed control [27] and has also been used under hooded sprayers for between row weed control [64]. WeedSeeker appears to be the only commercially available device for automatic plant detection in the agricultural industry.

Wang *et al*. developed an optical weed sensor using a five band multi-spectral sensor based on the spectral characteristics of weeds, crops and soil [58]. This system still had low spatial resolution but correct classification of crop vs. weeds was reported when the density of plants was above single plants.

2.5.2.2 Imaging sensors and machine vision

Higher spatial resolution is attainable with image captured from a video camera and more recently from a high-resolution digital camera. Plant detection is dependent on machine vision to recognize plants in the image, occasionally with the benefit of broadband spectral information from RGB cameras. Machine vision sensors have for a long time been limited by the image data processing time required – however the limitation on vehicle speed will decrease with increasing processing power.

The general process used with machine vision starts with image acquisition – either with a colour camera or perhaps with filters placed in front of a black and white camera sensitive to the visible and very near infrared. Image enhancement is applied to improve the quality of the image for subsequent processing. The result is another image with enhanced edges, contrast, colour or other improvement in image quality. Calculation of indices from individual waveband information may also be used to create a new image containing the red-green ratio, the red-NIR ratio where NIR is also available or some other combination. Segmentation then detects individual leaf and plant regions, separating them from the background soil. Feature extraction can involve analysis of leaf shape, texture analysis or plant organisation (via fractal dimension). Finally, classification determines which plant best matches the extracted features.

Textural features in each of four broad wavebands was used by Franz *et al*. [65] to discriminate between three broadleaf weeds and soybean. Image acquisition used a CCD camera in a laboratory setting with controlled lighting using four filters to provide broadband spectral information (blue, green, red and infrared). Classification using a discriminant analysis was successful when the patches used for texture analysis were selected manually.

Zhang and Chaisattapagon used a CCD camera with six different filters to capture images in a greenhouse environment from wheat and weeds [66]. They trialled colour, shape, and texture analysis in order to discriminate between the different plant species studied. The leaf shape and texture analysis (based on Fourier spectrum) were successful but were based on manual selection of the leaf areas used in the analysis.

These early machine vision trials were conducted under stationary, controlled lighting conditions without real-time constraints. However several systems have been trialled under field conditions with modern cameras and increased computing power. Tian designed a machine vision system with real-time use as the primary design goal [67]. A CCD camera captured images from an area covering multiple rows (3 m width) and a Bayesian classifier was used to detect plant density [68]. The plant detection was only applied to control zones in the

between row area, so this system is not capable of detecting single plants nor discriminating weeds from crop when the crop covers a larger area.

2.5.2.3 Hybrid spatial and multispectral sensors

A combination of narrow band spectral information and high spatial resolution appears to be the most likely solution to the problem of detecting weeds. High spatial resolution is desirable for spectral based sensors because it avoids the problem of spectral mixing. An imaging spectrograph has been used in several studies to provide both high spectral and spatial resolution. A single line from the ground is observed on a sensor which resolves each pixel into a spectral line. Vrindts used such a system to correctly discriminate corn, sugarbeet and weeds with an accuracy of greater than 90% [57]. However, this system was only tested with images collected while the device was stationary. Similar results were reported by Noble *et al*. for wheat and weeds [69].

Raymond *et al*. designed a system to measure reflectance in two narrow wavebands using red and NIR laser diodes and a photodiode to measure the response [70]. The modulated output beam is scanned across the ground providing a high spatial resolution. Only Green-from-Brown detection was attempted with this device but it was able to detect plants with a size as small as 5 mm wide at a speed of approximately 2 km/h.

2.6 Laser based spectral reflectance sensor

The Photonic Detection Systems prototype weed sensor described in Section 1.3 is a non-imaging spectral reflectance based sensor. It used two lasers in the red and very NIR bands to illuminate the ground and target plants. The use of lasers in place of LEDs provided reflectance properties of plants from a small part of the leaf area. This information was combined with 1-D spatial information acquired while the device travelled along the ground. The spacing between detection modules consisting of two lasers plus a photodetector significantly limited the potential to detect small plants. Leaf orientation also affected the leaf size determination and the device was very sensitive to distance from the sensor to the plant.

Further development of this spectral reflectance based weed sensor is part of a larger research project undertaken in collaboration between the Western Australian Centre of Excellence for MicroPhotonic Systems (COMPS) and Photonic Detection Systems, Pty Ltd (PDS). A prototype spectral reflectance based weed sensor using three wavelengths was developed by COMPS [10]. Three lasers were used (two red and one NIR) which created a structured light source to illuminate the ground and plants. The three wavebands were selected from a limited number of commercially available laser wavelengths and are within regions of the reflectance spectra which have previously been reported to provide sensitivity to different plant species.

The structure of the weed sensor is shown in Figure 2.5. The laser output beams were collimated with a 4 mm diameter and combined using wavelength selective filters. This arrangement ensured that when each laser was switched on it illuminated the same spot on the plant or ground. The single output beam from each laser module was divided into 14 beams using an optical cavity. The front surface of this cavity was coated with a high-reflection coating (around 90%) and the rear surface had a 100% reflection coating. The tilt angle of the cavity gave an output beam spacing of approximately 13 mm. A line scan camera provided measurement of the reflectance from each of the 28 spots over the 500 mm field of view. Each laser was sequentially turned on and an image captured from the camera. Software running on a computer controlled the operation of the lasers and camera as well as data processing. For each laser a peak was observed in the captured image. The peak values determined for each wavelength were used to calculate spectral slopes of the target plant and these slopes used to predict the target plant. The combination of high spatial resolution and multiple narrow waveband spectral resolution provided sufficient spectral information to discriminate several different plants and allowed detection of narrow-leaved plants [10].

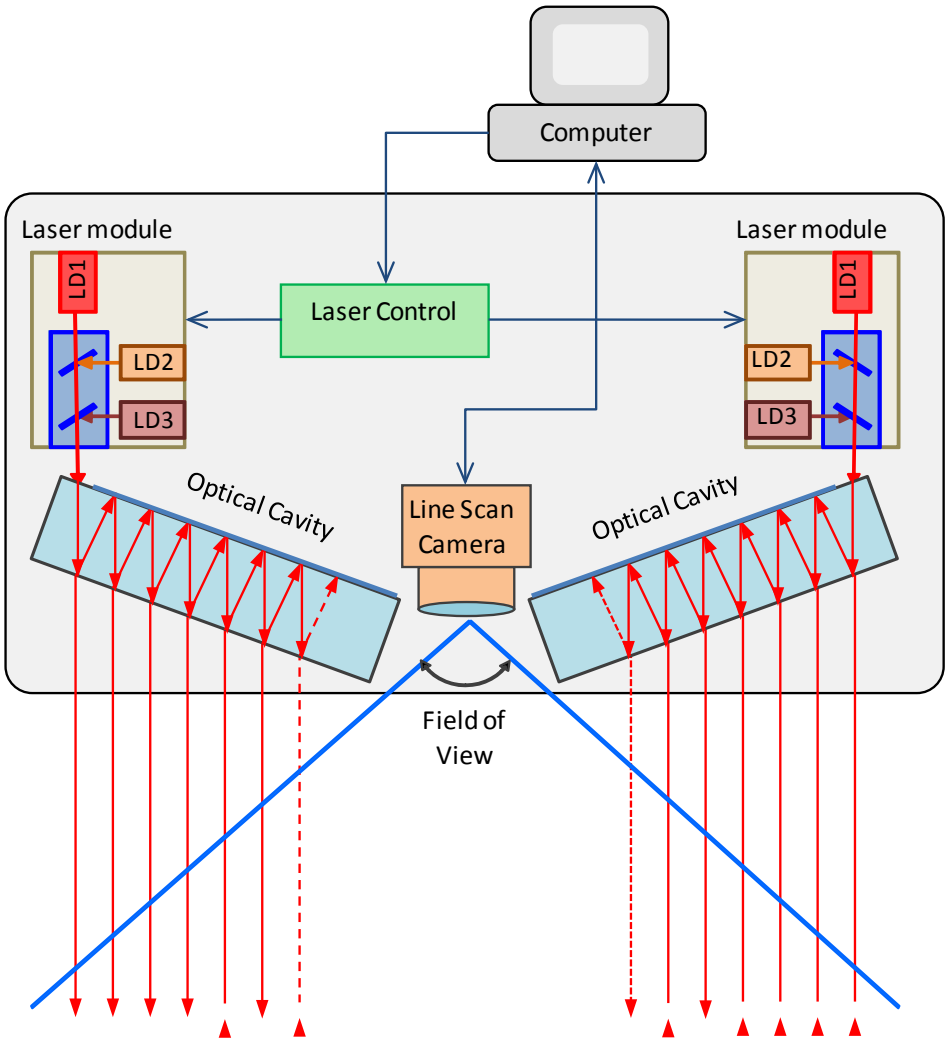

Figure 2.5. Laser based spectral reflectance sensor with lasers, optical cavities and line scan camera. Three optimised wavelengths are sequentially switched on for illumination along one optical path, striking the same spot on the leaf, stem or soil. An optical cavity enables multiple beams to be generated using a single laser source. A line scan camera monitors the intensity of light reflected by the plants or soil. The controller calculates plant spectral properties and detects target plants.

Figure 2.6 shows the principle of a real-time weed monitoring and spraying system based on this weed sensor which is able to detect weeds within a crop and apply herbicide only to the weeds.

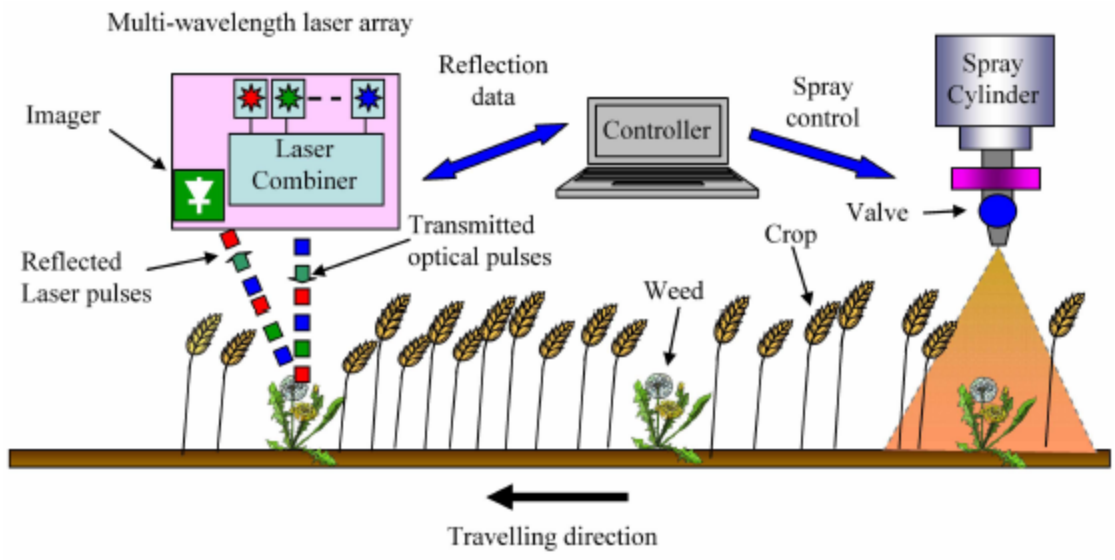

Figure 2.6. Principle of real-time weed detection and herbicide application (adapted from:[10]).

The prototype weed sensor described above was the starting point for this research project. Several limitations of the design prevented it from being used in outdoor field conditions. Throughout this project the design was developed to a point where it could be used to discriminate three different broadleaf plants at a speed of 5 km/h.

2.7 Summary

The management of weeds in agriculture is an expensive and time consuming activity for farmers. Integrated weed management is a holistic management technique which advocates the use of a broad range of weed control methods. The long term effects of any control method used need to be considered as part of the decision making process. With the size of farms continuing to grow, software based crop management tools are essential to synthesize the available spatial data and assist in crop management decision making. The emerging practice of precision agriculture provides an even greater volume of spatial data on the variability across the farm. This spatial awareness and the availability of technology have allowed the resurgence of crop management at a fine-grained scale. In the area of weed management however, site-specific weed control is limited to fallow or between row weed management because there are currently no commercially available precision agriculture devices

Table 2.1. Summary of approaches to real-time crop/weed discrimination.

Author	Approach Used	Limitations
Felton et al. [62].	Non-imaging spectral reflectance using ambient light with 2 narrow wavebands.	Weed/Soil discrimination only; limited to daytime operation.
NTech Industries Inc. [8].	Non-imaging spectral reflectance with 2 narrow wavebands.	Weed/Soil discrimination only.
Wang et al. [58].	Non-imaging spectral reflectance using artificial lighting with 5 wavebands.	Low spatial resolution; limited to laboratory conditions.
Franz et al. [65].	Multi-wavelength imaging with four wavebands (RGB and NIR) using texture analysis.	Not real-time; required manual image segmentation for best results.
Zhang et al. [66].	Multi-wavelength imaging with six wavelength bands using leaf shape and texture analysis.	Not real-time; required manual image segmentation for best results.
Tian et al. [67].	Low resolution NIR imaging using intensity thresholding or wavelet decomposition within management zones.	Weed/Soil discrimination only, thus limited to fallow or between row weed control.
Vrindts [57]	Hyperspectral line scan using ambient light and up to 12 narrow wavebands.	Not real time; reliant on uniform ambient light
Raymond et al. [70]	Multi-wavelength spectral scanning with 2 narrow wavelength bands.	Weed/Soil discrimination only; low speed (2 km/h).
Sahba *et al*. [10]	Multi-wavelength spectral line scanning with 3 narrow wavebands	Limited to laboratory conditions.

capable of discriminating between crops and weeds. The only exceptions to this are labour intensive manual spot spraying or weed mapping which relies on human decision making.

Previous research into plant classification and weed detection shows promise for the use of narrowband multispectral sensing to detect weeds in a crop. A summary of previous studies attempting to discriminate weeds from crop in real-time is presented in Table 2.1The reduction of spectral resolution to a smaller number of wavebands by discarding redundant information was able to maintain classification results. The research reported in this thesis builds on the multispectral sensor described in Sahba *et. al*., which uses a structured light source to provide improved spatial resolution [10]. Additionally, a survey of reflectance spectra was undertaken in two crops and important weeds. This allowed a discriminant analyses to identify wavebands useful for classification of plant species within a small range of wavelengths suitable for laser based spectroscopy. The detection of a small number of spectral reflectance features allows real time use on a spray boom, with the potential to correctly detect weeds under the required environmental conditions. The development of an optical weed sensor that is capable of operation under field conditions will lead to the development of a commercially-viable weed sensor capable of discriminating weeds amongst a crop. Such a sensor will provide a key component in precision agriculture practice and would result in substantial financial and environmental benefits through the reduction of herbicide use.

Chapter 3

Measurement of the Spectral Reflectance of Plants

3.1 Introduction

Spectral reflectance based sensors have shown the potential to be able to discriminate different plant species from each other and could be developed into an automatic spot spraying tool in agriculture. Successful development of such a sensor requires confidence that there is sufficient difference in the spectral properties of plants in order for discrimination to be possible. With this confidence it is then necessary to have a spectral reflectance sensor capable of measuring plant spectral properties in real time without the carefully arranged setup of a laboratory spectrometer.

This chapter covers the materials and methods used to measure the spectral reflectance of plants. A survey of spectral reflectance of four crops and the weeds growing amongst those crops was conducted as part of this research project. The spectrometer setup used to conduct the survey of leaf level spectral reflectance is described in Section 3.2. A prototype spectral reflectance sensor previously developed at the Centre of Excellence for Microphotonic Systems (COMPS) was outlined in Section 2.6. The components which make up this system are described and characterised in the rest of this chapter. The laser diodes and drivers used to control them are described in Section 3.3. The passive optical components used to create the structured light source from individual laser beams are described in Section 3.4. The line scan sensors used to record the intensity of reflected light are characterised in Section 3.5, along with an assessment of the required performance to reach typical farming vehicle speeds. Section 3.6 describes the ruggedisation of the prototype such that it will

maintain its performance in the high vibration conditions endured by agricultural implements. Lastly, the hardware required to independently control the prototype and perform data processing is described in Section 3.7.

3.2 Methods for spectral reflectance measurements

The difference in optical properties of plants can be used to discriminate between different species and monitor the status of plant growth, health, and water and nutrient stress. The diffuse spectral reflectance measured in the wide wavelength range from 400-2000 nm is used to investigate in which wavelengths the species differences are clearest. This information can be used to select the optimal wavelengths of light sources required in the system to discriminate plants described in this thesis.

3.2.1 Experimental setup for spectral reflectance measurements

The schematic diagram and the experimental setup used to measure diffuse spectral reflectance are shown in Figure 3.1 and Figure 3.2, respectively. Two fibre spectrometers are used to cover the wavelength range from 400-2000 nm. The visible spectrum is recorded by a USB2000 spectrometer which covers the range from 200-870 nm and the near-infrared (NIR) spectrum is recorded by a NIR256-2.1 spectrometer which covers the range from 870-2100 nm. A HL-2000 tungsten-halogen lamp with an emission spectrum from 360-2000 nm is used as a broadband light source. The sample is illuminated through a multi-core fibre ending in a probe oriented at 45° incidence. The diffusely reflected light is captured by the same probe and is divided between the two spectrometers using a trifurcated fibre assembly. Both spectrometers and the light source can be operated from a 12V battery power supply which allows spectral measurements to be made in the field. Field measurements allow the spectra to be measured a short time after leaf samples have been collected.

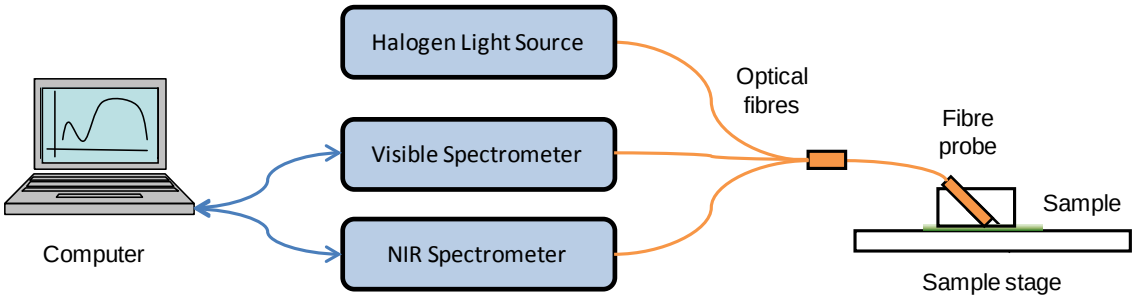

Figure 3.1. Schematic diagram of the setup for spectral reflectance measurements of plants and other objects.

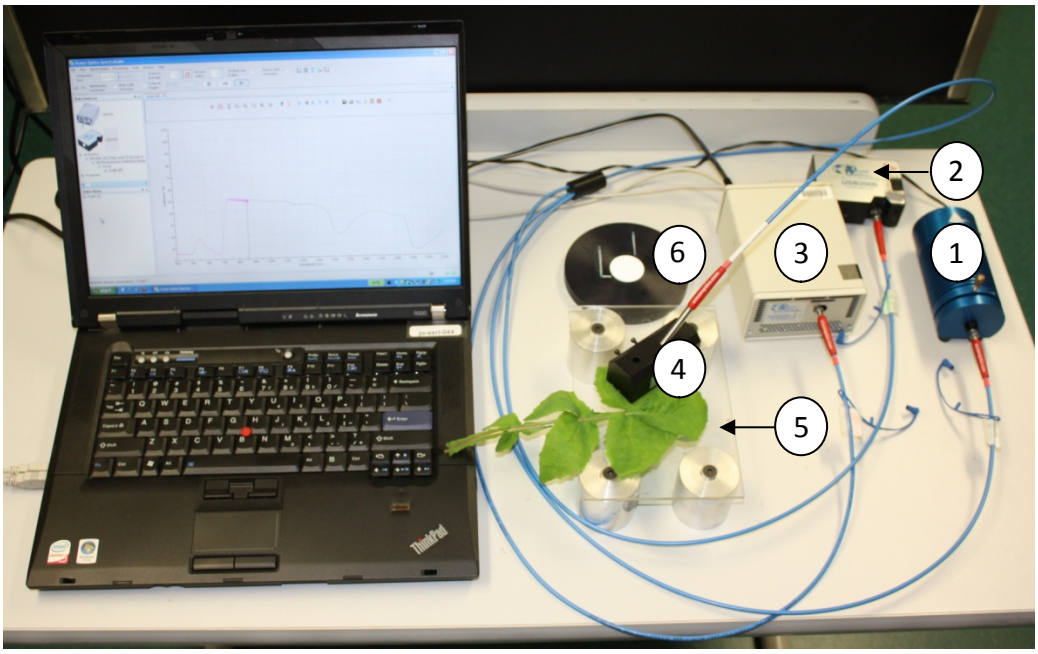

Figure 3.2. Setup used for spectral measurements of plants and other objects: 1) Halogen light source; 2) Visible spectrometer; 3) NIR spectrometer; 4) Multi-core optical fibre; 5) Acrylic stage; 6) 100% reflectance standard.

3.2.2 Procedure for spectral reflectance measurements

The reflectance spectra of plants were recorded using a laptop computer to control both spectrometers and record the data. The procedure required calibration of the system by recording a white reference spectrum from a 100% reflectance standard and a dark reference with the light source blocked. The standard used is a white polytetrafluoroethylene (PTFE) diffuse reflectance standard. Prior to this calibration the light source and NIR spectrometer were allowed to stabilize for five minutes. The NIR spectrometer uses a thermoelectric cooler to cool the sensor to -15°C. For each plant measured,

three leaves from the plant were collected and three spectra recorded from different positions of each leaf. Each leaf was placed on an acrylic stage to minimise back reflection of the light transmitted through the leaf. This is significant for the NIR spectrum because very little NIR light is absorbed by the leaf. The software used was supplied by the spectrometer manufacture. This software stores the calibration spectra, records the spectrum from each position on the leaf, and calculates the reflectance spectra using the calibration data. This calibration data was updated at the start of measurement for every plant to adjust for small changes in the lamp output and dark current over time.

3.2.3 Interpretation of plant reflectance spectra

A typical reflectance spectrum recorded from a green leaf is shown in Figure 3.3.The reflectance spectrum shows different behaviour across the visible to NIR regions of the spectrum. In the visible region (400-700 nm) the reflectance is low, less than 25% for all green leaves and as low as 5% in the red (650-690 nm) and violet and blue (400-490 nm) parts of the spectrum.

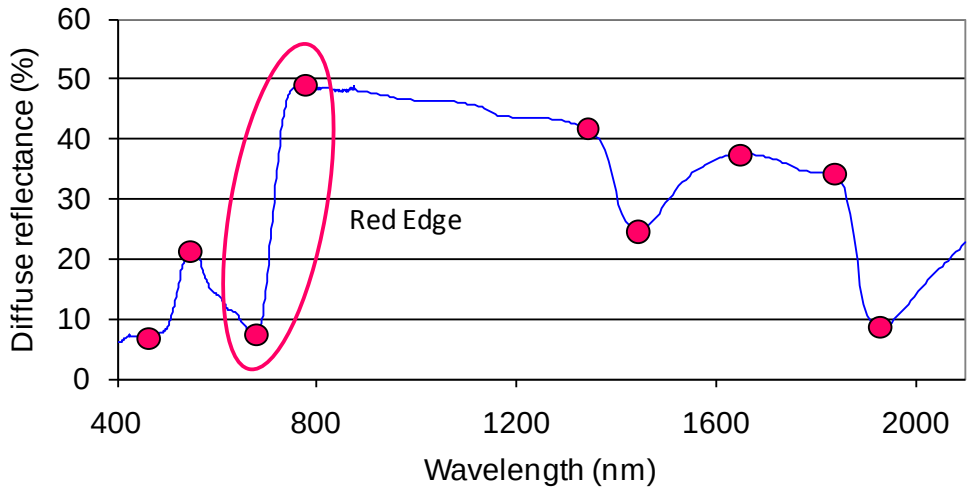

Figure 3.3. Example reflectance spectra recorded from a leaf showing characteristic wavelengths.

The system for discriminating plants discussed in the following section relies on differences in the slope of the spectral reflectance between some characteristic wavelengths. From Figure 3.3, several characteristic wavelengths can be identified which define the regions of high slope. The most striking feature is the red edge around 700 nm. This feature is commonly used to detect vegetation in

remote sensing applications and is the basis for vegetation indices calculated from reflectance at red (670 nm) and NIR (>750 nm) wavelengths. The other characteristic wavelengths considered are the peak of green reflectance at 530 nm and the inflection at 470 nm. These features are all related to the pigment concentrations discussed above and could be useful for the determination of plant type based on differences in their physiology.

The potential for use of this system in spot-spraying of weeds in sugarcane, cotton and other broad-acre crops is explored through a reflectance spectra survey presented in Chapter 5. The reflectance spectra survey gave an assessment of the potential for the three wavelength weed detection system to discriminate crop from weeds. In addition, a discriminant analysis explored the use of additional wavelengths to improve the discrimination rate and to validate the ability to discriminate based only on spectral reflectance at wavelengths of commercially available lasers.

3.3 Laser diodes and laser drivers

The weed detection system developed throughout this thesis determines spectral properties by illuminating the ground with light at specific wavelengths and capturing the reflected light. Using lasers as the light source for this system gives two main advantages over other light sources. The spectral linewidth for lasers is very narrow compared to other sources, from 5 nm wide to less than 0.5 nm wide depending on the type of laser. This allows narrow features of the reflectance spectra to be identified and used in discrimination. Secondly, laser output can be collimated in a narrow beam with low divergence. This allows detection of the spectral properties from small samples such as individual leaves on young plants and the narrow leaves of grasses. Additionally the spectral properties of different plants within the field of view of the sensor can be individually determined from the separate beams which are projected.

3.3.1 Laser specifications and selection of laser wavelengths

The most appropriate lasers for this project are semiconductor diode lasers. These lasers are cost effective, compact and available with output optical power ranging from approximately 1 mW up to 300 mW. Power consumption for the

low optical power range (<100 mW) of these lasers is less than 200 mW, making them suitable for portable applications. Laser diodes have good temperature stability of the wavelength and can be driven in either continuous or modulation mode by using either constant current or constant power laser drivers. There is a relatively wide range of commercially available wavelengths, particularly in red and NIR parts of the spectrum. Many laser diodes are available in rugged packaging which makes them less susceptible to mechanical vibration and impact than other types of lasers.

From Figure 3.3, the characteristic wavelengths in the visible and very near infra-red spectrum are 470, 530, 670 and 750 nm. The spectral slopes derived from these wavelengths are:

$$S_1 = \frac{R_{535} - R_{475}}{\lambda_{535} - \lambda_{475}} \quad (3.1)$$

$$S_2 = \frac{R_{670} - R_{535}}{\lambda_{670} - \lambda_{535}} \quad (3.2)$$

$$S_3 = \frac{R_{750} - R_{670}}{\lambda_{750} - \lambda_{670}} \quad (3.3)$$

Where R_λ is the reflectance value and λ_n is the wavelength in nanometers. Semiconductor laser diodes are commercially available for 670 nm and 750 nm.

There are commercially available lasers at 474 nm and 532 nm. These lasers use a complex optical process to generate the output beam. A semiconductor laser diode such as 808 nm is used to pump a neodymium-doped crystal medium which emits light at a longer wavelength. A non-linear optical crystal is then used to frequency double this light to produce the required output wavelength. The complexity of this process makes these diodes inefficient, less reliable and expensive for most commercial applications. More recently, blue laser diodes have also been developed in the wavelength range of 400-450 nm. The closest commercially available semiconductor laser diode to 532 nm has wavelength of 635 nm and maximum optical power of 30 mW.

The maximum optical power for the 670 nm laser diode is only 10 mW. At this wavelength the intensity of reflected light from green leaves is very low due to

the high absorption by chlorophyll. To improve the signal-to-noise ratio at this wavelength a laser diode with higher optical power is required. A laser diode with wavelength of 685 nm and maximum optical power of 50 mW is commercially available. Similarly for 750 nm, a suitable high power laser diode with wavelength of 785 nm is more readily available. The initial prototype used three lasers with wavelengths 635, 670 and 785 nm. In the second prototype the 670 nm laser diode was replaced by 685 nm, all of which are supplied by Blue Sky Research. These laser diodes were compact and were supplied with precision optics used to correct the aberrations of elliptical beams emitted from the laser diode. The output beam was collimated to a 4 mm diameter circular beam and had a near gaussian optical power distribution.

Laser diodes are frequently packaged with a monitoring diode (MD). This additional photodiode receives a fraction of the output light from the laser diode and produces a small current proportional to the output power. A schematic representation of the diode connections is shown in Figure 3.4.

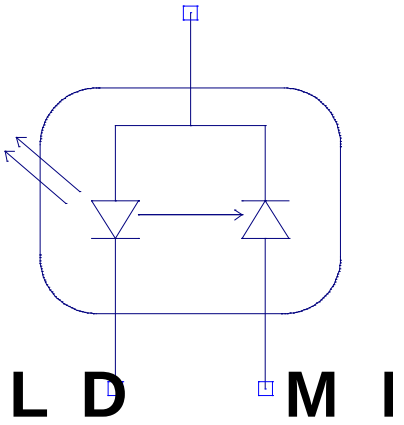

Figure 3.4. Schematic symbol for M-type laser diode (LD) with monitoring diode (MD).

3.3.2 Selection of laser drivers

To prevent damage and to operate laser diodes in continuous, modulation and pulsed mode a laser driver is required. Two types of laser driver are commonly used: constant current and constant power laser drivers. The constant current type uses a current source with a regulated current output. The constant power type uses feedback from the monitoring diode to regulate the current supplied to the laser diode. Both types of driver were used in the development of this

project based on ICs supplied by iC-Haus. The constant power driver used was iC-WJ and the constant current driver used was iC-HK. Figure 3.5 shows the block diagram and minimum circuitry required for these components.

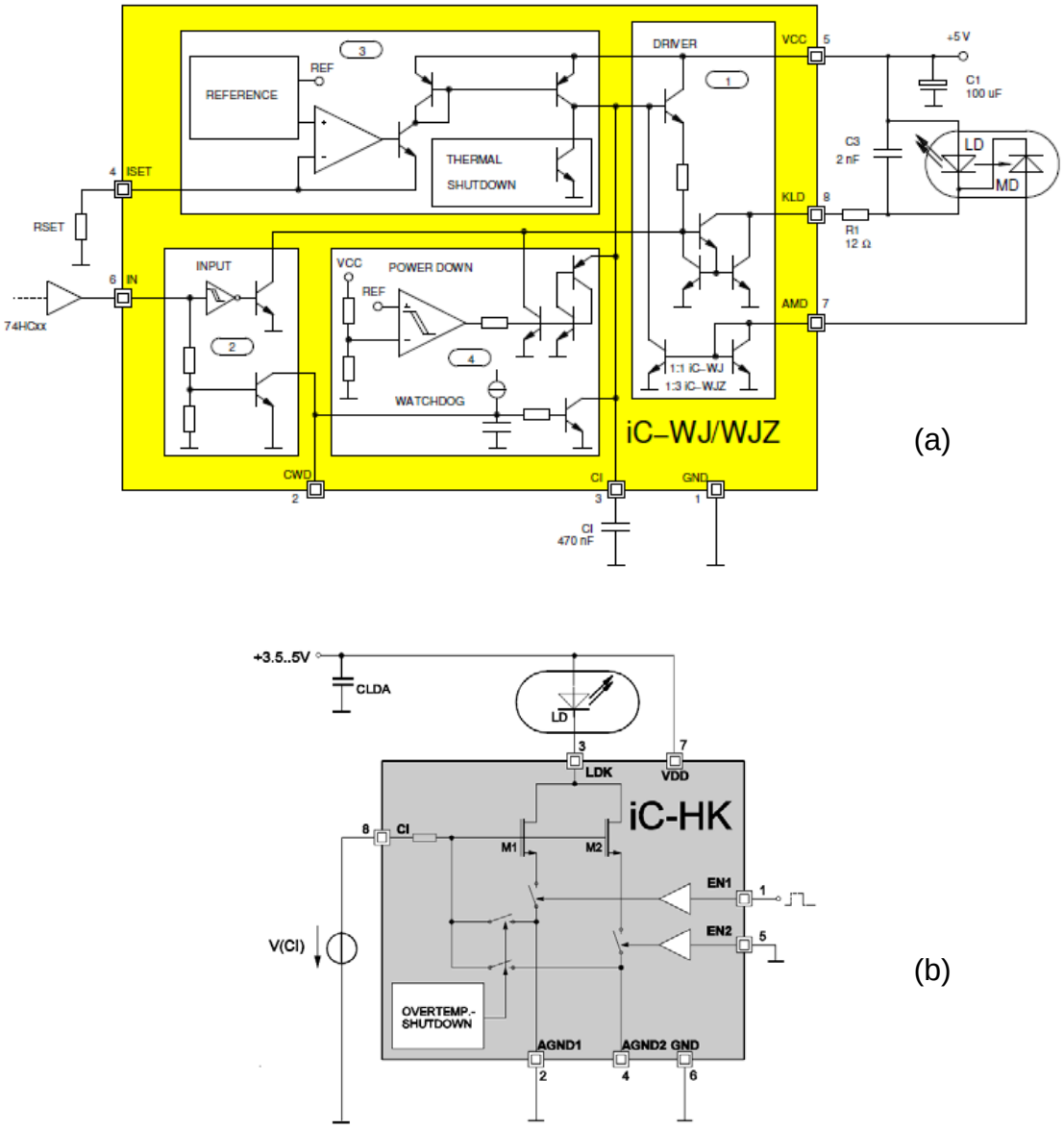

Figure 3.5. Block diagram and minimum circuitry required for (a) iC-WJ constant power driver and (b) iC-HK constant current driver (source: iC-Haus datasheets).

Figure 3.5 (a) shows the block diagram of the iC-WJ constant power driver and the minimum circuitry required to operate the laser diode. The output power is regulated by the value of R_{SET}, which determines the current passing through I_{SET}. A comparator matches the monitoring diode current by regulating the current suppled to the laser diode. This allows the driver to compensate for

changes in the efficiency of the laser diode, which is affected by temperature changes and by gradual degradation of the diode over its lifetime. The feedback from the monitoring diode allows the constant power driver to compensate for these changes in efficiency and provide a stable output power. This is simple in continuous mode but in pulsed mode or with arbitrary modulation the circuit design is more complex. The selection of component values for R_{SET} and CI in Figure 3.5 (a) depends on the average laser current and on the frequency of modulation. The operating conditions of the laser diode are then limited by R_{SET} and CI and if the switching frequency changes the laser output power would not be uniform within each pulse.

Figure 3.5 (b) shows the block diagram of the iC-HK laser driver and the minimum circuitry required to operate the laser diode. This driver uses a voltage-controlled current source to regulate the current supplied to the laser diode. A resistor divider can be used as the voltage source V_{CI} with a potentiometer to adjust the output power. Once the output power is set, the laser can be operated at any desired frequency without changing component values, solely by changing the input signal at EN1. The turn on time for the lasers using this circuit is determined by the speed of the iC-HK internal switches in series with the current source. This allows the laser to operate in a pulsed mode with frequency range from DC to over 100 MHz. The iC-HK has two channels in parallel which doubles the maximum current and also provides flexibility with multiple output power levels by independently switching one or both channels.

The disadvantage of constant current laser drivers is the lack of optical feedback. This causes the output power to change with changes in the efficiency of the laser diode which, as mentioned, can happen for a variety of reasons. For the iC-HK driver care also needs to be taken with oscillation of the laser current due to the fast switching. This can cause overshooting of the laser power which can cause failure of the laser diode if it is operated near its maximum output power.

Independent laser drivers were designed and built using a printed circuit board (PCB) that accommodated three drivers and included a connector for three laser diodes. The circuit diagrams for power and current drivers are shown in

Figure 3.6 and Figure 3.7, respectively. Both types of driver were used to control the laser diodes at various stages of the development of the weed sensor prototype. The description of the two types of laser drivers above shows clear benefits for each type of driver, however the operation of the weed sensor requires lasers be operated in pulse mode at variable frequency from 100 Hz to 1 kHz. In this mode of operation it is difficult to select component values for the constant power driver, which provide the required flexibility. The constant current driver was therefore the most suitable for our prototype development.

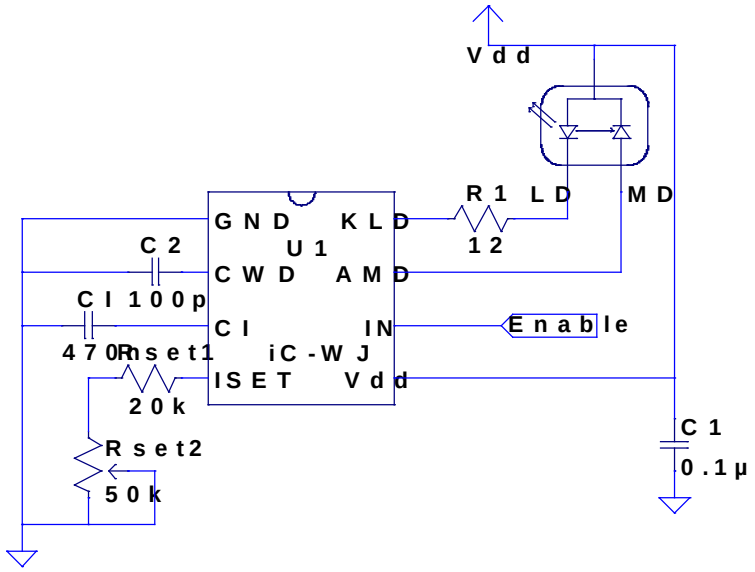

Figure 3.6. Schematic circuit diagram for iC-WJ constant power laser driver.

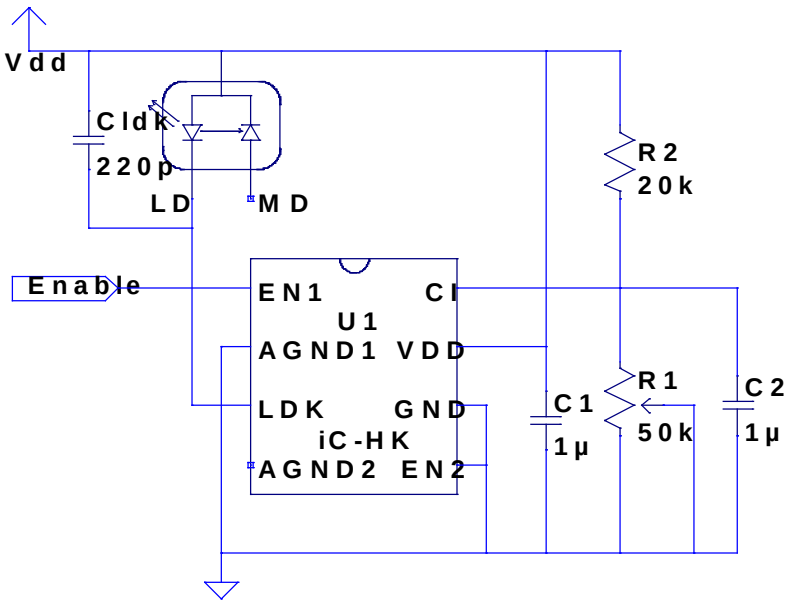

Figure 3.7. Schematic circuit diagram for iC-HK constant current laser driver.

3.3.3 Performance of constant current laser driver

Given the choice of constant current laser drivers the optical power stability becomes an issue. The operation of the weed sensor depends on reliable measurement of the reflected light intensity from a leaf at each wavelength used. This depends directly on the output power of the laser and any variation in the output power will result in a change in the spectral properties determined from the measurement of reflected light. The operation of the lasers using constant current laser drivers was evaluated independently to determine the turn on behaviour and the optical power stability.

Figure 3.8 shows the turn-on response of the lasers when pulsed with a frequency of 5 kHz supplied from a function generator. This is the highest frequency that would be required during normal operation of the weed sensor. A fast optical receiver connected to an oscilloscope recorded the response of the laser diodes over a period of 2 µs and triggered to begin recording 0.3 µs before the beginning of each pulse from the function generator. The oscilloscope was connected to a computer which controlled the collection and storage of data using LabVIEW software. Significant oscillation within the first microsecond is evident for the 785 nm laser. During the operation of the weed sensor a line scan is captured after each laser is turned on. The line scan acquisition typically takes from 50-200 µs and can begin within 1 µs of the laser turn on signal when the lasers are controlled by the constant current drivers.

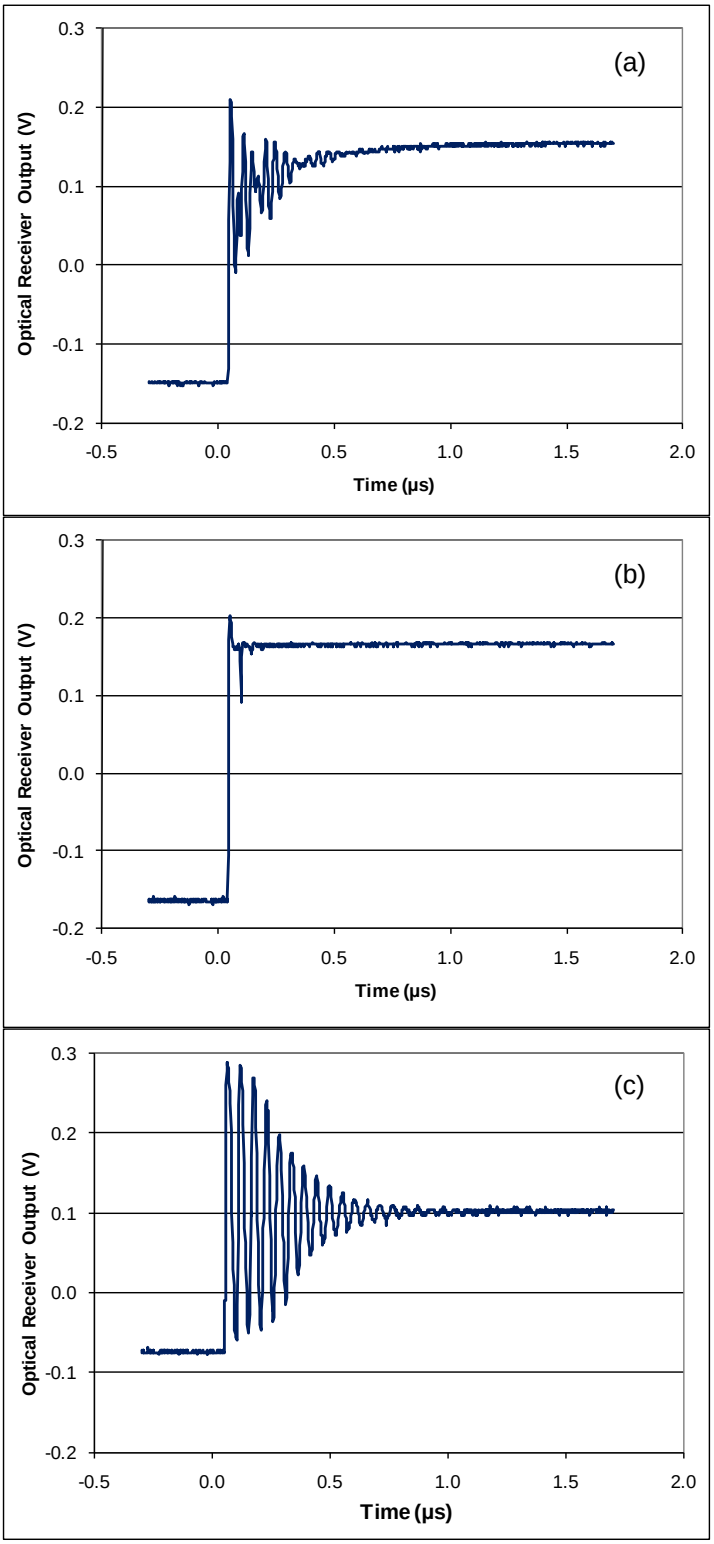

Figure 3.8. Turn on response of lasers using constant current drivers with driving frequency of 5 kHz and duty cycle of 50 %. Laser wavelength is (a) 635 nm, (b) 670 nm and (c) 785 nm.

The optical power stability of the lasers was evaluated by recording the optical power over a period of 10s. During this time the laser was turned on and left on until the end of the measurement. Each wavelength was recorded separately.

The lasers were installed in the weed sensor and the optical power of the first beam measured with a Newport power meter. The recorded output power when using constant power drivers shows the expected constant power with variation less than 1%. The stability of the output power when using constant current laser drivers varies depending on the laser wavelength. The reduction in output power was measured by monitoring the difference between the maximum output power and the power at the end of the 10 s measurement interval. Table 3.1 presents these results for both types of driver.

Table 3.1. Optical power for beam 1 over a period of 10s when using constant current drivers on independent driver PCB.

	Constant current laser driver			Constant power laser driver		
	635 nm	670 nm	785 nm	635 nm	670 nm	785 nm
Max Power (μW)	832	685	415	594	582	384
Final Power (μW)	711	664	380	591	581	383
Decay (%)	15	3	8	0.5	0.2	0.3

The optical power of the lasers using constant current drivers was not stable after the initial turn on of the laser. There was a reduction of up to 15% of the laser power which was most likely due to the effect of localised heating in the laser driver and the laser diode. An increase in temperature of the laser diode junction reduces the efficiency and therefore the output power of the laser. The independent driver PCB with constant current laser drivers used in this experiment did not have a thermal contact pad for the driver ICs. For the second prototype of the weed sensor a single PCB was designed to control the lasers, image sensor and data processing. This PCB included a thermal pad, which gave some improvement in the optical power decay. Figure 3.9 shows the total optical power of the 635 nm laser. The laser was pulsed at 125 Hz with a duty cycle of 25 % and the optical power recorded with the Newport power meter, using its statistics function to capture the data. This showed a decay of 5 % in optical power during the first three pulses and stable average optical power for the next 0.5 s. After one minute the optical power remained within 1 % of this stable output power. It is apparent that the optical power of the laser was not stable during the pulse. This effect was probably due to the thermal effects in the laser diode itself. The average power during each pulse was very stable and this was the important factor in determining reliable measurement by the weed sensor of the reflected intensity for each wavelength.

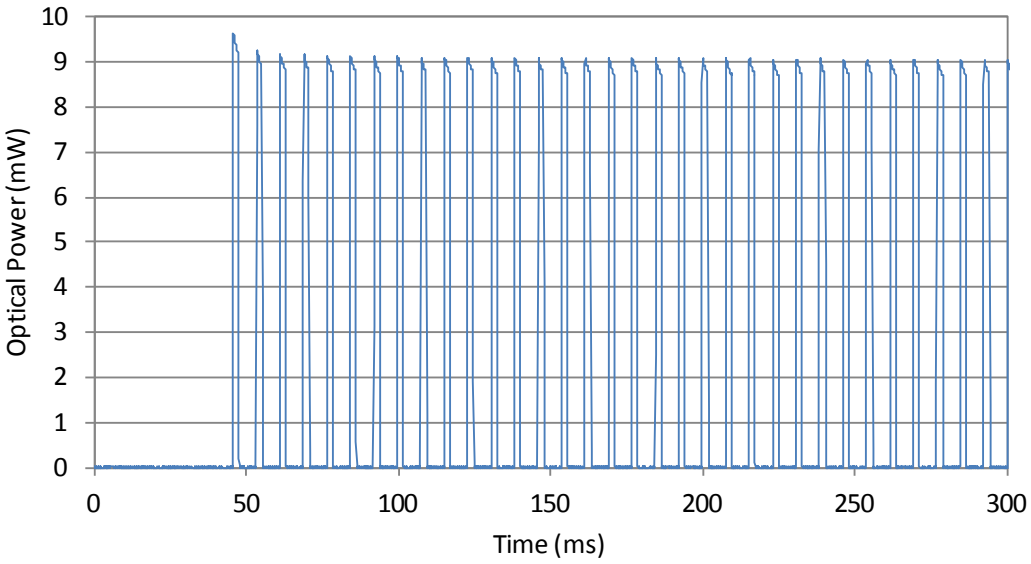

Figure 3.9. Optical power of 635 nm laser when using constant current drivers and pulse frequency of 125 Hz.

3.3.4 Improvement of constant current laser driver

Several modifications were made to the constant current laser driver circuit to improve the performance as characterized in the previous section. The second channel in the constant current driver was enabled permanently to provide a below threshold current to the laser diode while it is switched off. This modification reduced the change in current when the laser was switched on or off and also warmed up the driver and laser diode while they were switched off. The second modification was insertion of an inductor in the switching channel to lengthen the turn on time of the laser diode. This change was intended to suppress the oscillation in output power after laser turn on. The circuit diagram of the modified laser driver is shown in Figure 3.10.

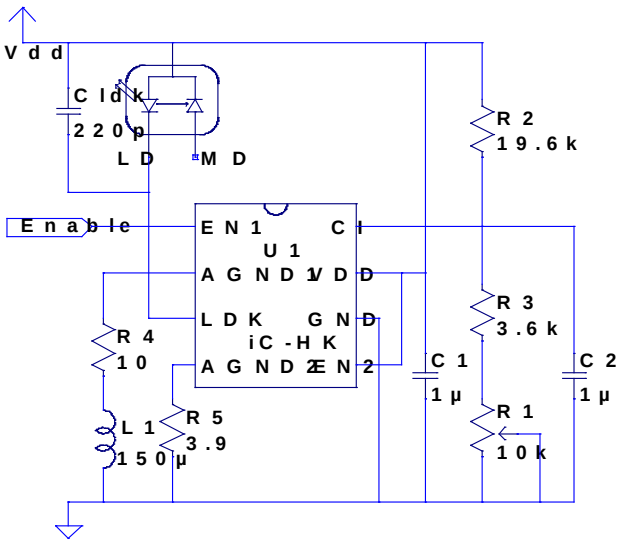

Figure 3.10. Schematic diagram of 2-channel constant current laser driver with additional inductance to lengthen turn on time.

The inductor L1 and resistance R4 in Figure 3.10 give a time constant of:

$$\tau = \frac{L}{R} = \frac{150\mu H}{10\Omega} = 15\mu s \tag{3.4}$$

Figure 3.12 shows the turn on response of the 785 nm laser when using this modified laser driver as measured by a fast optical receiver connected to a digital oscilloscope. The laser enable signal occurs at 0 µs and the laser reaches threshold around 5 µs later. After 35 µs the output power has reached its maximum value. The inductance used is certainly sufficient to remove the oscillation shown previously however it could be lowered to reduce the turn on time. The output power stability with this driver is also improved. Figure 3.11 shows the total optical power of the 635 nm laser after the first pulse and Table 3.2 shows the initial and final optical power for one beam from the weed sensor recorded over an 18 hour period while the lasers were continuously operating with a switching frequency of 120 Hz.

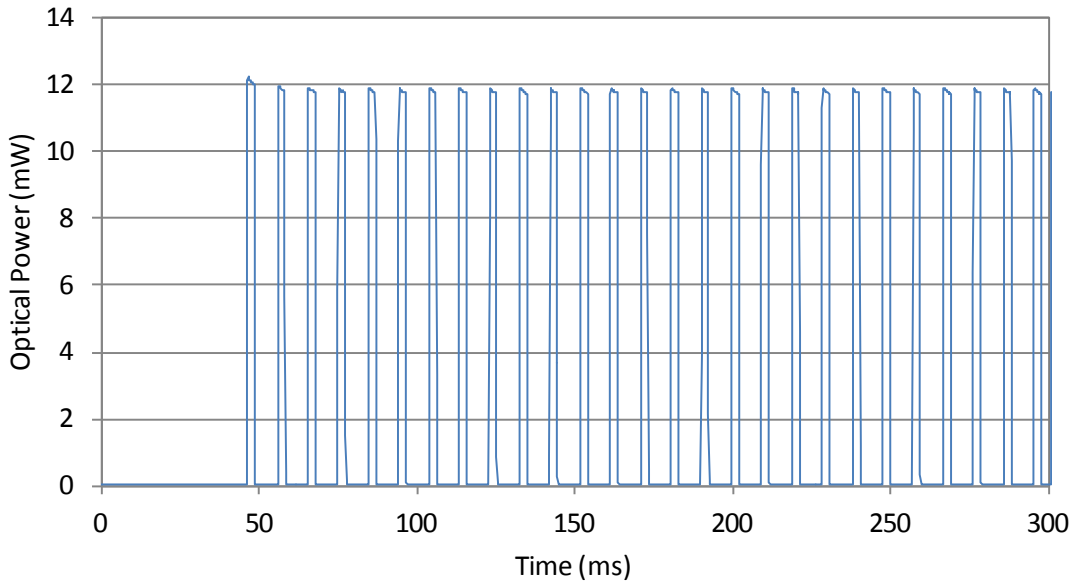

Figure 3.11. Optical power of 635 nm laser when using constant current drivers with additional inductance and pulse frequency of 120 Hz.

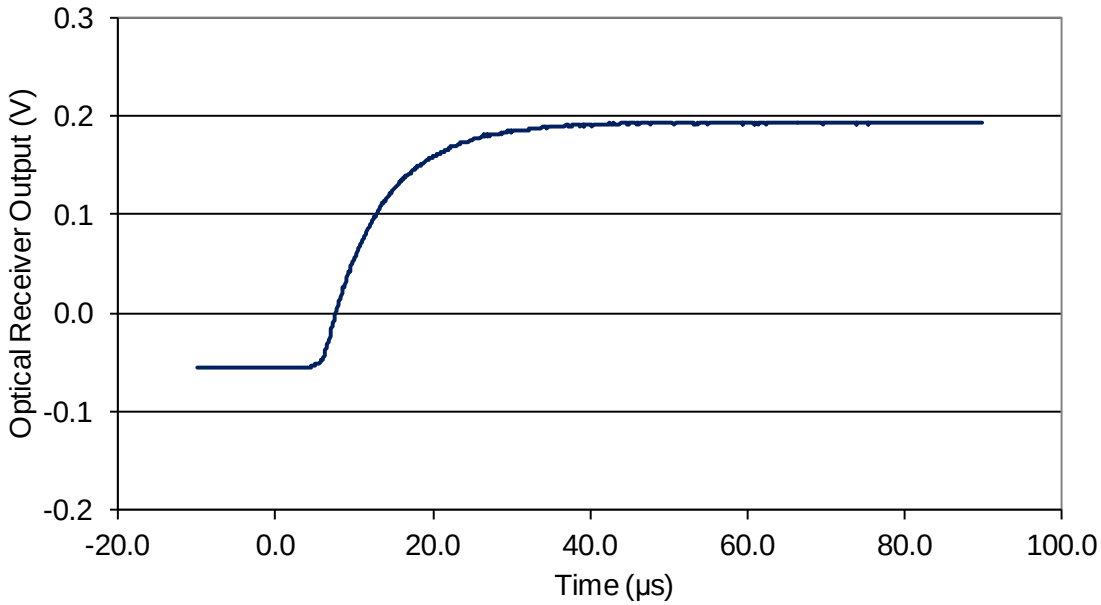

Figure 3.12. Turn on response of 785 nm lasers using constant current drivers with additional inductance to lengthen turn on time. The laser enable signal starts when time = 0 µs

Table 3.2. Optical power for beam 1 of two lasers over a period of 18 hours when using 2-channel constant current drivers.

	635 nm	785 nm
Initial Power (μW)	214	383
Final Power (μW)	220	366
Change (%)	3	5

The 2-channel constant current driver shows significant improvement in the laser optical power stability when compared with the original constant current driver. While the turn-on time is longer than necessary, this additional stabilisation time can occur during data transfer of the previous scan and has negligible impact on the speed of the weed sensor.

3.4 Thin film coatings

The illumination of multiple targets with light from multiple lasers as described in Section 2.6 required a beam combiner and a multi-spot beam generator. These optical components required specific reflectance and transmittance properties at the wavelengths of the lasers used for illumination. For each beam combiner a high reflectance at one wavelength and high transmittance at other wavelengths was required to minimise the loss of optical power. For the optical cavity a specified uniform transmittance was required over the range of laser wavelengths used so that the total optical power of the laser was distributed over all beams generated by the cavity. Thin film optical filters are well suited for this purpose because they can be designed to meet specific requirements on reflectance and transmittance over a wide range of wavelengths.

3.4.1 Thin film interference filters

Thin film optical filters made from layers of dielectric materials or metals have been in development and use since the 1930's. They are composed of a stack of layers of materials with different refractive indices and thicknesses less than the wavelength of light. There are many different structures of thin films made up of stacks of alternating layers of different materials. The interaction of light at the boundary of each layer results in partial reflection and transmission of the

light at each boundary. Multiple reflected and transmitted beams recombine at the top and bottom surfaces of the thin film and this recombination can be either constructive (additive) or destructive (subtractive) depending on the phase difference between the separate components [71]. The multiple reflected and transmitted components from a single layer thin film are shown in Figure 3.13.

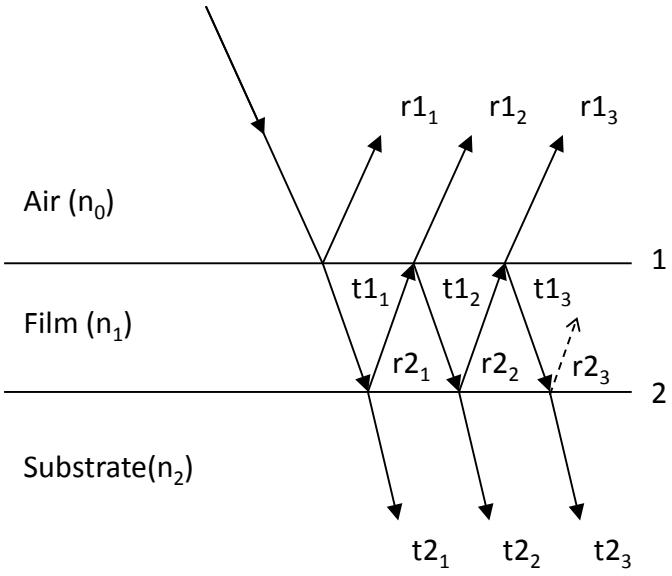

Figure 3.13. Multiple reflected and transmitted beams from the interfaces between air, a single layer thin film and substrate.

The reflectance and transmittance properties of thin film optical filters can be determined from the summation of the interference effects between the multiple beams transmitted through each interface. This depends on the angle of incidence and the refractive index and thickness of each layer which make up the thin film. Through selection of materials with different refractive indices and careful design of the layer structure and the thickness of each layer, it is possible to tailor the optical properties of the film for many different applications. Some of the applications of thin film optical filters include: antireflection coatings on lenses or substrates, high reflectance coatings on mirrors, band-pass filters, dichroic filters and band-stop filters. Each type of filter is characterised by the range of wavelengths for which they are transmissive and reflective [71].

3.4.2 Beam combiners for laser module

The arrangement of lasers and photodiodes used by Weed Control Australia, Pty Ltd, in their original weed sensor prototype required the target to be at a

specific distance from the sensor for a consistent measurement of the reflected light intensity. To overcome this problem the lasers need to be aligned up to the maximum distance from the sensor to the ground. This could be achieved by combining the output beams with two beam splitters oriented at 45°. One beam splitter (F1) combines the beams from the two visible lasers (LD1 and LD2) and the second beam splitter (F2) adds the beam from the IR laser (LD3) as shown in Figure 3.14. The beam combiner directs the beams from each laser into a single path making them collinear (or on the same line).

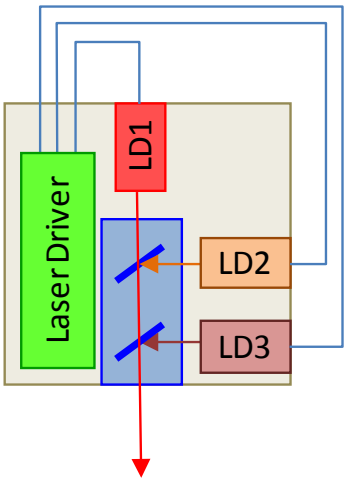

Figure 3.14. Schematic of laser module showing an independent laser driver PCB, three laser diodes and two thin film beam combiners.

The laser diodes are each held in place by a block of aluminium with a cylindrical hole slightly larger in diameter than the case of the laser diode. An adhesive is used to fix the laser diode in place. This aluminium block and the base of the beam combiner module also serve as a heat sink for the laser diodes. The output beams of the three lasers are aligned by careful adjustment of the position of the beam splitters, which are fixed in place with an epoxy adhesive.

To maximise the available power the beam splitters were coated with multi-layer thin film interference filters. Each thin film was designed to be highly transmissive below a cut-off wavelength and highly reflective above this cut-off wavelength. For F1 the cut-off wavelength was around 650 nm and for F2 the cut-off wavelength was near 730 nm. The range of reflectance and transmittance measured for four different beam splitters is shown in Table 3.3. Only the values which are desired to be high reflectance and high transmittance

are shown. A large variation is seen in the measured values, which is due to variation in the thin film manufacturing process and also a strong angular dependence, particularly for the 685nm reflectance from F1. During the alignment process it was possible to improve the loss from the beam combiner by careful adjustment of the angle of the 685nm laser and F1.

Table 3.3. Range of reflectance and transmittance of four different beam splitters used in the beam combiner.

	635nm	685nm	785nm
F1 R(%)		72-93%	
F1 T(%)	92-97%		
F2 R(%)			90-99%
F2 T(%)	91-97%	94-98%	

3.4.3 Optical cavity for multi-spot beam generation

The outgoing beams from each laser module were divided into 15 beams using a multi-spot beam generator. The multi-spot beam generator used in the weed sensor was a 200 mm long optical cavity with thin film coatings on the front and rear surfaces. The coatings of the rear and front surfaces had reflectivities of 99.5% and 92% respectively (both coatings were uniform for all wavelengths). An uncoated entrance window on the rear surface was used, through which the combined laser beam entered at an angle of 18º. This angle determined the spacing between the beams. The optical power for each beam was 8% of the internal beam power. The resulting array of 15 beams had a spacing of 15 mm. Using two laser modules and two multi-spot beam generators on either side of a central image sensor allows small plants to be illuminated by several beam whilst only requiring two sets of lasers to cover a 500 mm span. Note that the beam spacing is small enough to ensure all but the smallest plants are illuminated by at least one of the outgoing beams.

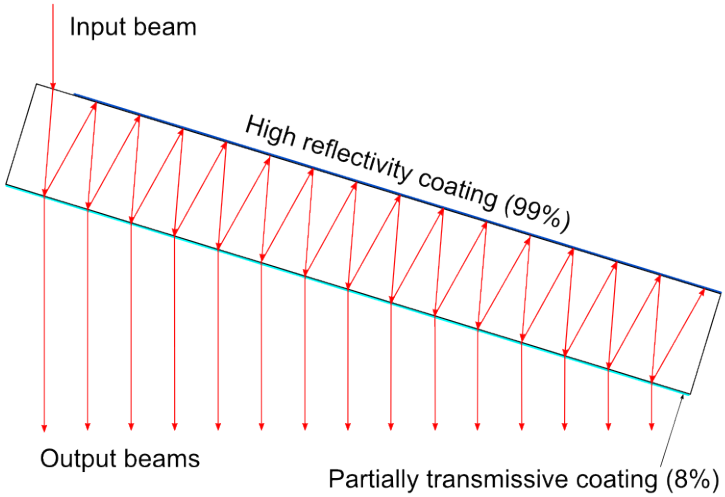

Figure 3.15. Generation of multiple beams through reflection in an optical cavity with uniform thin film coatings.

Figure 3.15 shows the optical path of the laser beam through the optical cavity. The alignment of the three laser wavelengths was maintained for all fifteen beams. This was important to ensure that the same spot on a leaf was illuminated by each wavelength laser. Figure 3.16 shows the optical power for each beam measured with a Newport 1918C optical power meter. The total power for the 785 nm lasers was relatively low to prevent saturation of the image sensor when measuring the response from a leaf which has high reflectivity for infrared wavelengths but low reflectivity for red wavelengths. The effect of the uniform cavity was a reduction in the optical power in each successive beam as the total optical power within the cavity was reduced.

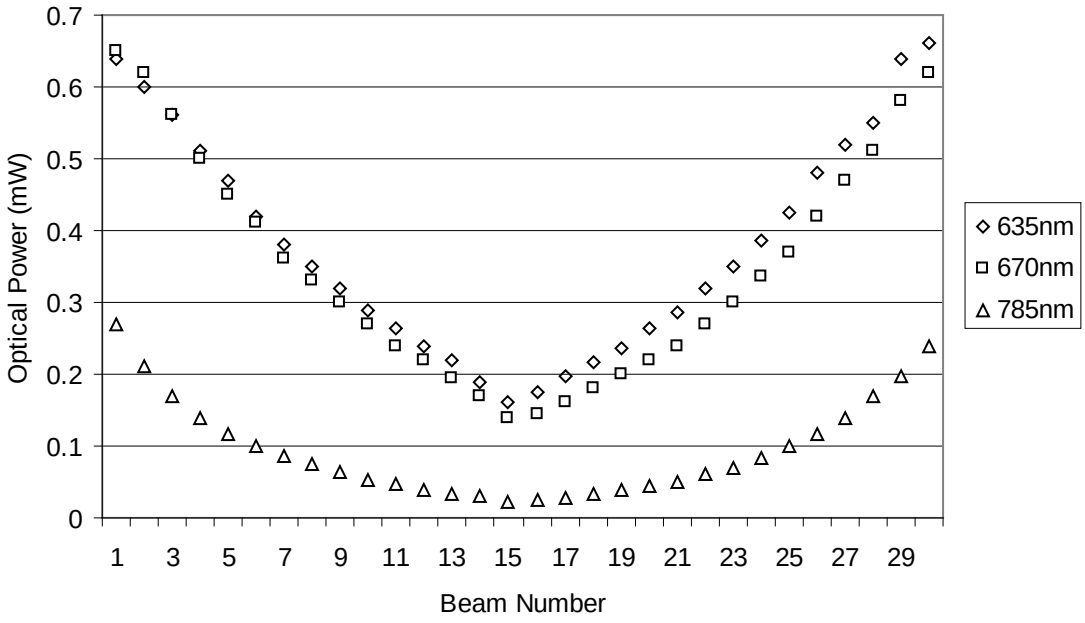

Figure 3.16. Beam optical power (BOP) for all 30 beams from prototype weed sensor at three wavelengths using optical cavities with uniform coatings. The optical power for 635 nm and 670 nm is 9 mW and the optical power for 785 nm is 3.5 mW.

In order to equalise the intensities for all beams, non-uniform coatings were needed at the front surface, as illustrated in Figure 3.17. Table 3.4 shows the transmission coefficients of the front surface required to generate 15 optical beams of equal intensities. Figure 3.18 shows the beam optical power for 30 beams generated by two optical cavities with different thin-film coatings for each beam. The input optical power was 10 mW for all lasers.

Table 3.4. Desired transmission coefficients (T) for multi-spot beam generator with uniform output power for 15 beams.

Beam No.	1	2	3	4	5	6	7	8	9	10	11	12	13	14	15
T (%)	5.8	6.2	6.6	7.1	7.7	8.4	9.2	10	11	13	15	18	21	28	38

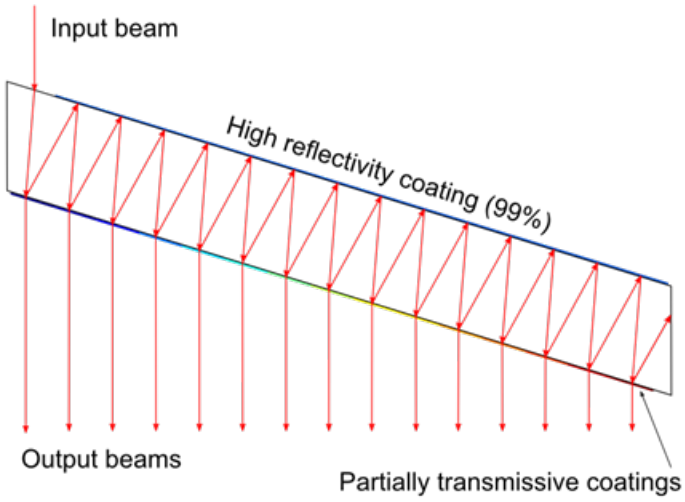

Figure 3.17. Generation of multiple beams through reflection in an optical cavity with individual thin film coatings for each output beam.

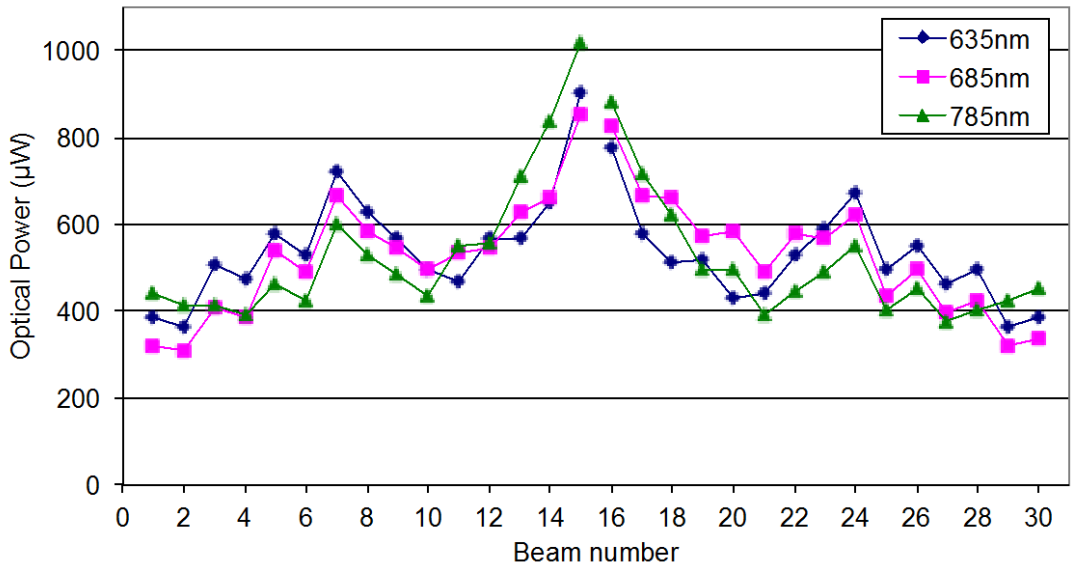

Figure 3.18. Beam optical power for 30 beams from weed sensor using two multi-spot beam generators with individual thin-film coatings for each beam. Input optical power is 10 mW for all lasers.

3.4.4 Solar filter

The image sensor used in the experiments measured the intensity of reflected light from each beam at the wavelength of each laser. These measurements were affected by the broad spectrum ambient light due to solar radiation. The spectrum of solar irradiation is shown in Figure 3.19, which shows the peak in the middle of the visible spectrum. The reflected intensity value recorded for

each beam is determined by the sum of the response of the image sensor to the ambient light reflected by the target plus the response to the reflected laser beam. The line scan sensor response to ambient plus laser light reflected from a green card reference is shown in Figure 4.7 (a). Under shaded conditions the signal due to ambient light is approximately equal to the signal from each beam, and under full sun, the ambient light signal is 5-10 times larger than the signal from each beam. In order to reduce the impact of ambient light on the measurement of reflected laser light, it is desirable to block out as much of the ambient light as possible.

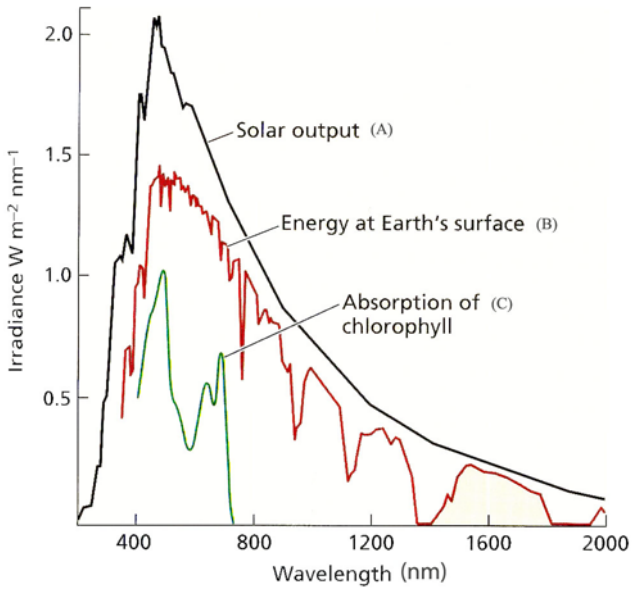

Figure 3.19. The solar irradiation spectrum above the atmosphere (A) and at sea-level (B). Spectrum C is the absorption spectrum of chlorophyll *a*, which absorbs strongly in the blue (about 430 nm) and the red (about 680 nm) regions of the spectrum (from Mauseth, 2003).

Other laser-based remote sensing applications use a narrow band pass optical filter to block more than 95% of the ambient light due to solar radiation. These filters have pass-bands at centre wavelengths close to the laser wavelengths used in the device and their pass-bands exhibit narrow bandwidths. They are typically made using an interference filter design because this design allows careful selection of the centre wavelength and the bandwidth in order to optimise the performance of the sensor. With a single pass band it is possible to have a transmittance above 95% at the centre wavelength. The design of the weed sensor requires high transmission for the three laser wavelengths and

suppression of unused part of the solar spectrum. Interference filters with multiple narrow bands are much harder to realize, and as the bandwidth of the pass bands is reduced, the transmittance at the centre wavelengths is also reduced. A feasible design for this application is a two-band-pass filter with pass-bands for the red and near infra-red regions of the spectrum. A filter with pass bands specified at 648±43 nm and 783±29 nm and transmittance above 95% in both bands was designed and manufactured by China Daheng Corporation. The transmission spectrum for this filter measured with a spectrophotometer is shown in Figure 3.20. Comparison with the spectrum of ambient light due to solar irradiation in Figure 3.19 indicates that a large fraction of the ambient light will be blocked by this filter.

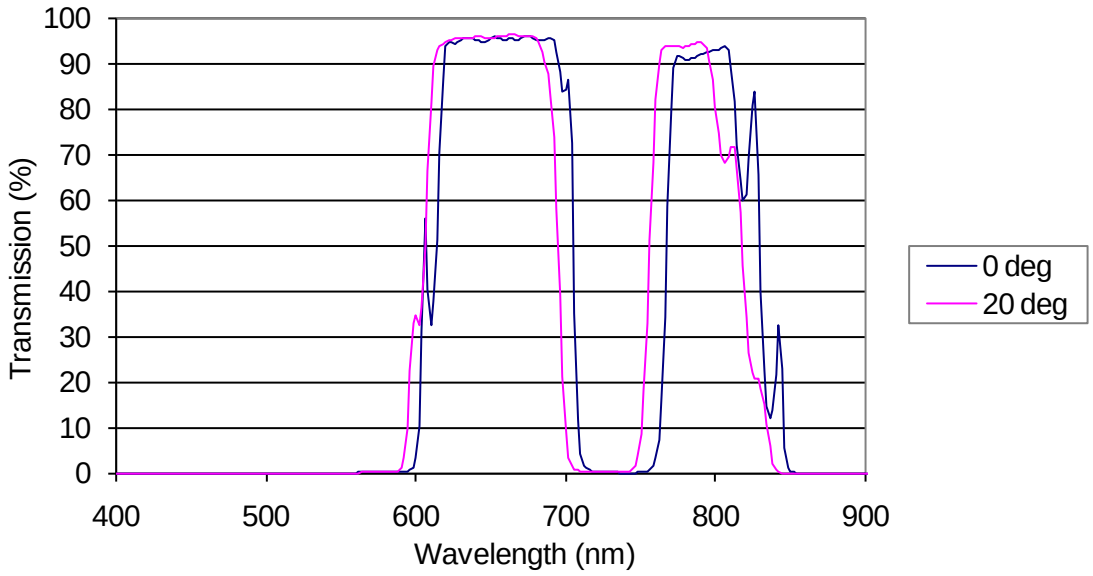

Figure 3.20. Transmission spectrum for solar filter measured at normal incidence (0°) and 20° incidence using a spectrophotometer.

The application of thin film filters presented in this section allows the generation of many output beams using only a small number of laser diodes and provides a significant reduction in the level of background light when the sensor is used in outdoor conditions.

3.5 Selection of image sensor

The image sensor shown in Figure 2.5 is used to measure the intensity of reflected light from each beam generated by the two multi-spot beam

generation cavities positioned on either side of the sensor. In order to give consistent results for objects with the same reflectivity, the sensor used for this purpose must exhibit high sensitivity, high frame rate and low noise. The intensity of each spot detected by the camera is dependent upon the optical power of each beam in the array, the spectral reflectance of the object and the geometry of the measurement setup. During the development of the weed sensor, three different line scan image sensors were trialled. The sensor used in the initial prototype, as described by Sahba [10], was a Spyder3 SG-10-01K40 line scan camera manufactured by Teledyne DALSA and designed for industrial machine vision applications. In the improved prototype described in Section 4.3 this camera was replaced with a custom built camera using a TSL3301 digital line scan sensor from TAOS Inc. The final prototype used an s9227-03 analogue line scan sensor made by Hamamatsu.

3.5.1 Image sensor performance criteria

Four main factors are considered in evaluation of the sensor, namely, i) the stability of the pixel response; ii) the sensitivity of the sensor; iii) the frame rate or line rate of the sensor; and iv) the cost of alternative devices. The geometry of the weed sensor was well suited to using a line scan sensor provided that the image of all 30 beams was carefully aligned with the optical axis of the lens and the single line of pixels on the sensor. The use of an area sensor was also investigated. The main advantage of using an area sensor is in alignment of the 30 output beams with the sensor; however, the frame rate of area sensors is much less than the line rate of line scan sensors.

The first factor considered for any potential sensor used was the speed of the sensor. The optical weed sensor was designed to travel along the ground at a speed of up to 15 km/h (≈ 4.2 m/s). As the array of laser beams was scanned across the ground, the response from the object was recorded sequentially for the two lasers of each wavelength. During a single measurement, four line scans were recorded by the image sensor: one for each wavelength laser and one for the background with all lasers turned off. The period of this measurement cycle had to be less than the time required to travel a distance of approximately 4 mm, equal to the diameter of the collimated beams from the laser module. This ensured that the reflected signal for each wavelength was

received from approximately the same spot on the leaf. The maximum speed meeting this requirement can be calculated from the sensor's operating parameters using the following equations:

$$\tau_{scan} = 4 \times \left(\tau_{exp} + \tau_{read}\right) + \tau_{proc} \tag{3.5}$$

$$v = s/\tau_{scan} \tag{3.6}$$

where τ_{scan} is the period of a complete scan, τ_{exp} is the exposure time, τ_{read} is the read-out time, τ_{proc} is the time required for data processing, s is the distance travelled, and v is the speed of travel. Equation 3.6 gives a limit on the period of a complete scan of:

$$\tau_{scan} = \frac{s}{v} = \frac{4\text{mm}}{4.17\text{m/s}} = 0.96\ \text{ms} \tag{3.7}$$

which, according to Equation 3.5, requires a line rate for the sensor of:

$$f = \frac{1}{\left(\tau_{exp}+\tau_{read}\right)} \approx \frac{4}{\tau_{scan}} = 4.2\ \text{kHz} \tag{3.8}$$

Equation 3.8 neglects τ_{proc} since data processing from one scan could be carried out during the image acquisition period of the following scan.

3.5.2 Spyder3 camera

The Spyder3 SG-10-01K40 line scan camera used is an off-the-shelf camera which used a CCD sensor with a dual line of 1024 pixels having 12-bit resolution. The line height was 14 µm and the pixel pitch was also 14 µm. The maximum frame rate of the camera was 36 kHz, but practically, this was limited by the exposure time (40 µs) and read-out time required. A C-mount lens was fitted to the camera, which had a focal length of 12.5 mm and adjustable aperture set to f/4. Figure 3.21 shows the spectral responsivity of the CCD sensor, which indicates a relative responsivity in excess of 85% for the wavelength range 620-800 nm. The high line rate of this camera was the reason it was chosen for the first prototype as it was suitable for operation at the speed required when used with farming equipment. However, the camera was too

expensive for use in a commercial weed sensor and was primarily chosen to show a proof of concept.

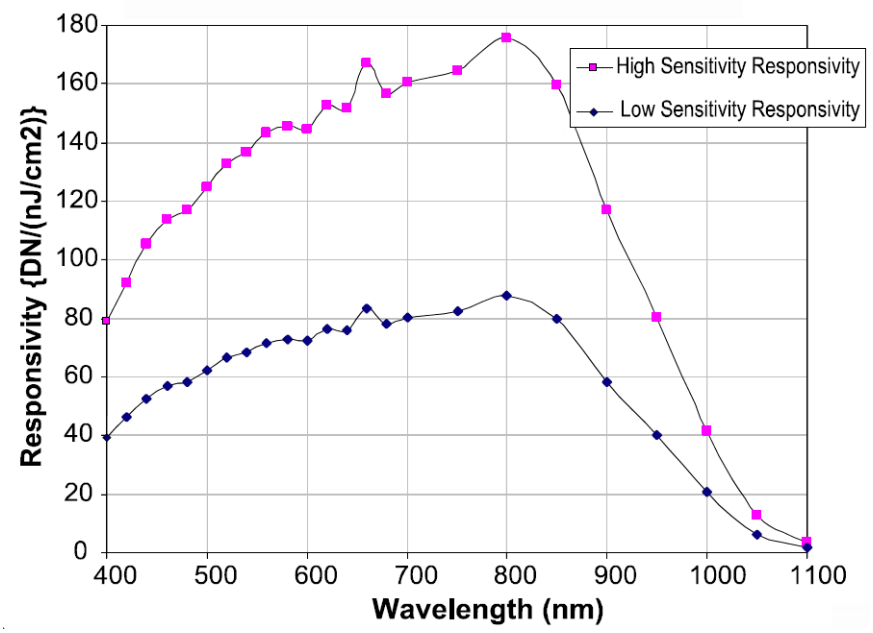

Figure 3.21. Spectral responsivity of Spyder3 line scan sensor (source: datasheet).

3.5.3 TAOS TSL3301 sensor

The TAOS TSL3301-LF is a linear optical sensor array with 102 pixels in an 8 pin dual-in-line (DIP) packaged IC. Each pixel is 85 µm high by 77 µm wide with a pixel pitch of 85 µm covering a total light sensitive area of 0.085 x 8.7 mm. The IC includes an analogue to digital converter with 8-bit resolution and uses a serial interface for control and pixel value readout. The maximum line rate is 10 kHz but with an integration time of 200 µs and readout time of 100 µs the line rate is reduced to 3.3 kHz. This is below the 4.2 kHz in Equation 3.8 but was still sufficient for a speed above 10 km/h.

The pixel response linearity of the TSL3301-LF sensor was characterised by using the line scan sensor in the setup shown in Figure 2.5 with the output beams incident on a reference card at a distance of 650 mm. The response of the image sensor was measured with all 3 wavelength lasers using beams 1 and 13 in order to test linearity across a large power range and test for wavelength dependence of the sensor linearity. The cavity used was the single coating type shown in Figure 3.15 which gave a much lower output power for

beam 13 then beam 1 (where beam number is counted from first beam closest to entry window of the optical cavity). The output power of beam 1 was adjusted to 600 µW using constant power drivers and decreased in increments of 100 µW down to 100 µW.

The image sensor response to beam 1 and 13 incident on the green card was recorded at each power setting and a peak value calculated using the method described in Section 4.3.2. Figure 3.22 shows a plot of the calculated peak value against optical power for each wavelength. The correlation coefficient seen in Figure 3.22 for all of these lines is greater than 0.99, indicating a strong linear pixel response of the TSL3301 line scan sensor.

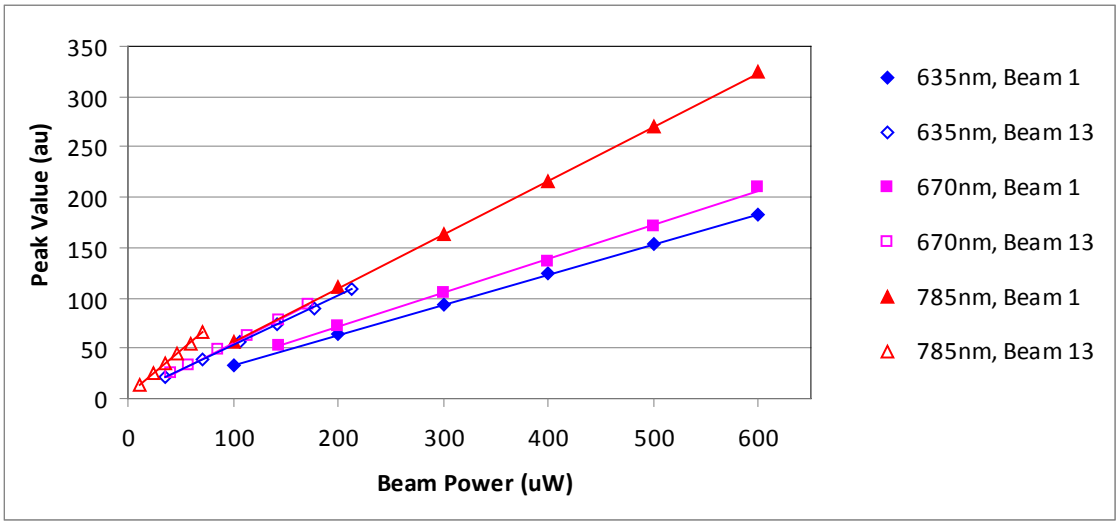

Figure 3.22. Linearity of TSL3301 response to beam optical power measured with two beams of weed sensor by adjusting laser output power.

Figure 3.23 (A) shows the relative spectral responsivity of the TSL3301 sensor, which exhibits high sensitivity in the region of 600-800 nm, as for the Spyder3 camera. A camera housing with C-mount lens attachment was designed to hold the TSL3301 line scan sensor for the second prototype of the weed sensor. The low cost of the TSL3301 line scan sensor combined with high speed made it a good replacement for the Spyder3 camera in the improved prototype optical weed sensor.

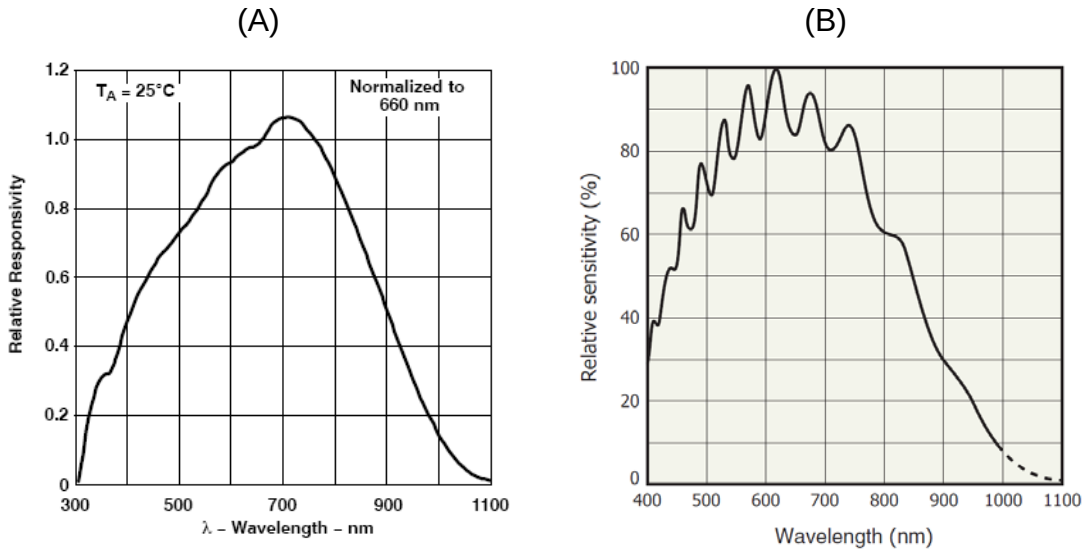

Figure 3.23. Spectral responsivity of (A) TAOS TSL3301-LF line scan sensor (source: datasheet) and (B) Hamamatsu S9227-03 line scan sensor (source: datasheet).

3.5.4 Hamamatsu S9227-03 sensor

The S9227-03 sensor is a small CMOS linear image sensor with a single line of 512 photodiodes and accompanying charge amplifiers. Each pixel is 250 µm high by 10 µm wide with a pitch of 12.5 µm and total active area of 6.4 x 0.25 mm. The pixel readout rate is up to 5 MHz with a voltage range of 4.3 V and dynamic range of 72 dB. The relative spectral responsivity of the sensor (without glass cover plate) is shown in Figure 3.23 (B). The sensitivity of this sensor is lower than the TSL3301 and therefore the exposure time required was longer. Depending on the output beam power the exposure time used was between 1-2 ms. The captured line scan was digitized by an analogue to digital converter (ADC) peripheral on the dsPIC microcontroller used in the control system. This ADC was operated at 512 kHz and 10-bit resolution giving a read-out time of 1 ms and overall line rate of between 200-300 Hz.

3.6 Opto-mechanical design requirements

The optical weed sensor reported by Sahba *et al*. is an implementation of the proposed design described in Section 3.3 [10]. The sensor illuminated plants using lasers of three different wavelengths and the intensity of reflected light at

each wavelength was measured using a line scan camera. The reliability of this measurement depended on precise alignment of the lasers and other optical components. This weed sensor prototype enabled some adjustment of the optical components but did not provide the necessary control process for precise optical alignment. This section describes the alignment requirements of the weed sensor and design considerations of the improved prototype.

3.6.1 Alignment requirements

The mechanical design of the prototype was reviewed and redesigned to improve the alignment capability of the prototype. At the same time the optical components were reviewed to improve the effectiveness of the weed sensor in an outdoor environment where the level of background light is significantly higher than under laboratory conditions.

The use of a centrally positioned linear sensor allows the detection of the reflected light signal for each beam over a large range of distance from the sensor. This requires all the laser beams to be carefully aligned with the optical axis of the lens and the active area of the image sensor. The three lasers in each laser module were mounted in an aluminium block which was fixed in place and had a hole bored for each laser. The output beams of the three lasers were aligned by careful positioning of the thin film beam combiners, which were then fixed in place with epoxy glue. Each laser module and corresponding multi-spot beam generation cavity was mounted on a stage made from an aluminium plate with two tilt adjustments. These allowed adjustment of the angle of the outgoing beam array. The camera was mounted on a separate stage which also had a tilt adjustment that allowed adjustment of the pitch. The two beam arrays could be made coplanar via this angle adjustment and then aligned with the camera.

Note that the beams from the lasers directed at the target must be precisely adjusted in order to sufficiently illuminate the image sensor’s active area. Precise alignment was also required to ensure the fraction of power in each reflected beam received by the image sensor is the same for each wavelength. The beam size of the lasers used was 4 mm. To ensure that a consistent fraction of power from each laser was received by the sensor the beam centre

for each laser was required to be within 1 mm or less. The alignment of the lasers to the image sensor was required over a working range of up to 1 m, therefore, including the distance travelled through the cavity for Beam 15, the maximum total beam path over which laser alignment was necessary was 2 m.

The polarisation angle of the three lasers in each laser module also required alignment. There are two reasons the polarisation angle was important. First, the beam splitters used to combine the three laser beams and the transmissive coating on the optical cavity were sensitive to the polarisation angle which affected the beam power; and second, the reflectance of leaf surfaces depends on the polarisation angle of the incident light. The thin film filter used on the beam combiner was designed for one polarisation. The efficiency of the desired reflection or transmission was reduced for the opposite polarisation, in some cases reduced from 90% down to 40%. This is particularly important for filters used to split or combine light of two wavelengths within 50 nm. The original design of the prototype required the polarisation of the three lasers to be aligned to avoid the reflected light signal being dependent on the polarisation angle of each laser.

3.6.1.1 Laser alignment

The laser module described in Section 3.4.2 combines the output beams of three lasers with an alignment process conducted during manufacture of the module. Each laser and thin film beam combiner was fixed in place in a solid aluminium block using epoxy glue. This construction reduced the ability to make further adjustment of alignment or the replacement of lasers. The laser module was then mounted on a large alignment stage which was a heavy aluminium plate.

Three alternative designs for the construction of the laser module were considered, namely:

i) A precision manufactured combiner made from a single block with three holes bored for each laser and slots cut for the thin film beam combiners. No adjustment capability was included in this design, which instead relied on precision manufacturing for alignment.

ii) A fibre based laser combiner with a fibre pigtail attached to each laser and a fibre coupler or linear waveguide coupler leading to an output collimator.

iii) A laser module with each laser independently adjustable and the beam combiners fixed in place.

The viability of design i) was evaluated experimentally. A beam combiner module was designed in collaboration with, and manufactured by, Raven Engineering. The combiner was manufactured from a single block of derlin which is an insulating thermoplastic with high stiffness. This combiner had no adjustment for laser diodes or thin film combiners, as shown in Figure 3.24. The alignment accuracy of this combiner was assessed by fitting lasers to the three holes bored into the block and inserting beam combiners into the two slots cut at 45°. The beam offset was measured by marking the beam circumference of each laser on a target at a distance of 1 m and measuring the offset of the three beam centres. This offset ranged from 3-7 mm for the three lasers. This result was explained by measuring the beam pointing accuracy of the same three lasers, which was found to be between 1.1-2.6 mrad and accounts for a beam offset of over 7 mm. The specified beam pointing accuracy for the laser packaging is 25 mrad. To have a beam offset of less than 2 mm at the working distance of 2 m for beam 15, the required beam pointing accuracy is 0.5 mrad. The laser manufacturer offered to select lasers with a better beam pointing accuracy than that specified but could not guarantee 0.5 mrad.

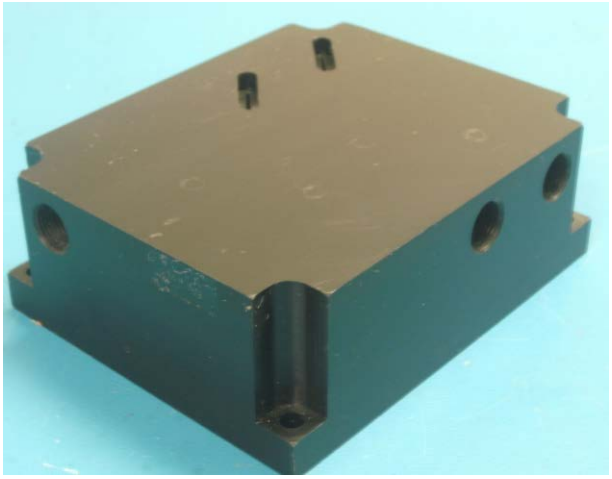

Figure 3.24. A precision manufactured combiner, made by Raven Engineering, using a single block with three holes bored for each laser and slots cut for the thin film beam combiners.

The use of optical fibre in design ii) provides an advantage in alignment of the outgoing beams. The alignment would be ensured by the containment of the beam within the fibre. However, the simplest design using fibre couplers would have high loss of optical power due to the efficiency of fibre couplers and the coupling loss from laser to fibre. These losses can be reduced by careful selection of the fibre used and custom design of the fibre couplers. However, this development process would be a significant effort in itself and result in a laser combiner module which is considerably more expensive than the thin film combiner based design.

Design iii) was a flexible and practical construction that offered independent adjustment of all laser beams. The concept for adjustment of the laser alignment was initiated after consideration of the problems with the first two designs. Mechanical adjustment gives four degrees of freedom for each outgoing beam: translation in the horizontal and vertical directions as well as tilt around the horizontal and vertical axes. The design was developed in collaboration with China Daheng Group.

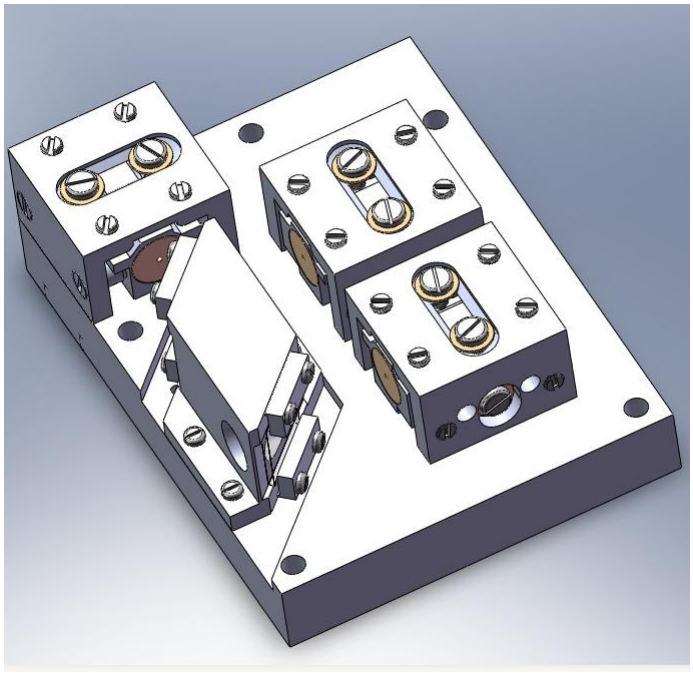

Figure 3.25. Model of laser module with three lasers and beam combiners showing adjustment allowing four degrees of freedom.

3.6.1.2 Polarisation alignment

The polarised nature of light emitted by lasers is not critical to the determination of spectral properties by the optical weed sensor however there are two reasons that the polarisation angle of each laser needs to be considered. These are the sensitivity of thin film filters to polarisation angle and the effect of polarisation angle on the reflectance of the leaf surface.

The sensitivity of thin film filters to polarisation angle is particularly important for filters used to split or combine light of two wavelengths within 50nm. The 670 nm wavelength laser has the lowest maximum output power of the three lasers and the efficiency of the thin film filters for 670 nm has a strong dependence on the polarisation angle. The polarisation angle of the 670 nm laser was therefore adjusted to ensure the maximum transmission of optical power from this laser.

The original design of the prototype required the polarisation of the three lasers to be aligned to avoid the reflected light signal being dependent on the polarisation angle of each laser. The polarisation alignment procedure doesn't specify the polarisation angle but only ensures that all the lasers have the same polarisation and that it matches what is required by the thin film filters.

A power meter is used to measure the output power of the laser module at 670 nm (after reflection from one filter and transmission through the second). The polarisation angle of the laser was adjusted by rotating the laser body until the maximum possible output power was obtained. A polarising filter was then aligned to the opposite polarisation by rotating the filter to minimise the transmission through the filter. This polarising filter was then used to adjust the polarisation angle of the other lasers by rotating each laser until the angle with minimum transmission through the filter had been found. Each laser was locked into place in its holder with a grub screw.

3.6.1.3 Line scan sensor alignment

The optical cavities either side of the line scan sensor project an array of laser beams. The light from these beams which was reflected by the ground and plants below the sensor was imaged by the lens and focused on the line of pixels in the line scan sensor.

The required alignment could be achieved by adjustment of the:

i) Camera height,
ii) Camera tilt (pitch of lens optical axis), and
iii) Rotation of sensor around optical axis of lens

The camera in the first prototype did not have adjustment for i) or iii). This alignment could only be performed by adjustment of the laser beam array. Due to the small pixel height in the line scan sensor it was required to precisely align the output beam arrays from the two optical cavities so that the beams imaged by the lens were uniformly incident on the pixel line in the camera. Figure 3.26 shows the image of seven beams incident on a line of pixels in the TSL3301 sensor. In this sensor the pixel height is 85 µm, six times higher than the 14 µm pixel height of the sensor used in the first prototype. The second example in Figure 3.26 shows the effect of misalignment of the sensor rotation with the outgoing beam array. The lack of adjustment for sensor rotation about the lens' optical axis combined with narrow pixel height made this alignment difficult and a time consuming process.

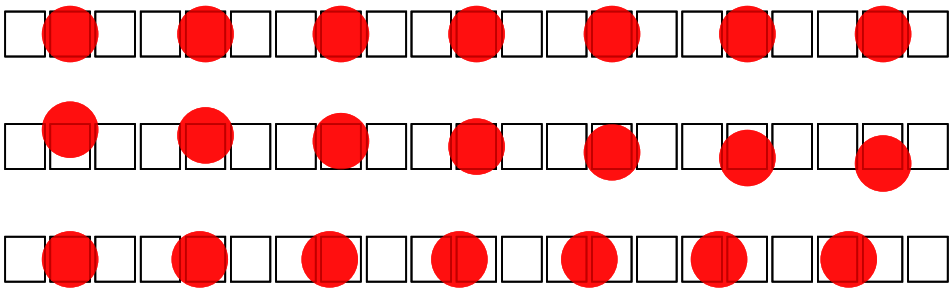

Figure 3.26. Alignment effects for line scan sensor with 102 pixels showing image of seven beams on 21 pixels.

3.6.2 Field of view

In designing this image sensor it is important to ensure that the lens is selected to have a focal length which ensures that all the beams are imaged by the line scan sensor. The first prototype used a 50 mm diameter lens resulting in a large gap between the two outgoing laser beams either side of the lens. A large gap of approximately 80 mm occurred when the sensor is scanned across the ground which resulted in any plant falling within that gap could not be detected. The only way to reduce this gap was to select a lens with a narrower diameter.

It is important to note that there is a range of lenses used in CCTV applications that have a narrow diameter, and that the focal length of the lens determines the field of view in combination with the length of the image sensor.

The required field of view for the camera is determined by the requirement that all 30 beams are visible at the minimum working distance. For a minimum working distance of 700 mm, the optimum focal length was found to be 12.3 mm. Therefore, an off the shelf lens with a focal length of 12 mm was selected from the range of commercially available lenses.

An experiment was carried out to check the maximum range at which the beams can be resolved with the TSL3301 sensor. It was observed that if the lens was chosen for a range of 800 mm then plants of height up to 200 mm were still within the field of view and successfully detected.

3.6.3 Component layout

Figure 3.27 shows the layout of the optical components in the weed sensor. The spacing between adjacent beams in the first prototype was 12 mm and the collimated beam diameter was 4mm. The spacing between the optical cavities was 70 mm to accommodate the lens of the line scan imager which had a diameter of 50 mm. In the second prototype a line scan imager with a smaller lens diameter was used to reduce the required spacing between the optical cavities to 35 mm, thus enabling 30 beams with a spacing of 15 mm to be generated by a 500 mm wide sensor module.

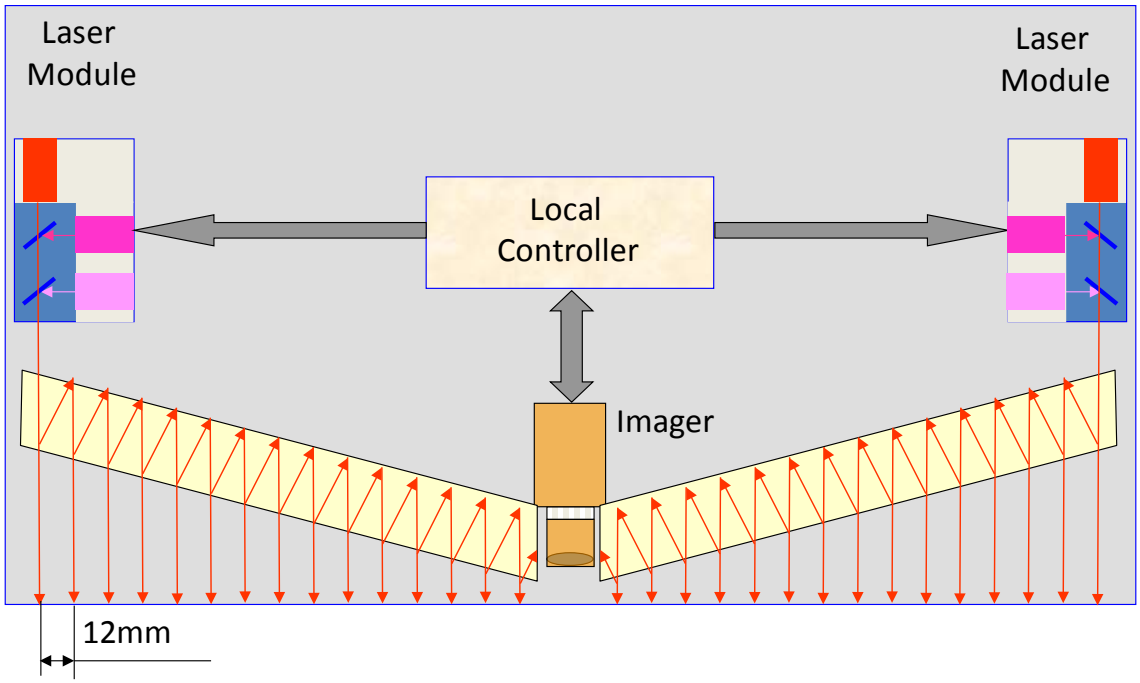

Figure 3.27. Layout of optical components in weed sensor.

3.6.4 Mechanical stress on cavity causing polarisation rotation

The stress applied to the optical cavity by the cavity holder induced mechanical birefringence in the cavity which rotated the beam polarisation. The resulting degradation in optical transmission for some beams reduced the signal to noise ratio. In order to suppress the birefringence some rubber spacers were used at the ends of the cavity to ensure that negligible stress was applied to the cavity.

3.6.5 Vibration testing

The prototype must be used in a harsh environment so it was necessary to test the tolerance of the laser sources and other optical components to mechanical shock and vibration. One laser module was subjected to vibration and shock testing. Three lasers and two thin film combiners were installed in this module, aligned and fixed in position with an epoxy resin. The laser module passed the vibration and shock testing and maintained the required alignment of the three lasers. Moreover the laser diodes were individually tested for shock and vibration tolerance by the manufacturer and they were found to be extremely robust and tolerant to shocks and vibration levels exceeding the levels that are expected to be encountered in the field.

Finally it is important to note that the complete system alignment requires the alignment of the individual components, namely the laser sources, the optical cavities and the image sensor, as described in section 3.7.1. The construction of the prototype was required to be sufficiently rigid so that this alignment was maintained when the system was operated in the field.

3.7 Control system hardware design

To be able to trial the weed sensor as a stand-alone unit that can travel over the ground at low speed required the development of a control system with high speed acquisition of the images and data processing. Using a microcontroller to control these functions is one solution to meet this requirement. A microcontroller is a single programmable integrated circuit which contains a processor (algorithmic logic unit or ALU), flash memory for program storage, volatile memory for temporary storage and a range of peripherals for input and output of signals (I/O). Microcontrollers are frequently used where a self-contained system is required to perform a dedicated task in a real time manner (*i.e.* with a predictable response time). These self-contained systems are referred to as embedded systems. An embedded system for the weed sensor requires a regulated power supply, a microcontroller, laser drivers, a communication system and supporting circuitry.

3.7.1 Selection of microcontroller

There is a very wide range of microcontrollers available covering many different architectures, data width from 8-bit to 64-bit and many different peripherals. The microcontroller chosen for the weed sensor was the Microchip 16-bit digital signal processor (dsPIC33F series). A digital signal processor is a microcontroller dedicated to signal processing and typically contains one or more arithmetic logic units optimized for efficient multiply and accumulate operations.

The Microchip dsPIC33F series of microcontrollers operate at a clock frequency up to 40 MHz and provide a broad instruction set and capable arithmetic logic unit (ALU). The ALU provides an integer multiply instruction which executes in a single cycle and a divide instruction which requires 18 clock cycles. These

instructions both operate on 16-bit integer or 16-bit fixed point fractional operands. The DSP core provides two 40 bit accumulators and a multiply and accumulate (MAC) instruction which executes in a single cycle. The series provides up to 256 kB of program memory, up to 30 kB of RAM, up to 85 general purpose I/O pins and many peripheral devices, some of which are optional depending on the device. In particular many chips provide a Controller Area Network (CAN) bus controller which simplifies the implementation of a CAN bus.

The functionality and suitability of this microcontroller was evaluated using a development kit to connect to and control the laser drivers and the image sensor. The algorithms for data acquisition, which will be described in detail in the following chapter, were implemented with the development kit. There was no problem with the interface to the lasers and image sensor nor with the algorithm for peak detection which operates only on integer data. Further data processing requires operation on rational numbers, specifically for the calculation of the normalised peak value and the spectral indices such as NDVI. Rational numbers can be represented using a floating point notation or a fixed-point fractional notation. The dsPIC33F does not have floating point support but the fixed point fractional format can be used. There was a floating point library available but the time required for multiplication and division operations depends on the value of the operands and in some cases can require several hundred instructions. The total time for data processing may exceed 0.5 ms, which was within the available time at low speed but would limit the maximum operating speed to under 10 km/h. Additional data processing tasks that may be required would further reduce the maximum operating speed and limit the flexibility of the discrimination process. Hence the fixed point fractional format was used to represent sensor response and calculated spectral properties.

3.7.2 Design of embedded controller

The PCB design process used Altium Designer to create the schematic, board layout and design files required to build the PCB. A block diagram of the controller is shown in Figure 3.28 which shows the signal connection between different components. Two versions of the PCB which controlled the weed sensor were made. Several issues were uncovered with the first design which

necessitated a redesign. This included additional functionality required to test laser operation and a voltage reference for the laser driver to improve the laser power stability. The monitoring diode in each laser is unconnected to the driver circuitry and can instead be used to ensure the correct operation of the laser. This is achieved with an op-amp in a trans-impedance amplifier configuration.

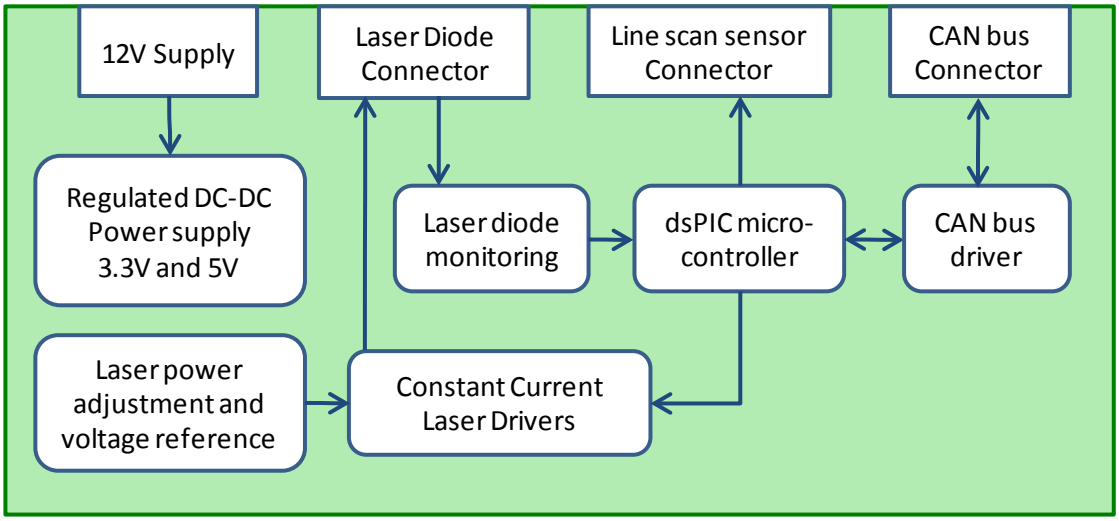

Figure 3.28. Block diagram of the main PCB for the weed sensor's embedded controller.

3.7.3 Spray controller with speed sensor

A separate PCB was designed and manufactured which monitors the vehicle speed and opens the solenoid valves which are connected to spray nozzles on the boom. The PCB would receive a positive strike signal when a weed is detected by the sensor. A position encoder attached to the wheel of the vehicle provided a signal with frequency proportional to the vehicle speed. One part of the spray controller software determined the vehicle speed from this signal. When a strike signal was received by the spray controller it calculated the delay and duration required to open the solenoid valve and spray the detected weed. The discrimination trials reported in Chapter 5 were conducted on a circuit and dye on the plants would interfere with detection. A signal tower was used to indicate plant detection rather than spraying the plant with dye, hence the spray controller was not required.

3.8 Summary

In this chapter the measurement of spectral reflectance has been discussed. A fibre spectrometer setup was described which has been used to conduct a survey of leaf level spectral reflectance for a range of crops and weeds. Measurement of spectral reflectance is a potential means for automated detection and spot spraying of weeds in a crop. This requires a proximate sensor which can be operated while traversing the ground behind a farming vehicle. The components which make up a prototype weed sensor have been described and characterised. Such a system requires reliable determination of the spectral properties of plants while travelling at a speed of up to 15 km/h.

The important design aspects of the prototype weed sensor were considered and where necessary, improved to meet the reliability required. These design aspects were:

i) the selection of lasers and laser drivers to illuminate plants with a stable optical power;
ii) the thin film coatings used in the passive optical components for generation of a structured light source;
iii) the selection of a cost effective and high performance line scan sensor;
iv) the optomechanical design of the sensor required to withstand vibration; and,
v) the design of a control system to allow independent operation of the weed sensor.

In Chapter 4 the integration of these components in a complete system will be discussed.

Chapter 4

Development of an Optical Weed Sensor

4.1 Introduction

The weed sensor design for each prototype developed was based on the principle of measuring spectral reflectance from leaves using lasers as a narrow-band illumination source. Each prototype used a laser module to align the output from three lasers using thin-film beam combiners. An optical cavity divided the laser module output into 15 evenly spaced and parallel beams. Each laser was sequentially turned on and the reflected light from the ground and leaves captured by a broadband line-scan sensor. A control system processed the data from the sensor and determined if the calculated spectral properties matched those of the target plants. This chapter will describe the initial prototype weed sensor and the further development of two revised models culminating in a working field prototype. For each revision of the weed sensor a description of the design and function will be given with reference to the components described in Chapter 3.

The first prototype was a bench-top demonstrator with limitations that prevented it from being tested under field conditions. The whole system was evaluated to determine its ability to collect and process data, to calculate spectral properties and to discriminate different plants under laboratory conditions. The main limitations of the prototype's design which prevented its use in field-testing were the low speed operation of the lasers illuminating the sample, the low signal to noise ratio of the image sensor and the lack of rigidity of the system which made the optical alignment highly sensitive to movement and vibration. Field-

testing also required operation using an embedded system that could function independently or be connected to a computer to collect discrimination results.

To overcome these limitations, the prototype was redesigned with a focus on the opto-mechanical system, building an embedded system and replacing some individual components. The redesign process is described in this chapter beginning with the evaluation and replacement of individual components. Two components were identified that required replacement: the laser drivers, which regulated the operation of the laser diodes, and the line scan sensor, which captured the reflected light. Following replacement of the sensor the software which operated the prototype was redeveloped and updated to interface with the new sensor. Once the required components had been identified, the opto-mechanical structure of the prototype was redesigned and a new prototype built which could maintain the alignment of the optical components. A micro-controller based system was designed and built to allow independent operation of the system. Lastly, software was developed to operate this system as an independent device.

The design of the final prototype was based on the second prototype but with replacement of the line scan sensor and refinements to the laser drivers and electronics for the embedded controller.

4.2 Initial prototype

4.2.1 Description of system

The initial prototype weed sensor was comprised of two laser combination modules, two multi-spot beam generators and a line scan image sensor, all mounted on a rigid base-plate and separate stages for optical alignment. The arrangement of these components is shown in Figure 4.1. Each laser beam combiner module and optical cavity was mounted on a separate aluminium plate. This whole section could be aligned with the line scan camera in the centre of the prototype by adjustment of the height at the centre and rear of the module.

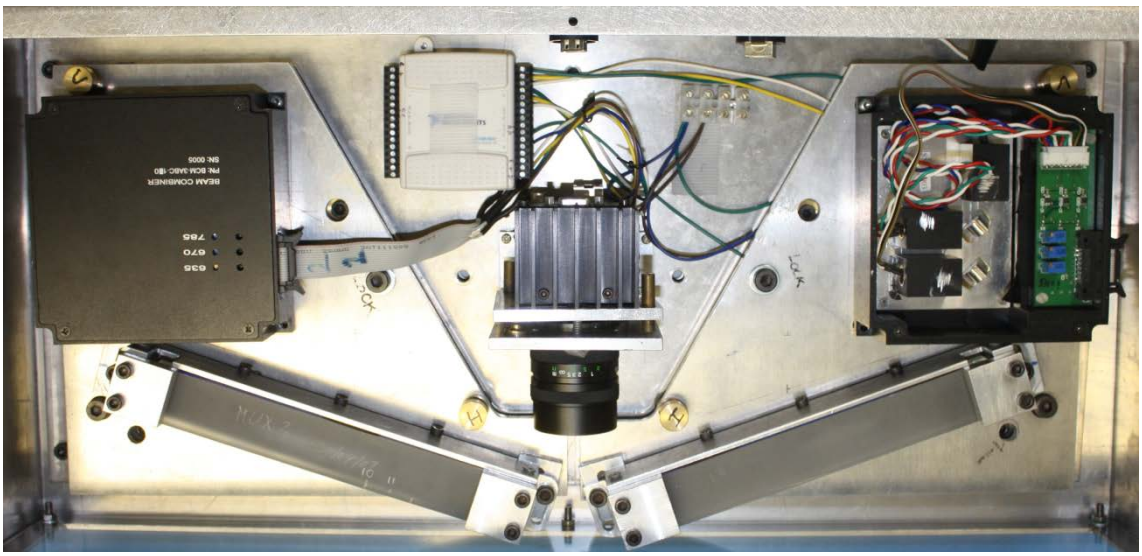

Figure 4.1. Photograph of initial prototype weed sensor showing layout of optical components.

The beam combiner used to align the three lasers is described in Section 3.5.2. It had each laser fixed in place and did not provide any adjustment of the individual laser diodes. The laser drivers used in this prototype were located on a PCB within the laser module and were of the constant power type described in Section 3.4.2. For the data collected under simulated dynamic conditions the laser drivers were replaced with independent constant current laser drivers. The optical cavity used for multi-spot beam generation has a uniform transmissivity coating creating 15 output beams with gradually decreasing optical power. The optical properties of this cavity have been described in Section 3.5.3. The optical beam power for the first beams emitted was near 700 µW for the red lasers and 350 µW for the 785 nm lasers. The intensity of the reflected light was recorded by a line scan camera located between the two optical cavities shown in the centre of the photograph in Figure 4.1. The camera used is a Spyder3 SG-10-01K40 manufactured by DALSA and is described in Section 3.62. A C-mount lens with 50 mm diameter, focal length of 12.5 mm and adjustable aperture and focus was used to image the reflected beams on the line scan sensor.

4.2.2 Control software and data processing

The control system for this initial prototype was software running on a Windows PC. The software was written with Microsoft Visual C++ and provided a

graphical user interface (GUI) to control the operation of the weed sensor. The functions of this software was to control switching of the lasers, capture of image data, processing of image data and discrimination of plants using spectral data. The interface between the PC and laser drivers was a National Instruments digital I/O device and the line scan sensor data was recorded via the camera's GigE ethernet connection. A flow chart showing the actions performed during a complete cycle is shown in Figure 4.2.

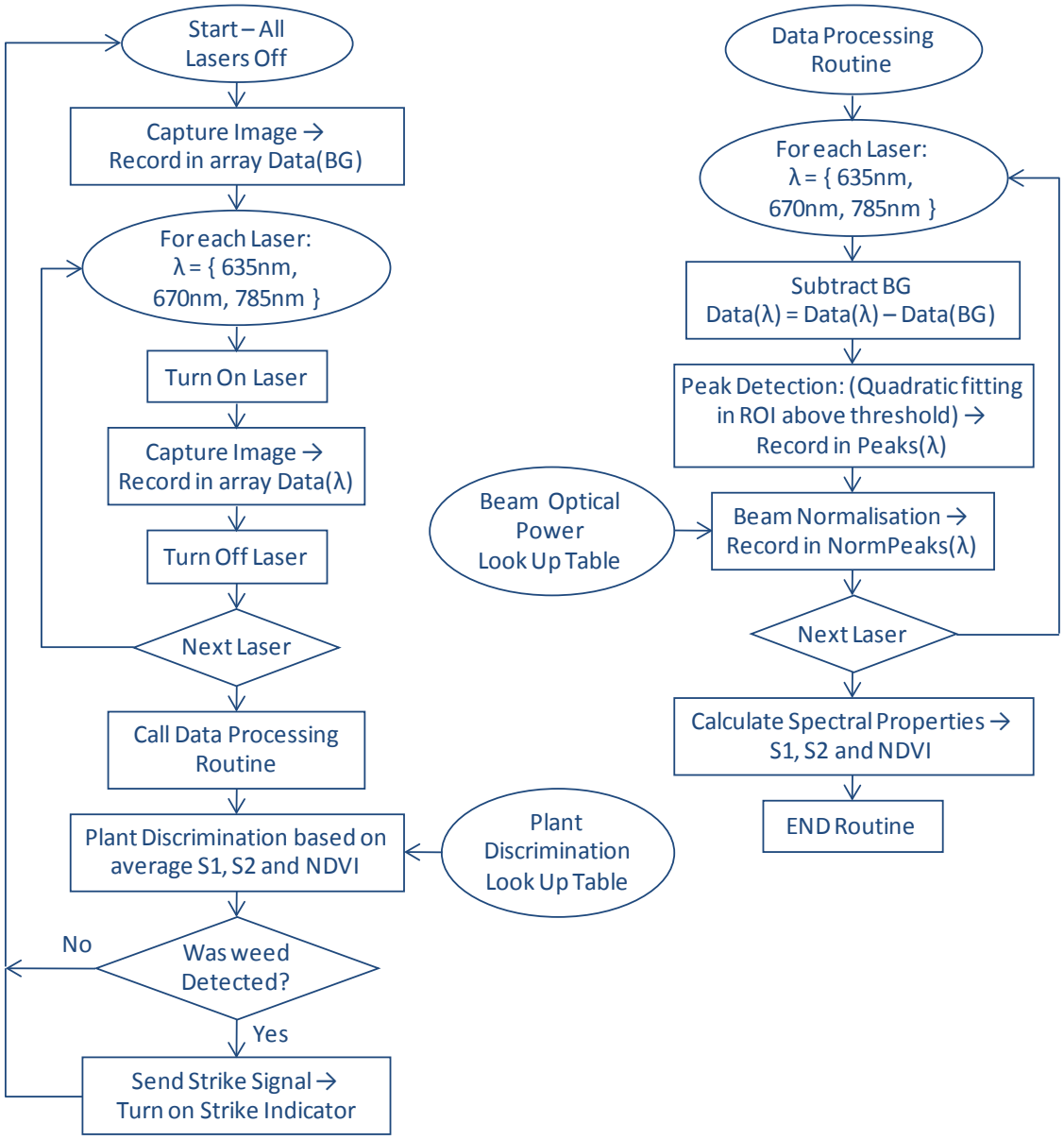

Figure 4.2. Flow chart for a single acquisition cycle used by the software controlling the original weed sensor prototype.

The detection cycle begins by switching on each laser and capturing an image of the reflected light intensity with the line scan camera. The captured image

has a peak for each of the 30 beams projected from the weed sensor. A peak detection algorithm searches the image for regions above a threshold which is automatically set slightly above the background intensity level. Within each region the maximum pixel intensity (I_λ) is found and stored. The detected peaks for each wavelength laser are checked to ensure that the peaks found correspond to each individual beam. Figure 4.3 shows the pixel response from one half of the line scan camera with 15 beams clearly visible. An alternative peak value calculation was later implemented using a quadratic fit which is also shown in Figure 4.3.

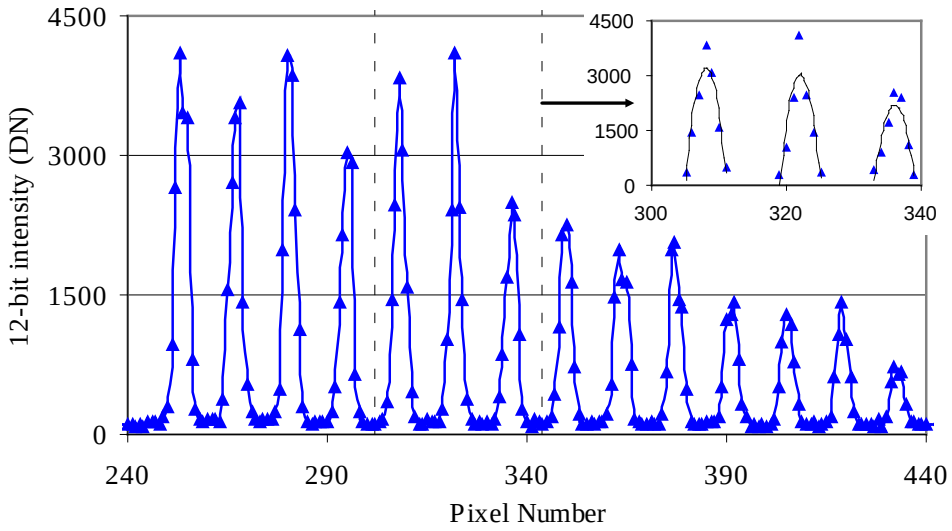

Figure 4.3. Intensity profile of 14 output beams from a 635 nm laser illuminating a background screen recorded by the image sensor. Inset shows quadratic fitting of measured intensity profile for three peaks.

Each peak is then corrected for the relative optical power of the corresponding beam using Equation 4.1, where P_λ is the beam optical power recorded using a Newport power meter.

$$R_\lambda = \frac{I_\lambda}{P_\lambda} \tag{4.1}$$

R_λ is representative of the reflectance of the surface on which the beam was incident but is not calibrated for the physical properties of the sensor. Two separate discrimination procedures are available using the corrected peak values R_λ. The “green from brown” discrimination calculates the normalised difference vegetative index (NDVI) from the corrected peak values for 670 nm

and 785 nm using Equation 4.2. When the NDVI is above a specified threshold a strike signal is generated which indicates that a green plant was detected.

$$NDVI = \frac{R_{785} - R_{670}}{R_{785} + R_{670}} \tag{4.2}$$

“Green from green” discrimination is based on calculation of a slope value which corresponds to the spectral slope between each pair of neighbouring wavelengths, shown in Equation 4.3. The range of slope values representative of four separate plants could be entered in the GUI. When both the calculated slope values are within the range specified for one of these plants a strike signal is generated which indicates which plant was detected.

$$S_1 = \frac{R_{635} - R_{670}}{\lambda_{670} - \lambda_{635}} \quad \text{and} \quad S_2 = \frac{R_{785} - R_{670}}{\lambda_{785} - \lambda_{670}} \tag{4.3}$$

In the bench-top demonstration version of the weed sensor the discrimination process based on results from individual beams was unreliable. The average value of NDVI, S_1 and S_2 was calculated for four beams of the weed sensor and the average value used in the discrimination process described above.

4.2.3 Performance and Refinement of Initial Prototype

The uniform coating on the optical cavity used in this prototype results in each subsequent beam having a lower optical power and the last beam (closest to the line scan sensor) has an optical power which is less than one third of the first beam (see Figure 3.16). The recorded intensity of the 15th beam was so low that it was frequently not found by the peak detection. For the experimental work performed with this prototype this beam was covered and not used in data processing.

The peak value calculated by the software was simply the maximum pixel value within each region above the threshold value. The response of the image sensor to the 14 beams incident on a green card reference is shown in Figure 4.3. The uncertainty in the peak value was equal to the uncertainty in each individual pixel value, which was very high, as discussed in Section 3.6.2. The shape of the detected peak is approximately Gaussian and this can be

used to reduce the peak value uncertainty by fitting a curve to the shape of the peak. Gaussian fitting would be the best solution but was not practical due to the complexity of non-linear regression. Quadratic fitting was chosen and implemented as a seven point quadratic fit centred on the maximum pixel value. The peak detection using this method is shown in the inset in Figure 4.3 and results in a reduction in standard deviation of the measured peak value. A disadvantage of this method is that the peak value is lower than that calculated with Gaussian fitting, particularly when the peak is narrow.

An improved design was required to solve the above issues, including: replacement of the Spyder3 line scan sensor to reduce the pixel noise; improvement of the constant current laser driver to increase optical power stability and modification of the uniform transmittance optical cavity which caused peaks with low power. To allow the prototype to be tested in the field, the opto-mechanical alignment system was reviewed and the computer replaced by an embedded control system.

4.3 Improved prototype

Following on from the assessment made of the performance of the original prototype the selection of components for, and the design of, each part of the system was carefully considered. The components used are described in Section 3 and included: laser diodes of three wavelengths (635 nm, 685 nm and 785 nm); constant current laser drivers; optical cavities having non-uniform transmittance on the front surface; the TSL3301-LF line scan sensor; and a custom designed PCB with microcontroller for independent operation. In addition, the opto-mechanical layout was revised to improve the coverage of ground illuminated by the lasers and improve the mechanical alignment of the system as well as its rigidity.

4.3.1 Description of System

Figure 4.4 shows the revised layout of the improved prototype with arrangement of optical components. All the components were mounted on a single base-plate made of 6 mm thick aluminium. Each laser diode was mounted in an alignment block along with two fixed thin-film beam combiners which made up

the laser module. This laser module is described as design 4 in Section 3.6.1.1. It allowed each laser to be independently aligned such that all beams were overlapping and aligned with the line scan sensor in the imager. Four laser wavelengths were used with this prototype – the 635, 670 and 785 nm combination was used initially with indoor experiments. During the outdoor trials the absorption of light from the 670 nm laser by leaves was so high that the signal to noise ratio of the peak detected by the sensor was very poor. The 10 mW maximum output power was insufficient so it was replaced with a 685 nm laser diode with maximum output optical power of 50 mW. The optical cavities are longer than those in the original prototype and positioned at a larger angle. This increased the spacing between beams from 12 mm to 15 mm and reduced the gap between the two beams closest to either side of the image sensor. The gap between the outside edge of the weed sensor and the outside beam was also reduced to 15 mm. The optical cavities with partially transmissive coatings on the front surface were replaced with cavities which had individual filters for each beam. For each subsequent beam the transmissivity is gradually increased in order to maintain a uniform output power. The properties of this replacement optical cavity have been described in Section 3.4.3.

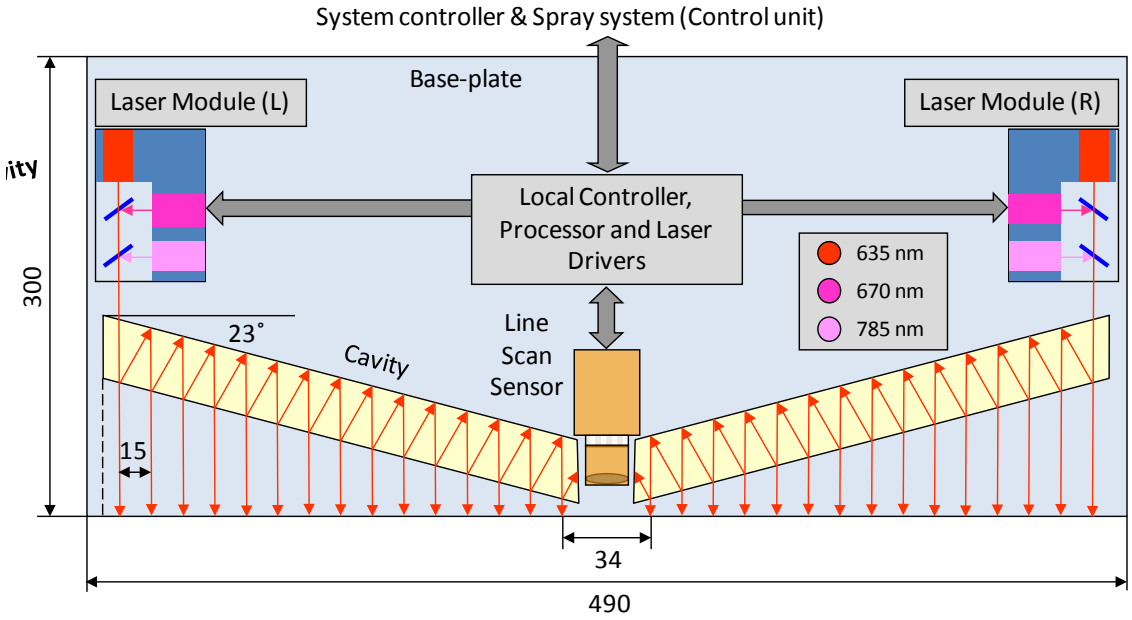

Figure 4.4. Layout of improved prototype showing laser modules, optical cavities and image sensor mounted on a single base plate.

An embedded controller was developed for this prototype which used a dsPIC33F microcontroller to control the lasers and image sensor and carry out data processing to determine spectral properties of the soil and plants. During the evaluation of the system a desktop computer continued to be used. The computer operated separately from the embedded controller. It used the same National Instruments digital I/O device as in the original prototype connected to a constant current driver version of the independent laser drivers and an evaluation board with serial interface to control the line scan sensor.

The prototype sensor was packaged within an aluminium case to prevent dust and water entry into the lasers, sensor and electronics. This case is made up of the 6 mm aluminium base with a rubber seal around the edge and a 1 mm aluminium lid. The lid includes an acrylic window to allow illumination of the ground and detection of the reflected lit as well as sealed connectors for power and control signal wiring.

4.3.2 Line scan sensor performance

The most important changes for plant detection capability with this version of the prototype were in stability of the measured reflectance. During experiments with the original prototype weed sensor the calculated spectral properties were observed to have a surprisingly high variability. The TSL3301-LF line scan image sensor described in Section 3.6.1.2 replaced the Spyder3 camera used previously. This line scan sensor proved to have much lower variability in the pixel response which gave repeatability in the measurement of spectral properties. The stability of the response of the TSL3301 line scan sensor was compared with that of the Spyder3 camera by recording the peak value detected by each sensor while a green card reference was sequentially illuminated by the 635, 670 and 785 nm lasers.

Figure 4.5 shows the variation in the digital response of the two optical image sensors over time to one spot on a reference sample. This spot was sequentially illuminated by 635, 670 and 785 nm laser beams at ten second intervals over a period of 10 minutes. The Spyders3 line scan camera readings (dashed lines) showed significant fluctuation for all three wavelengths in comparison with the TSL3301 linear sensor array (thin lines).

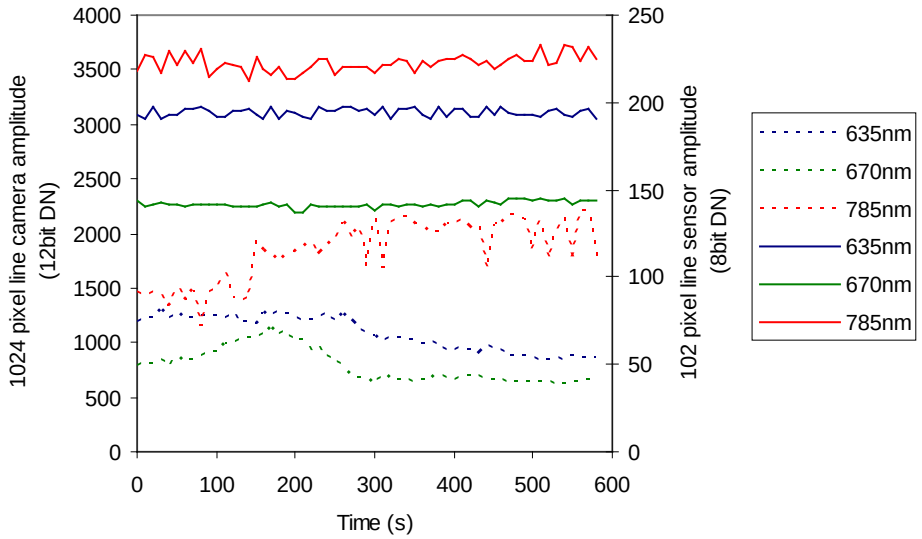

Figure 4.5. Response in digital numbers (DN) of two optical image sensors over time to one beam on a reference sample sequentially illuminated by 635, 670 and 785 nm laser beams. Dashed lines are for the Spyder3 line scan camera (left axis) and thin lines are for the TSL3301 linear sensor array (right axis).

Figure 4.6 shows a single line scan image recorded with this system with one laser turned on and all 30 beams incident on a reference card at a distance of 650 mm. The non-uniform coatings were used to generate the multi-spot beam array and generated an array with beam optical power similar to that shown in Figure 3.23. The increased beam power for the central beams is exacerbated in this case by the shorter distance to the sensor and reflection which is close to normal incidence. This effect was undesirable for the signal to noise ratio of outer beams but did have an advantage with peak detection. As outlined below, the peak detection began in the centre of the image and scanned towards the edge. The larger signal for the central beams ensured that they were always detected in the image even when the reflectance of the target was very low.

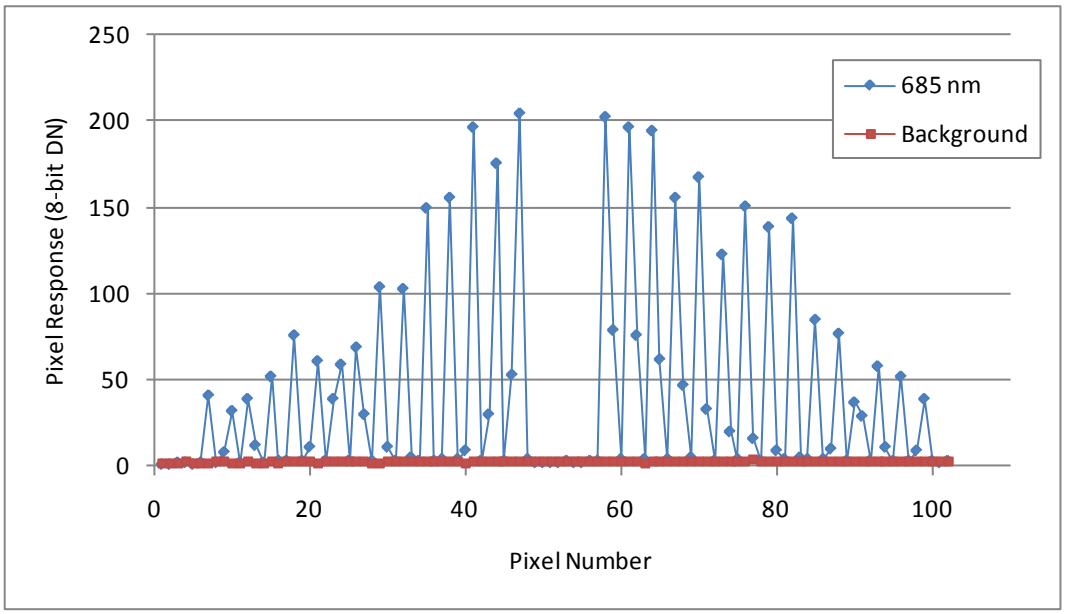

Figure 4.6 Single line scan image for TSL3301 line scan sensor with 685nm laser turned on. All 30 beams are incident on a reference card at a distance of 650 mm.

An optical filter to reject solar background radiation was fitted to the sensor in this prototype, as described in Section 3.5.4. The effect of this filter on the line scan sensor performance was measured by recording the response of the weed sensor with and without the filter to a reference card at a distance of 650 mm. The weed sensor was placed outdoors in a range of lighting conditions, including under shade and under full sun. The effect of the optical filter on the recorded peak value is shown in Figure 4.7 for shaded conditions, where the response of the image sensor is not saturated by the background light. The exposure time for both scans shown is 180 µs and the reduction in background light by the solar filter is clearly seen.

The average reduction in background level (after subtracting dark signal of 6 DN) over all pixels in the line scan is 75%. Without this reduction the response for nearly all beams is saturated in the line sensor. In order to have an unsaturated response for all beams the exposure time would have to be halved, which significantly reduced the signal to noise ratio.

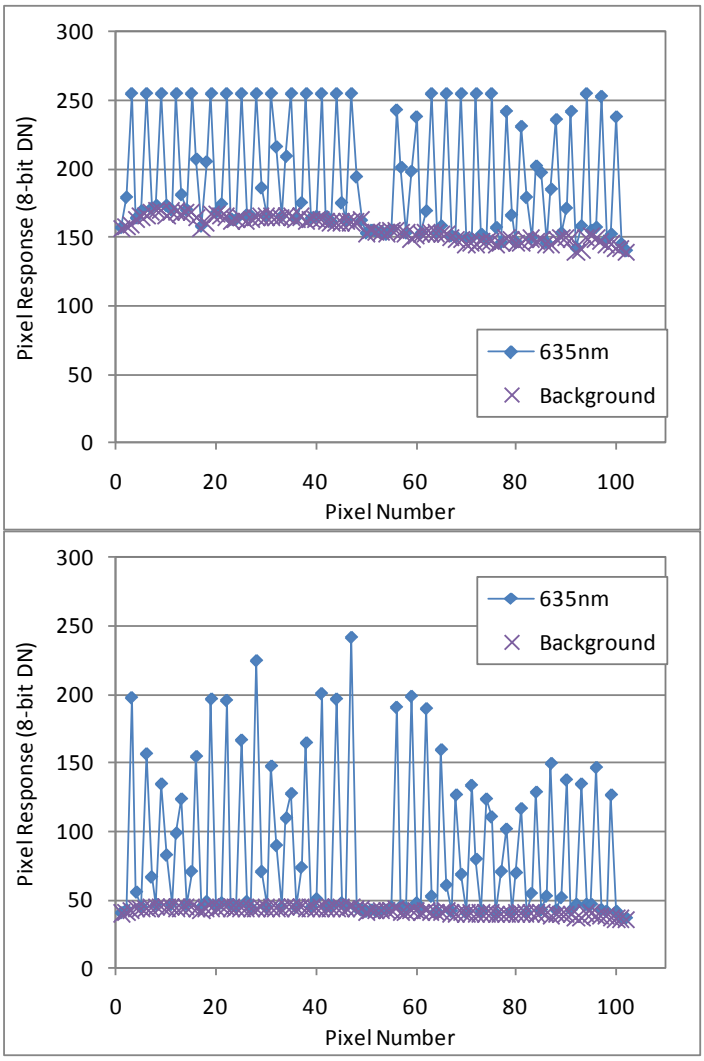

Figure 4.7. Response of line scan sensor to 30 beams illuminating a green reference card under shaded outdoor conditions (a) without solar filter and (b) with solar filter.

The high sensitivity of this sensor ensured the exposure time required was below 200 µs. With a read-out time of 100 µs, processing time of 200 µs and allowing a travel distance of 5 mm per scan, Equations 3.5-3.7 give a maximum travel speed of 7 km/h.

4.3.3 Development of control software

During the evaluation of the TAOS sensor as a replacement image sensor an evaluation board provided by the manufacturer was used. This evaluation board provided a serial interface to control the sensor and acquire data. The same National Instruments digital I/O device (NIDAQ) used in the original prototype was used to control the laser switching. There were two large sections of the

weed sensor software which needed to be adapted for the TAOS image sensor – the image acquisition and the peak detection. To simplify the process of rewriting these tasks and making further modifications to the Weed Sensor software the whole software program was rewritten in LabVIEW.

LabVIEW is a graphical programming environment allowing efficient programming which was introduced in 1986. Its design is centred on simplifying tasks involving instrument control, data acquisition and analysis, signal processing and data visualization. LabVIEW is a useful programming environment for ongoing development because it gives a flow chart representation of the algorithms used and allows immediate visualisation of the data flow at any point in the program [72].

The LabVIEW interface to the TAOS sensor used LabVIEW's built-in serial driver to communicate with the evaluation board. The NIDAQ device was controlled with the LabVIEW driver for the device which provided simple controls to configure the required outputs and switch each laser independently.

After initial testing of the TSL3301-LF sensor a LabVIEW version of the control software was developed. A flow chart of the scanning cycle is shown in Figure 4.8. The software included a data collection routine, a data processing routine and a graphical interface. The data collection routine switched each laser on sequentially and captured an image for each laser. The data processing routine detected peaks in each image, corrected these peaks for beam optical power and calculated the required spectral properties. The graphical interface provided control of the laser and sensor parameters and displayed the calculated peak data and spectral properties. A Green from Brown detection was also implemented based on a NDVI threshold and the collected data could be saved to a file for further analysis. The algorithms implemented in LabVIEW are very similar to those used in the software controlling the original prototype, except for the communication with the TAOS evaluation board and the peak detection.

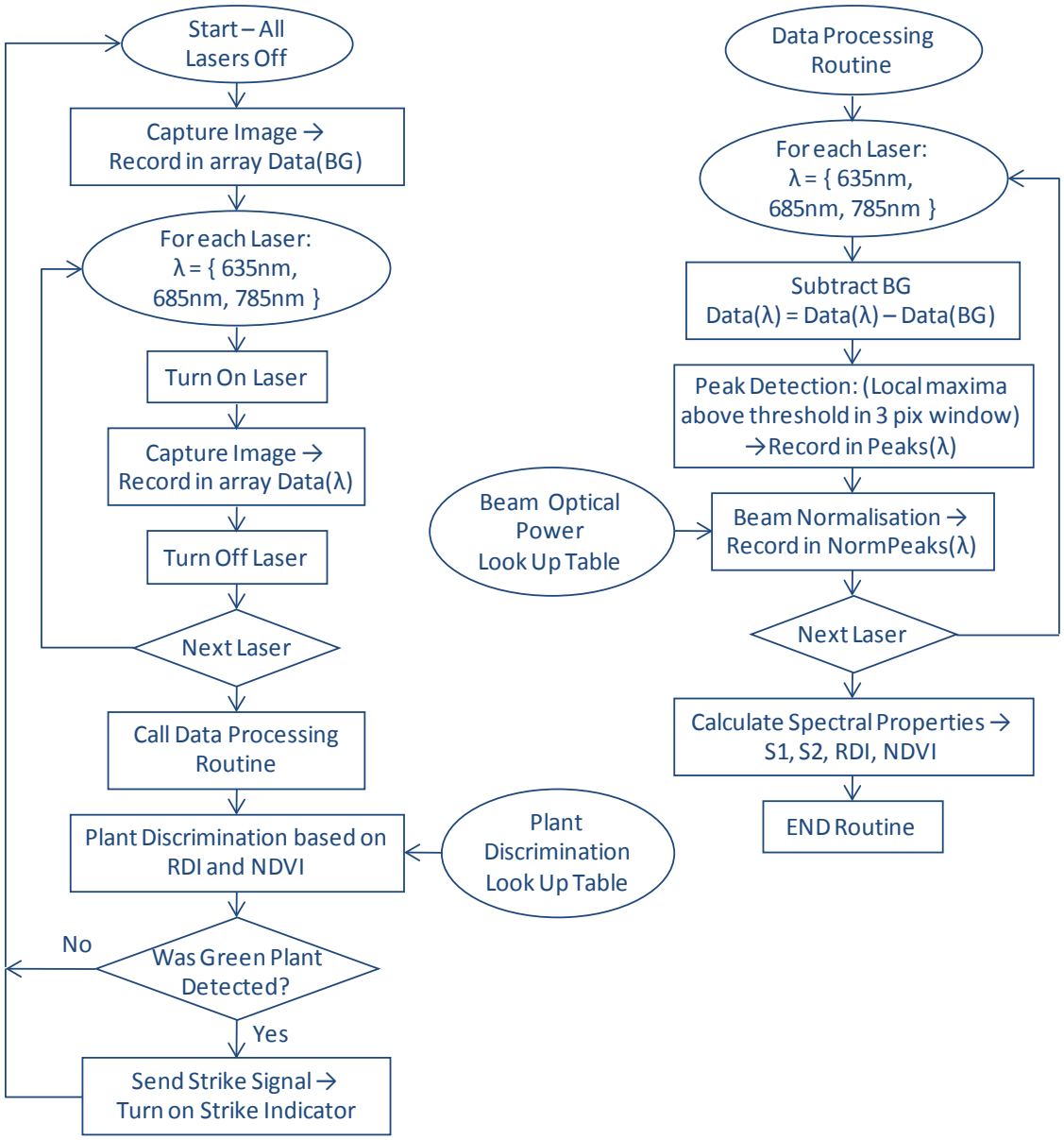

Figure 4.8. Flowchart for a single acquisition cycle used by software executed by the second prototype weed sensor.

4.3.4 Algorithm for peak detection

The TAOS line scan sensor has 102 pixels. Thirty beams were imaged with this sensor which implies there were at most 3 pixels per beam. Each beam is incident on one or two pixels leaving a gap of one pixel between each spot in the recorded image; see Figure 3.26 and sample line scans in Figure 4.6. The built-in peak detection routines were not used as they did not work well for such narrow peaks. This peak detection was also required in the software developed for the microcontroller used in the local controller. A simple algorithm for peak detection was developed and implemented in LabVIEW.

A three pixel window is scanned along the line scan image. If the centre pixel is a local maximum and is also above a pre-determined threshold then it is detected as a peak. The peak value calculation assumes only two of the three pixels are exposed to the reflected beam and the third pixel can be used to compensate for the background noise due to ambient light and sensor dark current. The peak value *Pk* is the sum of the two largest pixel values and is calculated using Equation 4.4.

$$Pk = Pix_2 + \max(Pix_1, Pix_3) - 2 \times \min(Pix_1, Pix_3) \qquad (4.4)$$

where Pix_2 is the centre pixel and Pix_1 and Pix_3 are the pixels either side. The window is scanned by shifting Pix_2 one pixel at a time until the whole image has been scanned or 15 peaks have been found in each half of the image. After outdoor testing it was apparent that frequently there was no intermediate pixel between two beams and the background subtraction actually reduced the peak value from its true value. A separate background scan was added to the scanning sequence and this scan was used for background subtraction in place of the above method.

4.3.5 Algorithm for plant discrimination

During the evaluation of the TAOS image sensor the only detection attempted was green from brown discrimination. The method used is the same as described in Section 4.2.1. The NDVI value is calculated for each beam using Equation 4.6. If the NDVI for any beam is greater than a threshold value then a strike signal is generated. Each beam has a strike indicator in the graphical interface. The NDVI threshold is adjustable to determine the value which will provide most reliable discrimination. The value used was typically between 500 and 600. For the purpose of display it was also useful to have a combined strike indicator which was activated when any individual strike was activated.

Once a beam had been determined to be green according to the NDVI, it was tested to determine if it matched any of the criteria for desired plants. Two different types of criteria were used during the testing of the improved prototype weed sensor. The slope method used in the original prototype was also implemented in the LabVIEW program. Slopes S1 and S2 were calculated

according to Equation 4.5. For each target plant a range of S1 and S2 were determined. If the calculated values of S1 and S2 for a beam both within the specified range, then the beam recorded a strike for that plant.

$$S_1 = \frac{R_{635} - R_{670}}{\lambda_{635} - \lambda_{670}} \quad \text{and} \quad S2 = \frac{R_{785} - R_{670}}{\lambda_{785} - \lambda_{670}} \tag{4.5}$$

During testing of the sensor it became apparent that there were many factors which affected the calculated slope values, particularly those which reduced or increased the intensity of light at all three wavelengths. Such factors included the distance from sensor to leaf, the orientation of the leaf and the exposure time of the line scan sensor. This is contrary to the results with the previous prototype; however these effects were most likely obscured by the noisy peak values recorded by the Spyder3 line scan camera. Normalization was required to account for these factors. In line with the NDVI a similar normalised difference index was calculated from the two red wavelengths. This value is labelled the RDI and is shown in Equation 4.6.

$$RDI = \frac{R_{635} - R_{670}}{R_{635} + R_{670}} \quad \text{and} \quad NDVI = \frac{R_{785} - R_{670}}{R_{785} + R_{670}} \tag{4.6}$$

The alternate plant discrimination method was based on the slope method, but with S1 and S2 replaced by RDI and NDVI. Again, for each target plant a range a characteristic range of RDI and NDVI was determined. If the calculated values for and beam matched the ranges for one of the target plant then a strike was recorded.

4.3.6 Embedded controller design

An important step in transferring the weed sensor from the lab to outdoor operation was the development of an independent embedded controller. The control system described in Section 3.8 was developed for this version of the weed sensor. The PCB designed for this purpose included a regulated 5 V and 3.3 V DC supply for the electronics, a dsPIC33F microcontroller, constant current laser drivers, and a CAN bus driver for communication.

After initial power on, or device reset, an initialisation routine was run to configure the microcontroller inputs, outputs and peripheral devices. Memory

used by the program was initialised, which included loading the beam optical power table and the plant discrimination lookup table into memory. The TAOS sensor was then initialised which required sending a reset sequence followed by a short period of continuous clock pulses without sending any data. This sequence prepared the analogue and digital circuitry in the sensor ensuring it did not return nonsense data. The TSL3301-LF has programmable gain and offset correction for the analogue to digital conversion which were in an indeterminate state after power on. The offset correction was set to 0 and the gain to 1 during initialisation.

Following the initialisation the program entered the main loop. This loop carried out the operations for a single scan as described above and ran continuously until the device was turned off. All the operations of the LabVIEW program were converted to run on the microcontroller including output of a strike signal for green from brown detection and for detection of the target plants. The strike signals controlled a visible indicator to monitor the detection results of the weed sensor.

4.3.7 Outdoor operation

A frame was made to hold the weed sensor at an adjustable height above the ground. Figure 4.9 shows the sensor mounted on this static test rig with the lid removed. This setup was used to determine the response of the sensor to different outdoor light conditions as reported above. Dynamic testing was conducted with the weed sensor mounted on a frame attached to the front of a quad bike as shown in Figure 5.11. The quad bike provided an important test for the weed sensor, namely whether the optical alignment would be maintained after being subjected to continuous vibration from the engine. After several hours of operation the prototype was brought back into the lab and the alignment of lasers checked. All six lasers were found to be maintained within the 1 mm tolerance at a distance of 1 m and the line scan sensor was still aligned with the output beam array.

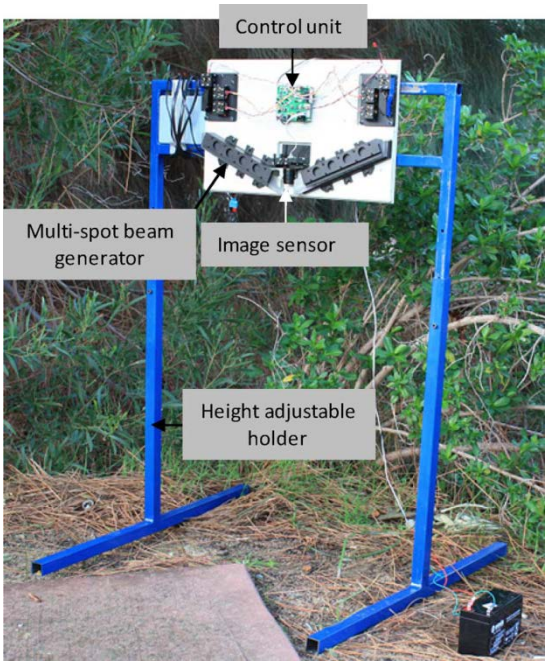

Figure 4.9. Improved prototype weed sensor on a static test rig for outdoor testing. Visible strike indicator not shown.

4.3.8 Discussion

The outdoor background light is a difficult problem for all optical weed sensors. With the solar filter employed in the weed sensor significant reduction in the recorded background level was observed. A signal was obtainable in sunny conditions provided that the exposure time was reduced, however reliable green plant detection was only possible under shaded conditions. With dynamic operation the effect of background light was more pronounced. The problem was not so much the light level but rapid, large changes in the background light level when the weed sensor travelled over surfaces with varying reflectance. Particularly problematic were plants themselves, which have a very high reflectance in the NIR compared to soil. The NIR light within the passband of the solar filter caused large changes in the recorded background level when travelling over plants.

Green from Brown detection was reliable under shaded conditions with some false positives on rough soil surfaces. Determination of spectral properties gave unreliable results because of low reflectance of leaves in the red wavebands and the corresponding low sensor signal. The low dynamic range of the line scan sensor's 8-bit digital output was the largest factor in this unreliability. The

discrimination performance of the improved prototype is presented in Section 5.4 and further improvements to the design are presented in the next section.

4.4 Final prototype

The final revision of the prototype weed sensor was designed to overcome the difficulty with determining accurate spectral properties of plants experienced with the previous prototype. It shares much of its design with the previous prototypes – the differences being replacement of the digital line scan sensor and a number of refinements which reduced the measurement error in recording reflectance from the leaf as well as variability in the calculated spectral properties. After investigation of the sensor response to a reference target, and monitoring the optical beam power with a high speed photodetector it was determined that both components needed improvement.

4.4.1 Description of system

The layout of optical components is the same as the previous prototype shown Figure 4.4. The laser modules, optical cavities and camera housing were all kept the same. The 8-bit digital line scan sensor was replaced with an analogue sensor with low noise and high dynamic range. The sensor used was an S9227-03 linear array described in Section 3.5.4. The choice of this sensor was a trade-off between low noise and sensitivity. Although the reduced sensitivity required an exposure time of 1-2 ms and slowed the scanning rate of the sensor considerably, the high dynamic range and low noise allowed evaluation of the discrimination performance of the weed sensor with more precise measurements of the leaf spectral properties. Additionally, the use of an analogue sensor allowed separate characterisation of the sensor performance and analogue to digital converter (ADC) performance. The constant current laser driver used with the previous prototype was refined to improve the output power stability using the circuit described in Section 3.3.3 to reduce ringing during the laser turn on and to minimise thermal fluctuations. The output power was also increased to approximately 20 mW for each of the red lasers and

15 mW for the 785 nm laser. This ensured a useable signal with the exposure time reduced to 1 ms.

Several improvements had been made to the electronic design of the local controller over the course of development. These improvements were incorporated into a modular design for the Controller PCB which included separate boards for the regulated DC power supply, microcontroller board, laser driver board, image sensor driver and the option to install the spray controller. The image sensor driver provided a clock to drive pixel readout, exposure time control and a buffer to interface the 5 V analogue output with the 3.3 V input of the dsPIC33F. The ADC peripheral on the dsPIC33F was used to digitise the pixel voltage. With the ADC operating in 10-bit mode it had a maximum sample rate of 500 ks/s resulting in a read-out time of 1.1 ms. Using Equations 3.5-3.6 and given 1 ms exposure time, 1.1 ms read-out time, 1.2 ms processing time and 5 mm travel distance, the maximum travel speed is 2 km/h. The processing time was more than 5 times longer than previously because the peak detection was more complicated and needed to scan through 512 pixels in place of 102. In practice, restriction of the plants used in discrimination trials to broad-leaved plants with a flat leaf surface allowed a travel speed of up to 7 km/h.

4.4.2 Data processing

Several changes were made to the data processing algorithms to accommodate the higher resolution line scan sensor and to improve the discrimination performance. Figure 4.10 shows a sample reading from the line scan camera when six beams are incident on a leaf. The scan for the 635 nm laser is omitted for clarity. Each beam covers from 5-9 pixels so a similar peak detection algorithm to that used in the original prototype weed sensor was employed. Each peak in the 785 nm scan is detected using the same region of interest (ROI) method as before. The quadratic fitting to determine peak value was replaced with a sum over the pixel values of each pixel within the ROI. These same ROIs were then used to calculate reflected intensity values for the two red lasers. This technique ensured that even when the local maxima for a beam was very small – even if below the threshold used to find peaks – the peak value could still be detected.

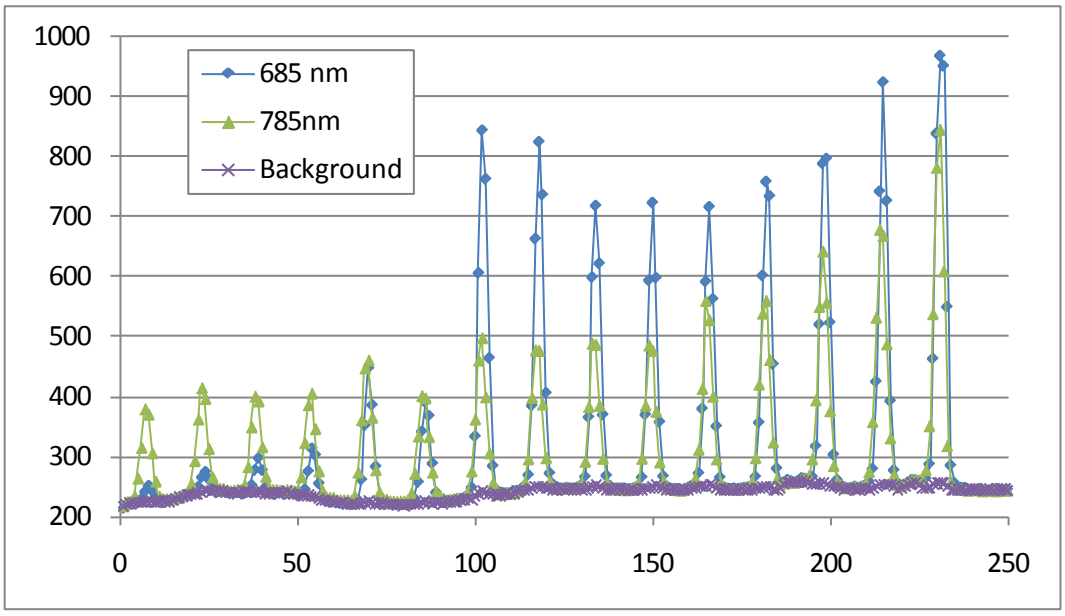

Figure 4.10. Line scan sensor reading for two lasers (685 nm and 785 nm) and the background scan using S9227-03 sensor. Only one half of the image with 15 beams is shown. Six beams from the outside edge of the weed sensor are incident on a leaf.

Investigation of the variability in the red laser peak values when the beam was incident on a leaf also led to a change in the spectral properties used for discrimination. Because both red peak values are low, the *RDI* value had significantly larger variability than the *NDVI* value. Instead, a second *NDVI* value was calculated using the 635 and 785 nm peak value, as shown in Equation 4.7. These two values are referred to as $NDVI_{635}$ and $NDVI_{685}$.

$$NDVI_{635} = \frac{R_{785} - R_{635}}{R_{785} + R_{635}} \quad \text{and} \quad NDVI_{685} = \frac{R_{785} - R_{685}}{R_{785} + R_{685}} \tag{4.7}$$

The common 785 nm peak value used in both NDVIs resulted in a strong correlation between the two values. This is evident in the scatter plots of spectral properties shown in Section 5.5. To accommodate this correlation the simple min/max range criterion used previously was replaced by a parallelogram criterion in the $NDVI_{635}$, $NDVI_{685}$ space. This allowed more compact range criteria to have less false negatives when the spectral properties recorded from a leaf were near the limit of the criterion for the plant. When a beam matched the discrimination criterion stored for a target plant, an individual beam strike was recorded. Initially any strike recorded would turn on the strike indicator but this proved to have a very high false positive rate for different

plants. A strike aggregation algorithm was implemented to reject individual beam false positives. This algorithm simply summed all the individual beam strikes for a target plant from a set of scans. If the aggregated sum of individual beam strikes was above the threshold then the strike indicator was activated.

A flowchart for the modified software is shown in Figure 4.11. The software for the microcontroller was written in C and made use of the library available to control the CAN bus driver. This allowed the prototype weed sensor to be controlled via the CAN bus with a laptop. A communication protocol was set up to allow control of each step in the single scan, to read out pixel data and results, to update the beam optical power table and the discrimination criteria for different plants and to put the weed sensor in and independent scanning mode. The interface on the laptop was programmed in LabVIEW and had similar functionality to the LabVIEW program used for the previous prototype. The program also allowed the recorded spectral data and discrimination results from the weed sensor to be displayed in real-time – albeit at a lower scan rate due to the time taken to transfer data over the CAN bus.

4.4.3 Discussion

The final version of the prototype weed sensor presented in this section has significantly improved upon the performance of the previous versions. Reliable indoor and outdoor discrimination of three plants was achieved with this sensor, as presented in Section 5.5. The critical factors in this improvement were stability of the output laser power and improved signal to noise ratio of the detected leaf reflectance. A low noise, high dynamic range line scan sensor provides reliable detection of the intensity of reflected light from leaves and soil. The data processing algorithms take advantage of the reliability of the 785 nm laser to determine the location of each beam in the image and for normalization of the signals from the two red lasers.

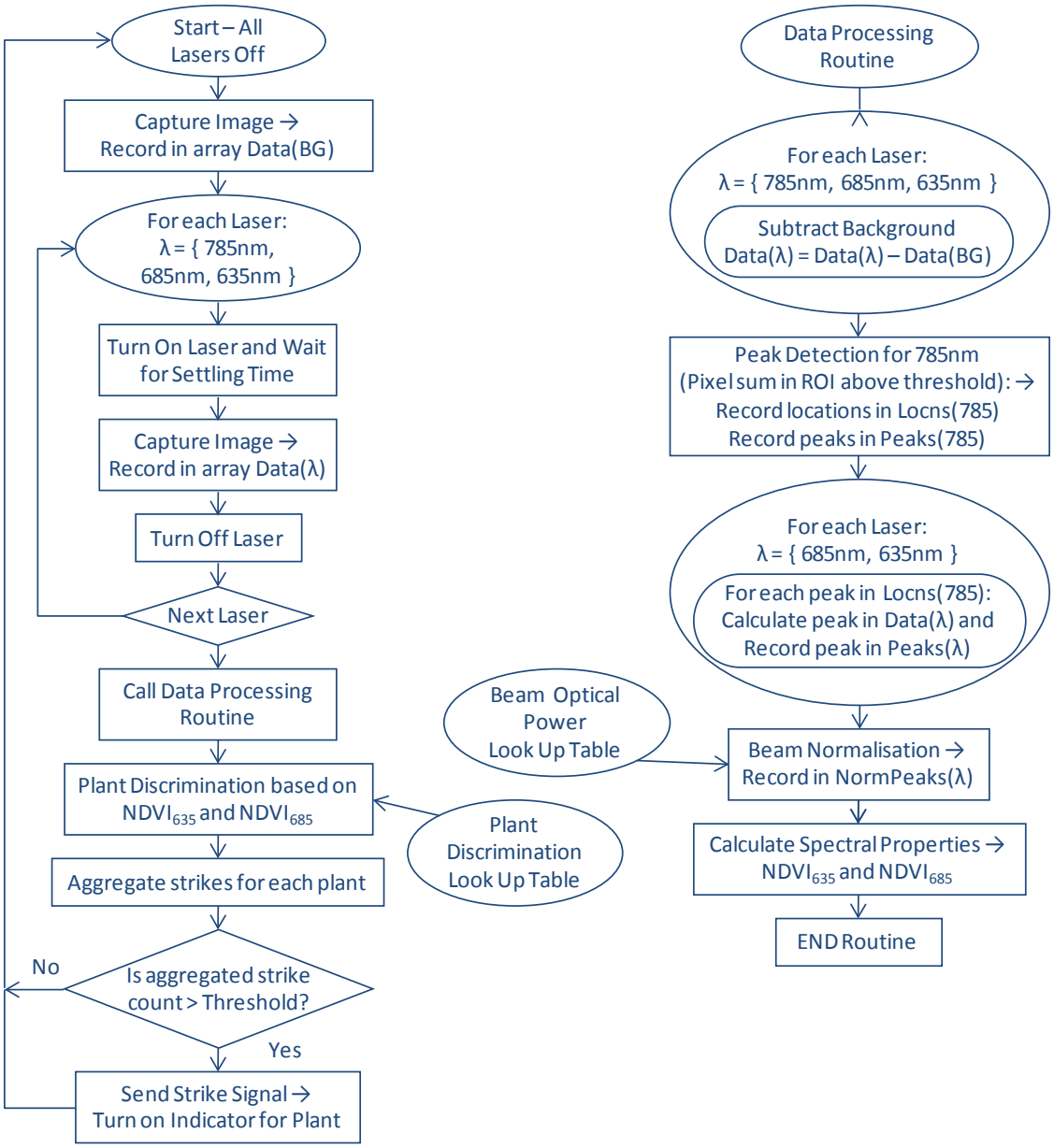

Figure 4.11. Flowchart for single scan operation run on the microcontroller of the final prototype weed sensor.

Additional spectral information could be determined with the addition of more laser wavelengths which would improve the reliability of plant discrimination. The use of only three narrow wavebands is a limitation imposed on this system by the sequential scanning nature of reflectance data acquisition combined with time constraints due to the travel speed. With consideration of the current speed of operation being well below the desired speed, the inclusion of additional lasers was not tested with this prototype.

The choice of line scan sensor was a compromise on the desired speed of operation of the weed sensor. There are however several possibilities to

increase the speed of operation. In addition there was another advantage to using the S92207-03 sensor. The tall pixel height simplified the alignment of the line scan sensor with the output beam array. It meant that the camera need not be perfectly aligned with the output beam array in order for all beams to be incident on the active area of the sensor. Even with a small shift in position the beams remained within the active area.

The potential improvement in speed of operation could be realized by a combination of the following:

i) Increasing laser power so that the exposure time can be reduced. All the lasers were operated well below their maximum output power, but it is also desirable to operate below the rated maximum for longevity of the laser diodes.
ii) Search for an alternate sensor with similar dynamic range to the S9227-03 but a higher sensitivity. Additionally a pixel count of 200-250 would be sufficient to provide the spatial resolution required and would halve the read-out time.
iii) Many linear sensors (including the S9227-03) have the capability of starting the following exposure while the previous scan is read out. This overlap of operations would reduce the total time for a single scan.
iv) Replacing the 4mm diameter lasers with 1mm diameter lasers. Focusing the beam power on a smaller point would increase the intensity on the central pixels and allow the exposure time to be reduced.
v) Faster microcontroller – this would reduce processing time and allow more complex algorithms to be used.
vi) Choosing a faster ADC for analogue pixel readout. Either an independent ADC or a microcontroller with faster peripheral ADC. If an independent ADC is used the speed of digital input of the microcontroller would be important too.

More complex algorithms were considered for both the plant discrimination and for the strike aggregation. Different shaped criteria as well as a generalised distance scheme and other statistical methods were considered for the plant discrimination. The aggregation method could also be improved to make better use of the clustering of individual beam strikes associated with an individual

plant. However, these methods would all require more processing time and the simple algorithms were sufficient to demonstrate successful discrimination of different plants as shown in Chapter 5.

4.5 Summary

Three revisions of the prototype weed sensor have been presented in this chapter. The important design elements have been explained and the effect of these components on the operation of the weed sensor shown. The difficulty measuring the spectral properties of plants from a moving platform are evident in the care required to have a stable and reliable system. This work has culminated in a design which is effective and will explore the potential of reflectance spectroscopy to discriminate different plants with only a small number of narrow wavebands.

Chapter 5

Experimental Data and Discussion

5.1 Introduction

A survey of the spectral reflectance of leaves from various crops and weeds was conducted to assess the potential application of the prototype weed sensor in several intensively farmed Australian crops. Six field trips to Queensland, Australia (Qld), were conducted over a period from July 2008 to Jan 2009, each about a month apart. Two farms were visited during these trips: a cotton and cereal farm near Dalby, and a sugar cane farm near Bundaberg, Qld. The spectral reflectance data collected during these field trips was used to conduct a discriminant analysis using a small number of wavelengths to show the potential for weed detection over the period of the growing season. There are many factors which affect the spectral reflectance of individual plants and this analysis gave a sense of the possibility for using such a system over the whole growing season.

At each stage of the prototype weed sensor's development, its ability to detect and discriminate between different plants was assessed. This assessment was carried out under various conditions: stationary in the lab, simulated dynamic conditions in the lab, stationary while outdoors and at low speed on a testing ground under shade. The initial prototype in particular could not be tested outdoors, but the second and final prototypes were attached to a quad bike for dynamic testing of their plant detection performance.

5.2 Spectral reflectance of crops and weeds

The spectral reflectance of leaves belonging to crops and weeds was recorded over a period of up to three months at two different sites in Queensland, Australia. The target industries were sugar cane and cotton farming. In addition two cereal crops were also examined, wheat and sorghum. The primary application for this work is to enable automatic detection of weeds for spot spraying. This requires classifying plants as either the crop or other plant (and therefore a weed to be sprayed). Previous studies with hyperspectral reflectance measurements found an increase in spectral resolution to be important for accurate identification and characterization of biophysical parameters such as species type [56]. With the increased spectral resolution there is some added complexity to using hyperspectral data. The increased volume of data leads to longer processing times and complex algorithms for data processing. The analysis of spectral data conducted here aimed to find optimal wavelengths for identification of these individual crops among their surrounding plants.

5.2.1 Survey for spectral reflectance of plants

The cotton (*Gossypium hisutum)*, wheat (*Triticum aestivum*) and sorghum (*Sorghum bicolor*) were located at Arrawatta farm near Dalby, Qld. Dalby is in the Darling Downs region of Queensland which is a productive agricultural region covering approximately 8 million hectares. Due to different growing seasons the wheat was recorded in July and September while the cotton and sorghum where measured monthly from October to January. Five weeds were monitored when they were present during this period: flaxleaf fleabane (*Conyza bonariensis*), sow thistle (*Sonchus oleraceus*), climbing buckwheat (*Fallopia convolvulus*), sesbania pea (*Sesbania cannabina*) and feathertop Rhodes grass (*Chloris virgata*). There are many more weeds which are prevalent on cotton farms in eastern Australia, these five are included in this survey due to their presence at Arrawatta farm and because they are widespread problems [73] or in the case of fleabane, emerging problems – particularly for minimum till farming operations [74].

Figure 5.1. Cotton field at Arrawatta farm, near Dalby, Queensland. (Photo taken December 2008).

The sugar cane (*Saccharum* spp.) spectral reflectance data was recorded at Fairymead farm near Bundaberg, which is in one of the main sugar growing regions on the east coast of Australia. Four visits were made to Fairymead from October to January where spectral reflectance of sugar cane and major weeds were recorded. The two weeds monitored were guinea grass (*Panicum maximum*) and Johnson grass (*Sorghum halepense*), both perennial grasses. Like all crops, competition from weeds in sugarcane can significantly reduce yield. In addition, the burden of perennial grasses can build each year culminating in yield reduction which makes cropping uneconomically viable. The available management options are to manually control the perennial grasses with hand-held spot spraying or to plough out the cane and perennial weeds and then replant the field (often with an intervening rotation crop for one season). The replanting cost is a significant fraction of the total cost for the 3-7 year production cycle. For this reason in particular, automated precision weed spot spraying in the sugarcane industry has significant potential economic benefits [75, 76].

Figure 5.2. A sugar cane field at Fairymead, near Bundaberg, Queelsland.

Two fibre spectrometers were used to measure the spectral reflectance over the range from 400-2100 nm. The fibre probe used examines a small area on a leaf (approx 3 mm in diameter) allowing the spectral reflectance of the leaf alone to be recorded. The diffusely reflected light is captured by orienting the fibre probe at 45° to the leaf – avoiding the specular reflection from the surface of the leaf. Both spectrometers could be operated from a vehicle battery power supply, along with a laptop for control and data recording. The detailed procedure used for spectral reflectance measurement is described in Section 3.2.

5.2.2 Discriminant analysis of spectral reflectance

The field surveys conducted during this project contributed to creating a database of spectral reflectance characteristics for several crops and a range of common weeds. The leaf level spectral reflectance data recorded closely matches the scale of the reflectance measurement made by the prototype weed sensor. However there is far greater spectral information available from the spectrometer which it is not possible to gather with single laser reflectance measurements. The use of this spectral data to validate the weed sensor design required significant reduction in the spectral information density. After selection of a small number of wavelengths, a discriminant analysis was performed to test the potential for discrimination of crop from weeds based on these selected wavelengths.

For each survey conducted a selection of spectral data was made from each crop and weed species. Samples from weeds which were flowering were recorded, but excluded from this analysis. The selection was based on

approximate age and size of the plants to include crops that were in their early growing stage (when in crop herbicide application is most important). Samples from young weeds only (i.e. not flowering) were included on the basis that the presence of old weeds is unlikely due to pre-emergent weed treatment.

For each species the selected samples were divided into two sets on a chronological basis. In each case the set from the youngest plants was used as a training set for the discriminant analysis and the other set was used to validate the discriminant criterion developed. The wavelengths selected for the analysis were based on the discussion in Section 3.2. Wavelengths included were based on readily available laser diodes and the wavelength of other prominent spectral features. The NIR spectrometer data (above 870 nm) was not used in this analysis because including them in the prototype weed sensor would require using a line sensor sensitive to NIR light and cooling the sensor to avoid thermal noise affecting the sensor response.

Prior to the discriminant analysis some pre-processing was required. The spectral resolution of the visible spectrometer is approximately 0.3 nm. For each wavelength chosen all data within a 3 nm wide band were averaged. This reduced the noise present in the spectral data, particularly near the extremes of the wavelength range. Despite the calibration process used which provided very good relative spectral reflectance there was a large error in the absolute reflectance due to geometrical effects in the optical setup. The proximity of the optical fibre probe to the sample meant any surface roughness or shift in leaf position changed the distance from probe to sample. The fraction of reflected light captured by the probe and returned to the spectrometer was affected by this distance. To prevent the discriminant analysis being affected by this error the variables used in the discriminant analysis were normalised difference indices, calculated in the same way as the NDVI used by the prototype weed sensor. Two wavelengths (750 nm and 785 nm) in the NIR plateaux of the reflectance spectra were used to normalise the other wavelengths using Equations 5.1 and 5.2. The complete set of wavelengths used was λ = 470, 530, 635, 670, 685, 750, 785 and 810 nm.

$$NDI_{750\_\lambda i} = \frac{R_{750} - R_{\lambda i}}{R_{750} + R_{\lambda i}} \times 1000 \qquad (5.1)$$

$$NDI_{785\_\lambda i} = \frac{R_{785} - R_{\lambda i}}{R_{785} + R_{\lambda i}} \times 1000 \quad (5.2)$$

Predictive discriminant analysis measures the variance in variables such as the NDI values (known as the predictive variables) and determines an equation which is a function of these variables. This discriminant criterion is then used to predict which group a sample belongs to, also known as classification. The software used to perform the discriminant analysis was Octave [77] with the 'nan' statistics package. Two classifiers were trialled: a linear discriminant analysis (LDA) and a generalised distance based classifier (GDBC) [78]. The GDBC consistently performed better than the LDA so only results based on the GDBC are presented here.

Combinations of two to six NDI values selected from those normalised by either 750 or 785 nm were entered into the discriminant analysis. For each combination of NDIs the discriminant analysis used the training set of data to determine a discriminant criterion. This criterion was then tested by applying it to the training set (re-substitution) and to the testing set (validation). Evaluation of the classification performance was based on the error rate from both sets, particularly the validation result. A slight emphasis was placed on the crop / weed and weed / crop overall error rates *i.e*. the weed-weed error rate is not as important.

5.2.3 Spectral reflectance of cotton, sorghum and wheat

During the six field trips to Arrawatta farm each of the three crops and five weeds were monitored when they were present. The wheat was harvested after the September trip and the sorghum and cotton germinated prior to the October trip. Average spectra for each species are shown in Figure 5.3.

For the discriminant analysis, only measurements taken prior to flowering and seed set were used. For wheat this meant that only the data for July was used; for sorghum, data from October and November was used; and for cotton, data from October, November and December was used. The weed spectra were selected to only include young weeds and those not yet flowering. This meant that there was only a small sample size which couldn't be divided into separate

training and testing sets. The classifier test therefore relied on re-substitution for the weeds which would decrease the error rate observed.

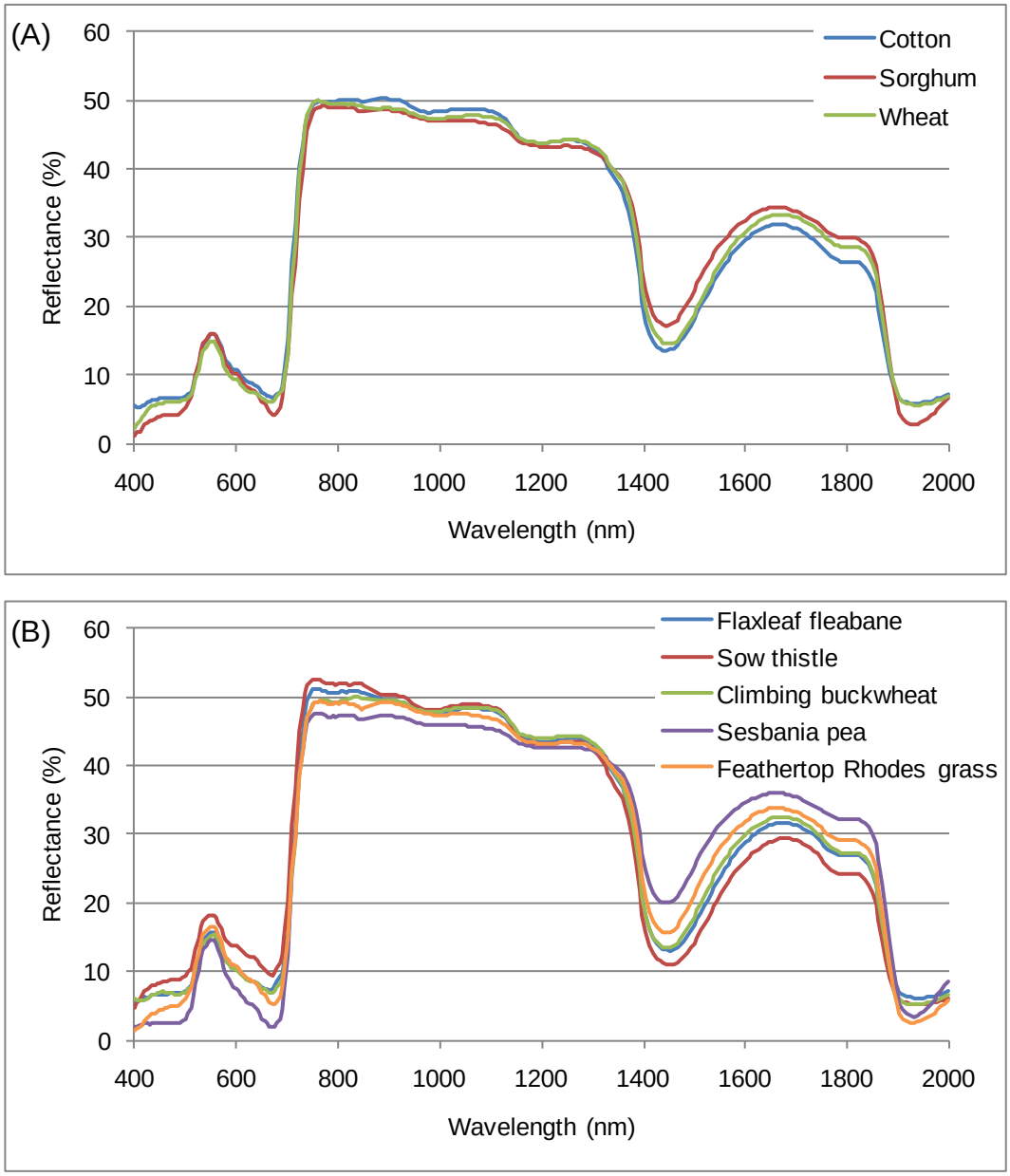

Figure 5.3. Average spectral reflectance curves for (A) three crops; and (B) five weeds. Spectra from Arrawatta farm near Dalby, Qld. A standard normal variate transform was applied to remove geometrical effects prior to averaging over multiple spectra for each species.

For all crops there was generally improvement in classification rate with increasing number of NDIs used, up to the maximum of five different indices. Tables 5.1, 5.2 and 5.3 give the classification results for test data with the

highest performing discrimination criterion. In most cases there was only a small difference between using 750 or 785 nm for normalization and a similarly small difference when using either the 670 or 685 nm NDI.

In some situations as few as two variables also provided good classification for sorghum. Two NDI provided equal performance for crop classification on the test data however weed classification was significantly worse. Similarly NDI_{785_635} and NDI_{785_685} correctly classified 30/36 of the cotton training samples in the training set and 31/36 from the testing set. Again, the error rate for weeds classified as crop increased from 0% to 5%.

Table 5.1. Classification results for cotton and weeds using a Generalised Distance Based Classifier with 5 normalised indices: NDI_{785_470}, NDI_{785_530}, NDI_{785_635}, NDI_{785_670}, and NDI_{785_810}.

	Predicted Species						Total	Error % total
Actual Species	Cotton	F. F.	Milk thistle	C. B.	S.P.	Ft. R. grass		
Cotton	32	4	0	0	0	0	36	3.3
Flaxleaf fleabane	0	18	1	0	0	0	19	0.8
Milk thistle	0	0	15	0	3	0	18	2.5
Climbing buckwheat	0	1	0	11	0	0	12	0.8
Sesbania pea	0	0	1	0	16	0	17	0.8
Feathertop Rhodes grass	0	0	1	0	0	17	18	0.8
							120	10.8

Table 5.2. Classification results for sorghum and weeds using a Generalised Distance Based Classifier with 5 normalised indices: NDI_{750_470}, NDI_{750_530}, NDI_{750_635}, NDI_{750_670}, and NDI_{750_810}.

	Predicted Species						Total	Error % total
Actual Species	Sorg.	F. F.	Milk thistle	C. B.	S.P.	Ft. R. grass		
Sorghum	12	0	4	0	0	2	18	5.9
Flaxleaf fleabane	0	15	0	4	0	0	19	3.9
Milk thistle	0	0	16	0	2	0	18	2
Climbing buckwheat	0	1	0	11	0	0	12	1
Sesbania pea	0	0	1	0	16	0	17	1
Feathertop Rhodes grass	0	0	0	0	0	18	18	0
							102	13.8

Table 5.3. Classification results for wheat and weeds (training set) using a Generalised Distance Based Classifier with 5 normalised indices: NDI_{750_470}, NDI_{750_530}, NDI_{750_635}, NDI_{750_670}, and NDI_{750_810}.

	Predicted Species						Total	Error % total
Actual Species	Wheat	F. F.	Milk thistle	C. B.	S.P.	Ft. R. grass		
Wheat	28	3	0	1	0	0	32	3.4
Flaxleaf fleabane	0	16	0	3	0	0	19	2.6
Milk thistle	0	0	16	0	2	0	18	1.7
Climbing buckwheat	0	1	0	11	0	0	12	0.9
Sesbania pea	0	0	1	0	16	0	17	0.9
Feathertop Rhodes grass	0	0	0	0	0	18	18	0
							116	9.5

These results are promising for the use of a weed sensor with only three wavelengths but the scope of application will be limited. There is a need to

determine the extent to which these differences in spectral properties are maintained with a wider range of growing conditions. Additionally the prototype weed sensor would not be able to perform as well as classification based on carefully collected spectral reflectance data with a calibrated spectrometer if it relied on spectral data alone. However, there is the potential to extract and use leaf size information, particularly for a crop like cotton, with the dynamic nature of the data collection. Combined with the spectral information this would be able to provide an effective sensor for precision spot spraying of weeds in cotton and other broad-acre crops.

5.2.4 Spectral reflectance of sugar cane

During the four field trips to Fairymead spectral reflectance measurements were undertaken with five different varieties of sugarcane and the two weeds which are most problematic: guinea grass and Johnson grass. During the final trip in January all the cane plants were above 1.5 m in height. It would not be feasible to apply herbicide at this stage due to the crop height and density so these results were not included in the analysis. The guinea grass and Johnson grass reflectance measurements used were selected from those made at times when the weeds were not flowering. Figure 5.4 shows the average spectral reflectance from a small number of samples for these three plants. There is only small variation evident; however a discriminant analysis demonstrated the potential to use spectral reflectance properties to detect guinea grass in particular, and to a lesser extent Johnson grass, in sugar cane.

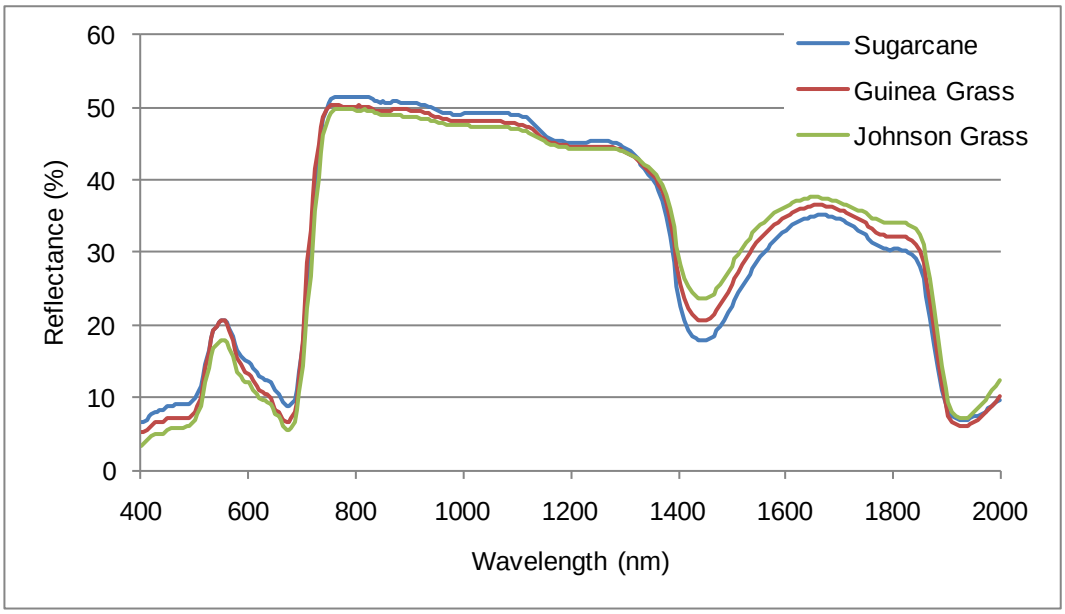

Figure 5.4. Average spectral reflectance curves for sugarcane and problem weeds at Fairymead farm in Bundaberg. A standard normal variate transform was applied to remove geometrical effects prior to averaging over multiple spectra for each species.

A total of 200 sugar cane samples, 66 guinea grass samples and 44 Johnson grass samples were selected for this analysis. As described above these samples were divided based on chronological order so that the training set contained samples recorded from October and November, and the validation set contained samples from November and December (and January for guinea grass). As for cotton, wheat and sorghum there was improvement in the error rate with increasing number of indices. With most combinations of indices there was also little change in error rate with either 785 or 750 nm used for normalization. The best combination of indices was found to be: NDI_{750_470}, NDI_{750_530}, NDI_{750_635}, NDI_{750_670}, and NDI_{750_810}. Tables 5.4 and 5.5 give the classification results for re-substitution and for validation of the discriminant criterion.

Table 5.4. Classification results for training data using a generalised distance based classifier with 5 normalised indices: NDI_{750_470}, NDI_{750_530}, NDI_{750_635}, NDI_{750_670}, and NDI_{750_810}.

Actual Species	Predicted Species			Total	Error % total
	Sugar cane	Guinea grass	Johnson grass		
Sugar cane	83	3	14	100	11
Guinea grass	0	33	0	33	0
Johnson grass	1	1	20	22	1.3
				155	12.3

Table 5.5. Classification results for validation data using a generalised distance based classifier with 5 normalised indices: NDI_{750_470}, NDI_{750_530}, NDI_{750_635}, NDI_{750_670}, and NDI_{750_810}.

Species	Predicted Species			Total	Error % total
	Sugar cane	Guinea grass	Johnson grass		
Sugar cane	73	10	17	100	17.4
Guinea grass	3	30	0	33	1.9
Johnson grass	12	3	7	22	9.7
				155	29.0

In the re-substitution test the weeds classified as crop error rate is very low (3.6 %) but crop classifieds as weeds error rate is 17 %. Most of these samples are assigned to Johnson grass. The validation test results are not as good, particularly classification of Johnson grass, where over half the samples were classified as sugar cane. The error rate for sugar cane also increased with 27 % classified as either guinea grass or Johnson grass. While these error rates seem high it may be possible to use this information to target guinea grass while leaving 90 % of the sugar cane. Due to the way sugar cane grows a small number of lost plants early in the growing season need not affect the yield because neighbouring plants can utilise the resources made available. Additionally the longer term effect of better guinea grass control within the crop row can provide significant economic benefit.

With only three wavelengths the error rate is significantly higher. Table 5.6 shows the classification results for the validation set using the best combination of three wavelengths: λ = 635, 685, 785 nm. This is a poor result, however targeting of guinea grass alone may still be feasible. This analysis included a larger variation in spectral reflectance due to the sampling of plants over a period of four months. While a weed sensing system needs to be able to operate without manual adjustment of discrimination parameters, the error rate for guinea grass detection may be low enough when the system is calibrated for the spectral reflectance properties at one particular growing stage. There were insufficient guinea grass samples collected at a single growing stage from a single field trip to undertake a discriminant analysis.

Table 5.6. Classification results for validation data using a generalised distance based classifier with 2 normalised indices: NDI_{785_635}, NDI_{785_685}.

Species	Predicted Species			Total	Error % total
	Sugar cane	Guinea grass	Johnson grass		
Sugar cane	50	20	30	100	32.3
Guinea grass	8	23	2	33	6.5
Johnson grass	13	5	4	22	11.0
				155	49.8

A potential problem with both this analysis and the one in Section 5.2.3 was that the NDI variables used in the analysis were normalised with the same reflectance value, either R_{750} or R_{785}. Some form of normalisation is required and using a single reflectance value to do so may be the best option. However, it would also be possible to form NDI values where there are no wavelengths in common and conduct a similar discriminant analysis.

There is a need to determine if the prototype weed sensor would be capable of the same discrimination performance, particularly with a reduced number of wavelengths and additional error in measurement of the spectral response. Additionally the weed sensor would be able to use leaf size information and leaf density information as suggested by Rees *et al.* [75] which is not available in this discriminant analysis. This capability would ultimately lead towards the

development of a weed sensor for use in the precision spraying of guinea grass in sugar cane.

5.3 Experimental data for initial prototype

The initial prototype weed sensor was developed prior to the start of this thesis. It's potential to discriminate four different plants was reported in [10] and the discrimination of four plants is shown in Figure 5.5. Each box surrounds the slope data recorded for each plant and is derived from the mean +/- 2 times the standard deviation for the spectral slopes of each plant. Due to the high variability of the line scan camera reported in Section 3.6.2 it was necessary to calculate the slopes as an average of the slope for four beams.

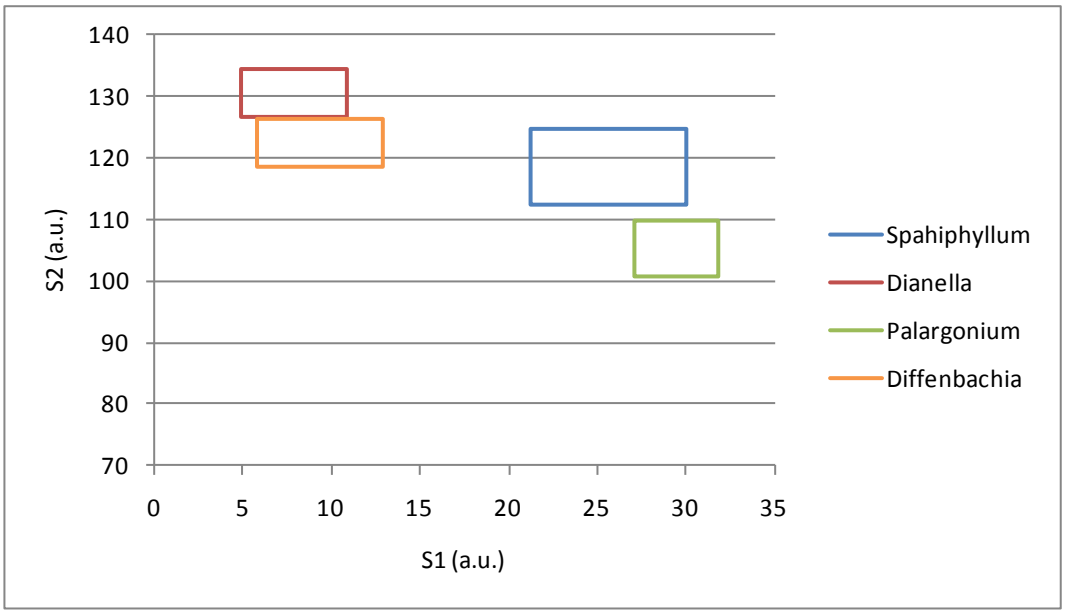

Figure 5.5. Discrimination of four plants based on slopes S1 and S2. (Source: [10].)

The ability of the initial prototype weed sensor to detect plants at typical farming speed was tested by simulating vehicle movement with leaf samples mounted on a rotating stage. This test was conducted under static conditions and at average linear velocities of 7 and 22 km/h with a single leaf of Spathiphyllum fixed to the rotating stage. For this experiment the laser drivers were replaced with constant current drivers to allow the lasers to be switched at the high speed required. The weed sensor was continuously carrying out the operations described in Section 4.2.1 and recorded the calculated spectral properties of the

leaf whenever it was detected – determined by the NDVI value being larger than a threshold of 500. All calculated values of S1, S2 and NDVI presented in Figure 5.6 are for 30 mm wide Spathiphyllum leaves covering 4 laser beams at distances of 58 cm, 69 cm and 80 cm from the weed sensor. Each data point is an average over 10 measurements from each of four laser beams illuminating the leaf. There is no significant change in the calculated values of S1, S2 and NDVI for variation in the distance to the leaf sample or for simulated speeds of 7 and 22 km/h. These results were reported in Paap *et al.* [79].

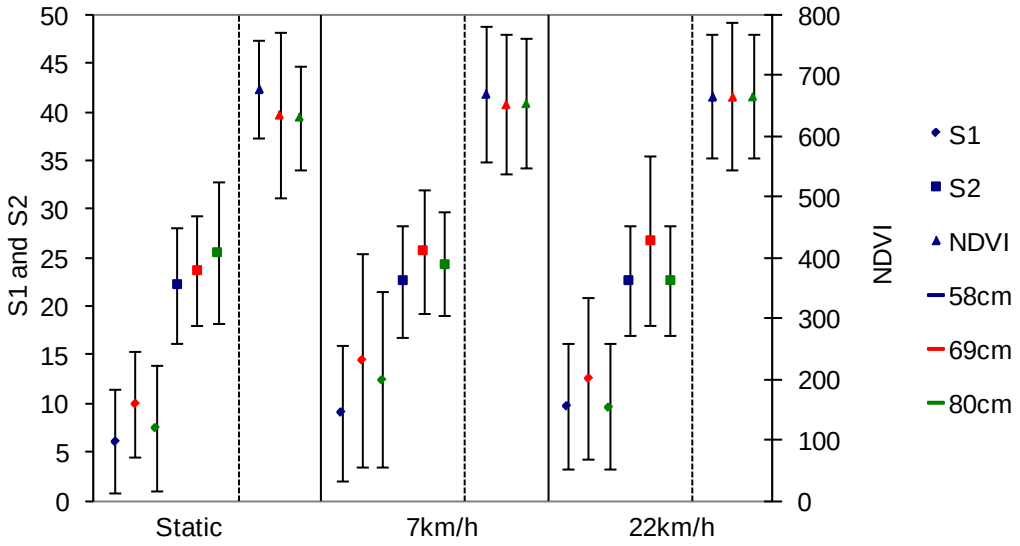

Figure 5.6. Average values of S1 (diamond), S2 (square) and NDVI (triangle) for static, 7 km/h and 22 km/h measurements of Spathiphyllum leaf at different distances. S1 and S2 are plotted against the left axis and NDVI against the right axis. Blue – 58 cm; Red – 69 cm; and Green – 80 cm.

5.3.1 Initial plant discrimination results

In order for the weed sensor to be used without the requirement of a large leaf covering four beams it was required that each beam be able to discriminate plants individually. A static discrimination trial with single leaves from four plants was conducted using the quadratic peak fitting method to determine peak values and the spectral slopes calculated independently for seven of the 28 beams. The four plants used were *Spathiphyllum sp.*, *Anthurium sp.*, *Acacia saligna* and *Eucalyptus marginata*. Forty measurements were recorded by each beam across the surface of the leaf. The average and standard deviation

of the slope values recorded from each leaf by a single beam are shown in Figure 5.7. There is significant overlap in this case which prevents this data being used to discriminate the plants reliably. The increased variability with respect to Figure 5.5 includes the increase due to using only a single beam in place of averaging over four beams and additionally includes variation from the surface of the leaf.

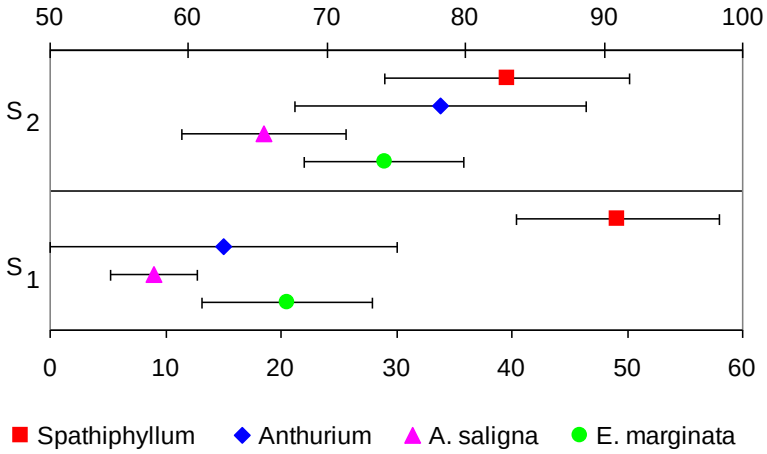

Figure 5.7. Spectral slope values determined by initial prototype weed sensor for single leaves from four plants under static laboratory conditions. Average S1 and S2 ± standard deviation of 40 samples across the surface of the leaf.

This analysis of the performance of the weed sensor highlighted the need for an improved prototype. The variability of the measurements presented in Figure 5.6 and Figure 5.7 is due to fluctuations in the response of the line scan sensor and variation in the optical power of the laser diodes in time. Additionally the reduced optical power in beams closer to the sensor resulting from the uniform coating on the optical cavity was too low to be used for measurement of leaf spectral properties. These problems were addressed in the second prototype weed sensor.

5.4 Experimental data for improved prototype

The goal for the design of the prototype weed sensor was for the sensor to be able to reliably discriminate between a limited number of plants with as little as a single leaf illuminated by any one of the thirty beams. Meeting this goal would ensure that the sensor when used in agriculture would be able to detect and

spot spray weeds down to a size of 30 mm across. The development of the prototype described in Section 4.3 worked towards this goal by improving the stability of the reflected light measurement and building a robust device which could be operated independently under outdoor field conditions.

5.4.1 Discrimination criterion

Discrimination of plants with the original prototype weed sensor was only possible when the slope values were averaged over four beams incident on the same leaf. The reduction in variability of the sensor response achieved with the improved prototype allowed individual beams to be used for discrimination. This improvement is reflected in the results shown in Figure 5.3. The prototype weed sensor was used to measure the reflectance of the same four leaves used in the experiment shown in Figure 5.6. The values of spectral slopes for the same four leaves are shown. These values were determined from a single beam and are the average of 40 measurements of S_1 and S_2 ± standard deviation across the surface of the leaf.

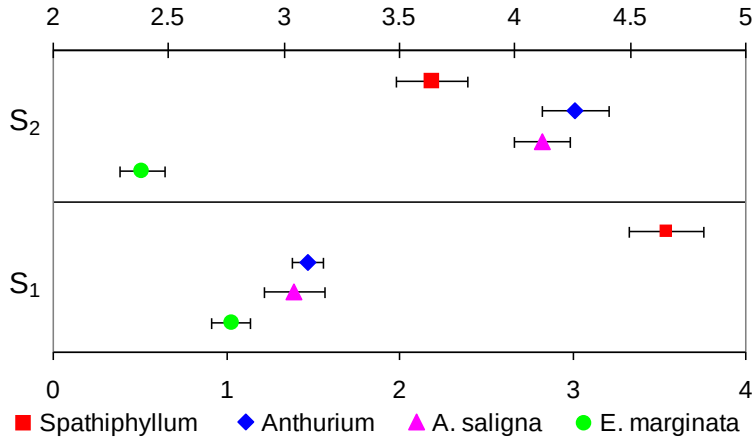

Figure 5.8. Average slope values S_1 and S_2 (arbitrary units) for four sample plants as determined by the improved prototype weed sensor, PDU2. Error bars represent standard deviation of 40 samples across the leaf surface.

This was a promising result but there was still difficulty using each individual beam. The discrimination criterion which were determined from this experiment could be used to discriminate three of the four plants from each other. There was considerable overlap between the recorded slope values for Anthurium and for *A. saligna* and these two plants were detected as the same plant. However,

when this same criterion was applied to other beams it failed to correctly classify the plants. Several methods of compensating for this beam variation were explored. Figure 5.9 shows the results of one of these techniques trialed. The slope values calculated with the standard algorithm show significant difference from each other and the corrected values are an improvement, but not sufficient to use the same criteria for each beam. Additionally some beams showed overlapping slope values for the two leaves and other beams were separated.

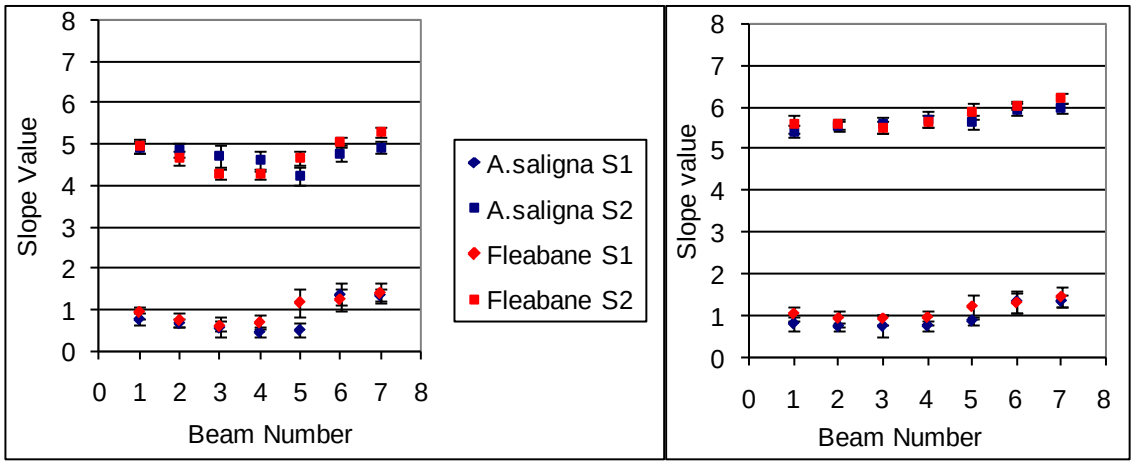

(A) (B)

Figure 5.9. Slope values for two plants measured with seven different beams (A) using standard algorithm and (B) using a correction determined by characterisation of each beam with a reflectance standard.

Using the same data, two normalized difference indices (RDI and NDVI) were calculated and are shown in Figure 5.10. The same correction was also applied to the NDIs. There is a clear separation between the NDVI values recorded for the two plants and the values are reasonably uniform across the seven beams. The RDI values are also separated for each beam individually but several beams show large differences in the average value. The corrected NDVI and RDI values appear to have improvement in the beam variation. This data was recorded using the computer and LabVIEW software described in Section 4.3.3. Following on from this work the embedded controller described in Section 4.3.6 was built. The controller was initially used to demonstrate green from brown detection in dynamic outdoor conditions as opposed to the stationary laboratory work carried out up until that point. However the green from green algorithm

implemented in the controller used the NDIs in place of the slopes used previously.

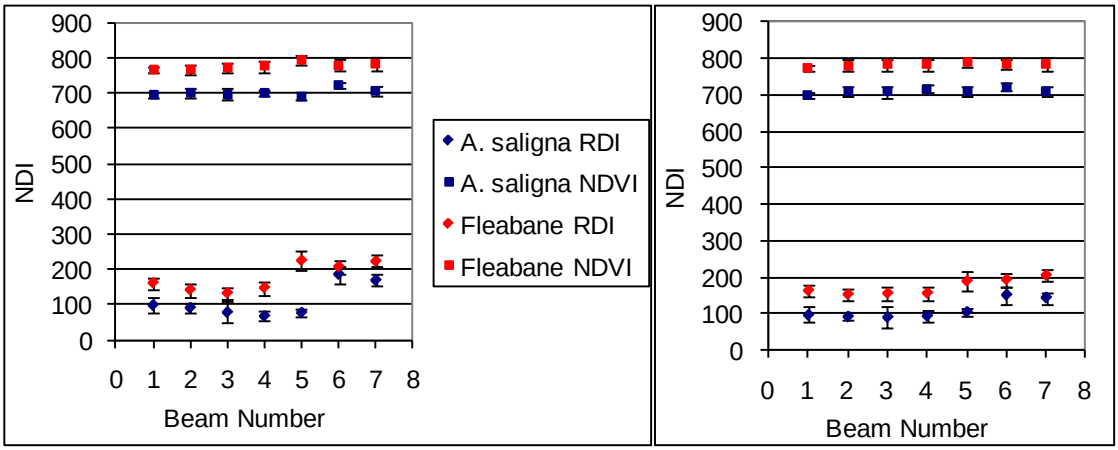

(A) (B)

Figure 5.10. NDI values for two plants measured with seven different beams (A) using standard algorithm and (B) using a correction determined by characterisation of each beam with a reflectance standard.

5.4.2 Outdoor dynamic testing

The slope values used previously worked well under laboratory conditions. For outdoor dynamic conditions the slopes were no longer suitable because there are many factors which influence the reflected light and affect the slope values. The normalization of the NDI values removes many of these factors and provides consistent measurement of the spectral properties of a target.

The outdoor testing with the improved weed sensor prototype began with static testing to determine the effect of background light on the sensor. The solar filter used on the camera was effective at blocking a significant fraction of the background light, but the prototype could only be operated reliably in shady conditions. The green from brown performance was very good. The sensor was able to detect lawn reliably when driving on and off paths around the lawn. Small patches of grass were also detected, even when only one beam was incident on a small patch. Green from green detection under outdoor conditions was not successful and even indoors proved to be unreliable. The design of the weed sensor was refined further as described in 4.4 in order to solve this problem.

5.5 Experimental data for final prototype

The final revision of the prototype weed sensor was designed to overcome the difficulty with determining accurate spectral properties of plants experienced with the previous prototype. The prototype described in Section 4.5 had significantly improved response for the red lasers reflected from leaves. However it was also more sensitive to background light and required a shroud to be operated during daytime, even in shady conditions. Figure 5.11 shows the prototype (PDU) and aluminium shroud mounted on a frame attached to the quad bike. A sunkisses plant can be seen in the middle of the shroud in front of the laser beam array.

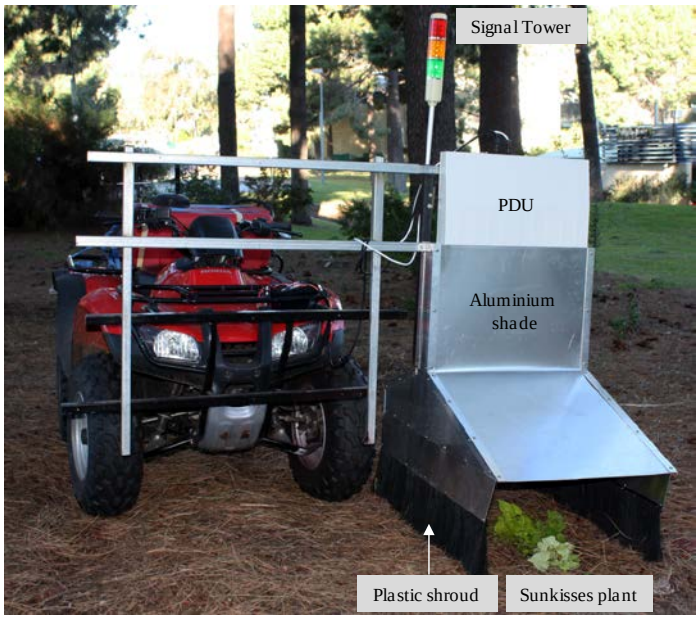

Figure 5.11. Dynamic testing of the final prototype weed sensor assembled on a quad bike. An aluminium shroud with plastic brushing down to the ground on the sides is used to block background light.

5.5.1 Dynamic testing

Figure 5.12 shows the four images captured in single scan while the quad bike travelled at approximately 3 km/h. Only one half of the camera's field of view is shown. Several leaves are covered by beams in the centre of the image as can be identified by the beams with a high 785 nm response and a low 685 nm response. Several examples of data which were difficult for the original algorithm to process can be seen. From the right hand side, between the first

two beams the 785 nm response is significantly above the background level. This is believed to be due to the high fraction of near infra-red light scattered from the surface of leaves and then reflected back to the image sensor from another leaf or part of the leaf. The fourth beam from the right has very low response for all wavelengths. This beam was likely obscured in part by a leaf or only a fraction of the beam incident on a leaf. Discrimination with this beam would not be reliable, but the peak must be detected so that the remaining peaks are assigned the correct beam number prior to peak normalization. Lastly, the ninth/tenth beams are problematic. There may be one beam incident split over two leaves or two beams which have almost been merged on the line scan sensor. This beam should also be rejected as spectral properties calculated from the beam are likely to be inaccurate.

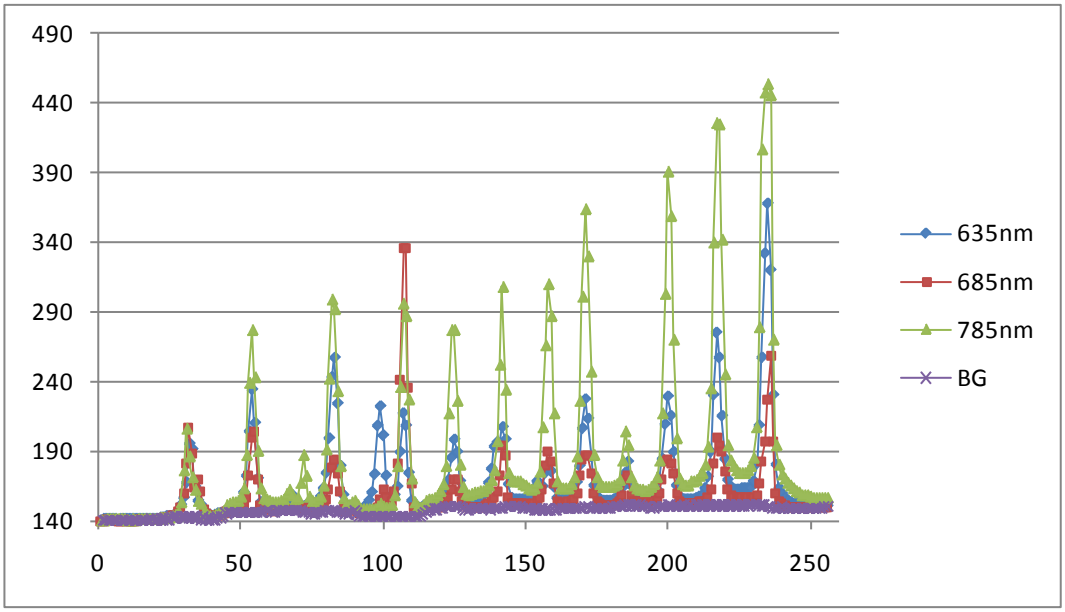

Figure 5.12. Line scan data from final prototype weed sensor over a sunkisses plant. Response for 15 beams visible in half of the field of view. Travel speed was 3 km/h. Eight of the beams entirely incident on a leaf. Several beams are obscured from the sensor by the plant.

5.5.2 Discrimination of three plants

The discrimination performance of the weed sensor was tested with a discrimination trial carried out with three plants growing in pots (anthurium (*Anthurium andraeanum*), sunkisses (*Ipomoea batatas* var. sunkisses) and dandelion (*Taraxacum officinale*)). To determine the discrimination parameters

$NDVI_{635}$ and $NDVI_{685}$ the spectral properties of a leaf for each plant were measured under laboratory conditions. Ten sets of data from three spots on each leaf were collected. The angle of each leaf was 20° from normal incidence of the incident light to avoid specular reflection returning to the line scan sensor. Figure 5.13 shows the calculated $NDVI_{635}$ and $NDVI_{685}$ parameters for three plants. The values for these parameters are concentrated in three non-intersecting parallelograms. The coordinates for each parallelogram were determined and used as the initial discrimination criterion for the outdoor dynamic test.

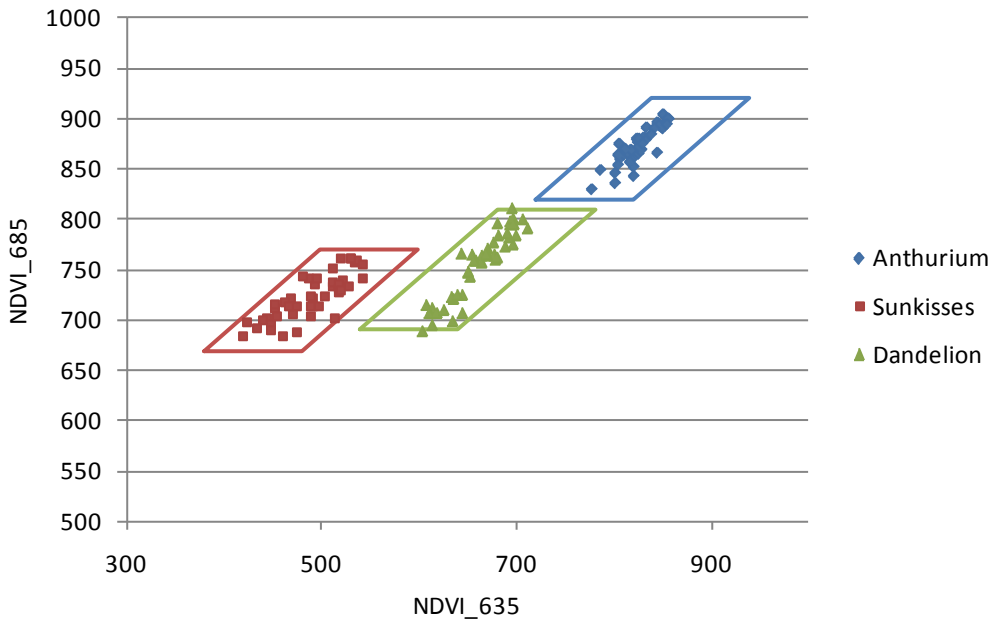

Figure 5.13. NDVI scatter plot for single leaves from three plants using final prototype weed sensor in laboratory conditions.

The three plants were placed in the ground on a testing circuit and the quad bike driven around the circuit at an average travelling speed of 3 km/h. The spectral properties were recorded for a single pass over each plant and are shown on a scatter-plot in Figure 5.14. The distribution for each plant is significantly more spread out under dynamic conditions for a number of reasons. The variation of spectral reflectance across the plant is one factor and the dynamic nature of the measurements is another. Additionally some of the points in the graph will have been measured with one of the scans recording a beam half on or half off the leaf. The simple aggregation method described in Section 4.4.2 is sufficient to correctly detect each plant with a threshold of 15.

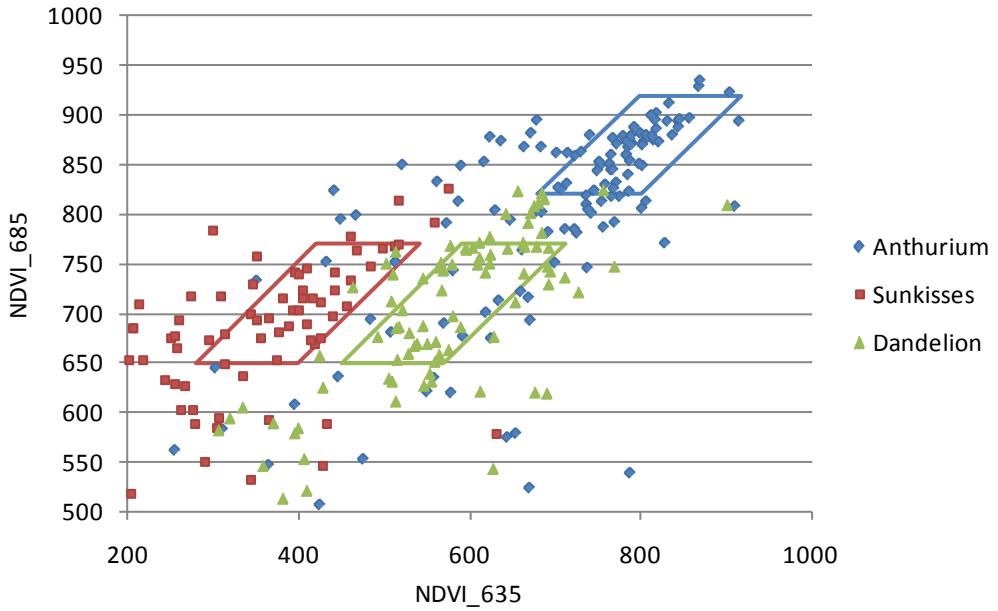

Figure 5.14. NDVI scatterplot for a single pass over three plants recorded by final prototype weed sensor travelling at 3 km/h. Each plant is correctly detected with an aggregation threshold of 15 and no false positives are recorded.

These discrimination criteria determined from one single plant specimen for each species were tested on multiple plants for two of the species (anthurium and sunkisses). Four of each plant species were placed on the testing ground and the quad bike driven around the circuit at a speed of approximately 5 km/h. The detection rate for all four anthurium plants was 100%, but the detection rate for sunkisses was lower, ranging from 3 out of 10 to 9 out of 10. See Table 5.6 for results. No false positives for either plant were recorded. Further investigation of the plant labelled Sk4 showed that it had a slightly different average NDVI values across the leaf surface. A slight adjustment of the discrimination criterion allowed all of the plants to be detected on 90-100% of passes over the plant.

Table 5.6. Detection results for 8 plants of two species in a discrimination trial with the final prototype weed sensor.

	Detection Result		
Actual Plant	Green	Sunkisses	Anthurium
A1	10	0	10
A2	10	0	10
A3	10	0	10
A4	10	0	10
Sk1	10	9	0
Sk2	10	7	0
Sk3	10	7	0
Sk4	10	3	0

5.6 Conclusion

A survey to measure spectral reflectance of crops and common weeds over a period of the growing cycle was conducted. Broad-acre cotton, sorghum and wheat were measured on one farm over a period of 2-4 months along with the problem weeds (as identified by the farmer) growing in or near those crops. Another survey was conducted over four months at a sugarcane farm to monitor the spectral reflectance of sugar cane and two major weeds: guinea grass and Johnson grass. Discriminant analyses were carried out using a limited number of narrow wavebands selected from the survey data. There were good results for cotton, sorghum and wheat using five normalised difference indices formed from six wavelengths. In sugarcane, guinea grass was the most well separated weed and could be detected with 6 wavebands. Using only the three wavebands corresponding to the lasers used in the prototype weed sensor presented here did not give a good result for the combined data from the whole growing season. There is the potential for good results when limited to a single stage of the crop growth, or a combination of the spectral data and spatial features.

The prototype weed sensor developed throughout this thesis is capable of limited discrimination of green plants. It is based on measuring the spectral reflectance at three narrow wavebands using illumination by laser light. Developing a stable and fast laser switching circuit combined with measuring the reflected intensity using a high dynamic range line scan sensor have proved to be the most important steps in improving the performance of the weed sensor. It has been demonstrated to reliably detect two different broadleaved plants at a speed of 5 km/h with several different possibilities for increasing the speed of operation without affecting the discrimination performance. The prototype weed sensor needs to be tested on the farm to determine which crops it might be used in and which weeds it will be able to detect and spray.

Chapter 6

Conclusion and Future Development

6.1 Summary of results

The presence of weeds in agriculture affects the production and quality of crops grown and can also harm the health of livestock. In agricultural crops, weeds compete with crops for water, light and the nutrients in the soil. Competition from weeds reduces the quantity of the harvested crop and can affect quality through contamination. The presence of weed material that harbours pests and diseases may also adversely affect the crop. Management of agricultural weeds increases the production cost of crops through the required investment in machinery and expenditure on labour and herbicides. This thesis describes the development of a spectral reflectance based sensor for plant discrimination which has the potential to be used in real-time spot spraying of weeds. The project achieved the following:

- Development of the hardware for a prototype weed sensor which transferred plant discrimination capability from the laboratory to an outdoor dynamic trial.

- Development of an embedded controller for this prototype and the software to reliably calculate spectral properties of different plants and discriminate those plants from each other.

- Demonstrated discrimination of green from brown at 10 km/h in outdoor conditions with the sensor attached to a quad bike.

- Demonstrated successful discrimination of three plants from each other at 5 km/h in an outdoor trial with a shroud to block ambient light.

- Showed the potential to discriminate cotton and sugarcane from important weeds growing amongst those crops with > 85-95% accuracy. The analysis used only a small number of narrow wavebands extracted from leaf level spectral reflectance measured with a spectrometer.

6.2 Weed detection with laser-based spectroscopy

Precision agriculture promotes site specific crop management to regulate the inputs to a crop in a way which accounts for the natural variability that exists in the field. This encompasses variation in soil properties, water and fertilizer needs, and crop health. Combined with yield mapping and spatial information technology, variable rate application technology can deliver the optimum rate throughout the crop in order to maximise the farm productivity. Weeds can currently be managed in a site specific way either when there is no crop (fallow weed control) or using weed maps produced from a combination of remote sensing and manual scouting. These weed maps are limited by the time and labour taken to produce them and generally are not as detailed as the true variability in weed density.

An on the ground weed sensor that could detect weeds within the crop in real-time is a missing piece of technology for precision agricultures. Such a sensor would allow variable rate application of herbicides to weeds where it is needed. This would provide significant economic benefit and savings in herbicides and would be an important part of sustainable agricultural practices that increase productivity while minimising degradation of the environment.

The spectral reflectance of plants has been one focus for research into the development of a weed sensor. Remote sensing with multispectral and hyperspectral imaging in the visible and near infrared bands has been used for measurement of a wide range of biophysical parameters, including: vegetation cover, biomass, chlorophyll content, nitrogen and phosphorous deficiency and water stress. Hatfield *et. al*. [53] reviews the wide range of applications and means by which remotely sensed spectral reflectance has been used. This

strong relationship between plants and their spectral reflectance is promising for the development of a weed sensor but also highlights the difficulty brought about by the wide range of factors which can influence spectral reflectance.

Proximate sensors attached to a vehicle provide the ability to be used in real-time. There has been a broad range of research in this area from wide band spectral imaging with colour filters or colour cameras to hyperspectral sensing with spectrographs. These approaches have been reported to provide discrimination of weeds from a number of crops under the conditions they were conducted in. An alternative approach has been machine vision. Image processing involves segmentation of the leaves and plants from the background followed by further analysis to identify the plant. This could include determining leaf shape features, plant organization, texture analysis or combinations of these and other methods. The challenge for all these different methods of plant discrimination is to continue to be reliable under field conditions with non-uniform lighting and changing environmental conditions.

The weed sensor design developed in this thesis is based on the principle of measuring spectral reflectance from leaves using lasers as a narrow-band illumination source. This design was previously described in Sahba *et.* al. [10]. Two revisions of this prototype were developed during this project and all three prototypes were tested for their ability to determine the spectral properties of plants and to discriminate between different species. Each prototype used a laser module to align the output from three lasers using thin-film beam combiners. An optical cavity divides the laser module output into 15 evenly spaced and parallel beams. Each laser is sequentially turned on and the reflected light from the ground and leaves captured by a broadband line-scan sensor. A control system processed the data from the sensor and determined if the calculated spectral properties match those of the target plants.

A survey was conducted which measured the spectral reflectance of cotton, sorghum, wheat and sugarcane crops along with the major weeds growing amongst these crops. This survey was conducted over the growing season in order to assess the impact of changing conditions on the reliability of spectral reflectance to discriminate weeds from the crop. A discriminant analysis of the spectral reflectance data was performed to determine the potential for

application of the prototype weed sensor to weed management in the two cropping systems.

6.3 Conclusions

A weed sensor design based on the principle of measuring spectral reflectance from leaves was the starting point for this project. The weed sensor has been developed through collaboration between the Western Australian Centre of Excellence for MicroPhotonic Systems, Photonics Detection System, Pty Ltd, Australia, and China Daheng Group, China. The outcome of this collaboration was the development of a sensor which used lasers as a narrow-band illumination source to investigate the spectral reflectance of a target leaf. The prototype used a laser module to align the output from three lasers using thin-film beam combiners. An optical cavity divided the laser module output into 15 evenly spaced and parallel beams. Each laser was sequentially turned on and the reflected light from the ground and leaves captured by a broadband line-scan sensor. Crucially, the alignment of lasers and image sensor ensured that for every calculation of spectral reflectance the reflected intensity levels were collected from the same spot on the ground or on a leaf. A control system processed the data from the sensor and determined if the calculated spectral properties matched those of the target plants. This prototype was a bench-top demonstrator with limitations that prevented it from being tested under field conditions.

The system was evaluated to determine its ability to collect and process reflectance data, to calculate spectral properties and to discriminate different plants under laboratory conditions. The main limitations of the prototype's design which prevented its use in field-testing were assessed and an improved prototype designed to address the problems. The low signal to noise ratio of the image sensor, the lack of rigidity of the system and an embedded system that could function independently were addressed with two revisions to the design of the prototype. In addition, the opto-mechanical layout was revised to improve the coverage of ground illuminated by the lasers and the mechanical alignment of the system as well as its rigidity.

An improved prototype using these new designs was built which used laser diodes of three wavelengths (635 nm, 685 nm and 785 nm), constant current laser drivers, optical cavities having non-uniform transmittance on the front surface, a high speed digital line scan sensor, and a custom designed PCB with microcontroller for independent operation. The fast line scan sensor greatly improved variability compared with the original camera and this allowed reliable detection of green-from-brown. This capability was confirmed with the prototype weed sensor mounted on a quad bike and driven at a speed of up to 10 km/h. This is an improvement over the currently available technology as detection was successful even for weeds as small as 30 mm across. The green-from-green performance of this prototype remained unreliable due to errors in calculated NDVI and RDI values. The error originated from the low R_{670} and R_{685} reflectance values combined with low dynamic range of the 8-bit analogue to digital converter (ADC). In addition, the low pixel count of the line scan sensor caused difficulty resolving beams when they were incident on uneven surfaces.

The final prototype design built was a robustly packaged optical sensor with improved laser output stability and a high dynamic range, low noise analogue sensor. The data processing algorithms were improved by taking advantage of the reliability of the 785 nm laser to determine the location of each beam in the image. Normalization of the signals from the two red lasers with the 785 nm laser also improved the reliability. Under dynamic conditions the false positive rate was high and an aggregation algorithm was implemented to contend with this issue. The final design reliably performed green from green discrimination for three plants at a speed of 5 km/h. The rugged packaging ensured reliable operation of the sensor in a high vibration environment while protecting the sensor from dust, water and the outdoor environment.

The choice of line scan sensor was a compromise on the desired speed of operation of the weed sensor. Its lower sensitivity increased the required exposure time and the time to complete a single scan. The sensor was also more sensitive to background light and a shroud was attached to operate in daylight. Another issue with the design of the sensor is shading of the viewing area. Incident light from beams on the soil or leaves lower down can be obscured by leaves closer to the sensor.

There is a great potential for use of this prototype weed sensor for spot spraying weeds in crop. The spectral survey and analysis conducted shows sufficient difference in spectral reflectance of some crops and weeds over a long period of the growing season. For cotton and sugarcane the crop was correctly classified 85-95% of the time. Most importantly this prototype weed sensor has achieved reliable discrimination of green plants with a low number of narrow wavebands.

6.4 Future research and development

There is still work to be done before the weed sensor can be used to spot spray weeds amongst a crop. The operation of the sensor is reliable for short periods of time but over longer time spans the reliability of the system needs to be improved. The current scan rate of the sensor has to be increased to enable detection of narrow leafed plants at vehicle speeds greater than 5 km/h. The weed sensor then needs to be trialled with crop and weeds to determine how reliable it will be and what the limitations are.

Long term reliability requires temperature control of the lasers because changes in the ambient temperature lead to changes in the optical power which affects the calculated normalised difference indices (NDIs). The solution for this is to implement a temperature controller for the laser diodes.

There are several possibilities to increase the speed of operation. A higher sensitivity sensor without significant reduction in dynamic range or increase in read-out noise would allow reduction in exposure time. Increasing the laser power would also allow a shorter exposure time. The separate operations of exposure, readout and data processing are performed sequentially. These could be overlapped to reduce the total time for a single scan.

The spectral reflectance properties of crop and weeds have many sources of variation. The brief survey reported in Chapter 5 and many other surveys need to be built on to determine which crop and weeds could be reliably discriminated with 3 or 4 wavelengths (i.e. 2 or 3 NDIs) and what conditions are required for this to be successful. Calibration of the system at a particular point in the growing cycle which accounts for environmental factors may be necessary to

increase the discrimination rate. It is likely that limited spectral information would need to be combined with spatial information. An improved aggregation algorithm could take advantage of plant shape and leaf size information, particularly with a faster sensor. There is also the possibility to use one or more additional lasers to improve discrimination capability – however this would depend on the availability of a compact, cost-effective laser diode with a wavelength in the green to blue range.

The data processing available with the embedded controller used was sufficient for the discrimination of the plants used in this study. In order to extend this capability it is expected that more complex algorithms will need to be employed, including the improved aggregation algorithm mentioned. It would also be possible to combine the spectral information measured with higher resolution spatial information using an imaging camera. This would certainly require more complex data processing and a more powerful processor to maintain the real-time performance.

The realization of a reliable plant discrimination sensor has potential for significant herbicide savings and economic benefit as well as environmental benefit. It would be another piece of the puzzle that is currently missing in precision agriculture technology.

Bibliography

[1] Natural Resource Management Ministerial Council, "Australian Weeds Strategy—A national strategy for weed management in Australia," NRMMC, Department of the Environment and Water Resources, Canberra, ACT, 2007.

[2] Australian Bureau of Statistics, "Natural resource management on Australian farms, 2006-07," ABS, Canberra, Cat. no. 4620.0, 2008.

[3] Australian Bureau of Statistics, "Value of agricultural commodities produced, Australia, 2006-07," ABS, Canberra, Cat. no. 7503.0, 2008.

[4] J. Sinden, R. Jones, S. Hester, D. Odom, C. Kalisch, R. James*, et al.*, "The economic impact of weeds in Australia," CRC for Australian Weed Management, Technical series #8, 2004.

[5] B. M. Sindel, "The history of integrated weed management," in *Australian weed management systems*, B. M. Sindel, Ed., Meredith, Vic., 2000.

[6] D. D. Buhler, "Challenges and opportunities for integrated weed management," *Weed Science,* vol. 50, pp. 273-280, May 2002.

[7] B. Whelan, "Current status and future directions of PA in Australia," in *Proc. 2nd Asian Conf. on Precision Agriculture*, Pyeongtaek, Korea, 2007, pp. 60-71.

[8] NTech Industries Inc. (2012). *WeedSeeker home page,* [Online]. Available: http://www.ntechindustries.com/weedseeker-home.html

[9] S. M. Swinton, "Economics of site-specific weed management," *Weed Science,* vol. 53, pp. 259-263, Mar-Apr 2005.

[10] K. Sahba, S. Askraba, and K. E. Alameh, "Non-contact laser spectroscopy for plant discrimination in terrestrial crop spraying," *Opt. Express,* vol. 14, pp. 12485-12493, Dec 2006.

[11] J. Dodd, R. J. Martin, and K. M. Howes, Eds., *Management of agricultural weeds in Western Australia* (Bulletin 4243). Perth, Western Australia: Dept. of Agriculture, 1993, 272 pp.

[12] Australian Bureau of Agricultural and Resource Economics, "Statistical tables," *Australian Commodities,* pp. 541-577, September quarter, 2007.

[13] R. L. Zimdahl, *Fundamentals of Weed Science*, 3rd ed. Burlington, MA, USA, 2007.

[14] Australian Bureau of Agricultural and Resource Economics, "Climate change," *Australian Commodities,* pp. 657-676, December quarter, 2007.

[15] B. M. Sindel, "Weeds and their impact," in *Australian weed management systems*, B. M. Sindel, Ed., Meredith, Vic., 2000.

[16] Australian Bureau of Statistics, "Land management and farming in Australia," ABS, Canberra, Cat. no. 4627.0, 2009.

[17] J. E. Pratley, "Tillage and other physical management methods," in *Australian weed management systems*, B. M. Sindel, Ed., Meredith, Vic., 2000.

[18] A. Storrie and T. McGillion, "Herbicide resistance," in *Integrated weed management in Australian cropping systems*, T. McGillion and A. Storrie, Eds., Adelaide, SA.: CRC for Australian Weed Management, 2006.

[19] A. Johnson, "Weeds," in *Weed control in central NSW*: Dept. of Agriculture, NSW.

[20] A. Zoschke and M. Quadranti, "Integrated weed management: *Quo vadis*?," *Weed Biology Manage.,* vol. 2, pp. 1-10, Mar 2002.

[21] G. Roberts and G. Charles, "Integrated weed management (IWM) – guidelines for Australian Cotton Production," in *WEEDpak – a guide for integrated management of weeds in cotton*: Australian Cotton CRC, 2002.

[22] N. Q. Zhang, M. H. Wang, and N. Wang, "Precision agriculture—a worldwide overview," *Comput. Electron. Agriculture,* vol. 36, pp. 113-132, Nov 2002.

[23] B. Koch and R. Khosla, "The role of precision agriculture in cropping systems," *J. Crop Production,* vol. 9, pp. 361-381, 2003.

[24] M. Robertson, P. Carberry, and L. Brennan, "The economic benefits of precision agriculture: case studies from Australian grain farms," Grain Research & Development Corporation, Mar 2007.

[25] C. Timmermann, R. Gerhards, and W. Kühbauch, "The economic impact of site-specific weed control," *Precision Agriculture,* vol. 4, pp. 249-260, Sept 2003.

[26] D. A. Peters, "Evaluation of weed control and economic benefit of a light-activated sprayer in cotton," Ph.D. dissertation, Agronomy, Texas Tech University, 2003.

[27] D. Brownhill, "Using 'Weedseeker' spot spraying technology in cropping systems," in *Proc. of the 10th Annual Symposium on Precision Agriculture in Australasia*, Sydney, Australia, 2006.

[28] T. Cook, "Weed detecting technology: an excellent opportunity for advanced glyphosate resistance management," in *18th Australiasian Weeds Conference*, Melbourne, Victoria, 2012, pp. 245-247.

[29] R. B. Brown, J.-P. G. A. Steckler, and G. W. Anderson, "Remote Sensing for Identification of Weeds in No-till Corn," *Trans. ASAE,* vol. 37, pp. 297-302, Jan-Feb 1994.

[30] S. Downes, L. Wilson, G. Kauter, T. Farrell, and K. Knight, "Bolgard II resistance management plan," in *Cotton Pest Management Guide*, S. Mass, Ed., Orange, NSW: Industry & Investment NSW, 2009.

[31] G. Charles, I. Taylor, and G. Roberts, "Integrated weed management in the cotton farming system: why should the industry adopt this approach?," in *11th Australian Cotton Conference Proceedings*, Broadbeach, Queensland, 2004.

[32] Australian Bureau of Statistics, "Agricultural commodities, 2009-2010," ABS, Canberra, Cat. no. 7121.0, 2011.

[33] Queensland Cane Growers Organisation Ltd. (2012, February). *About the Australian sugarcane industry,* [Online]. Available: http://www.canegrowers.com.au

[34] R. J. Davis, R. Bartels, and E. J. Schmidt, "Precision Agriculture technologies: Relevance and application to sugarcane production," National Centre for Engineering in Agriculture, Toowoomba, Queensland, Publication 1002265/1, 1997.

[35] G. Cox, H. Harris, and D. Cox, "Application of Precision Agriculture to sugar cane," in *Proceedings of the 4th International Conference on Precision Agriculture*, St Paul, Minnesota, USA, 1999, pp. 753-765.

[36] J. Dodd, "Comparison of the eradication programs for kochia (*Kochia scoparia* (L.) Schrad.) and skeleton weed (*Chondrilla juncea* L.) in Western Australia," in *11th Australiasian Weeds Conference*, Melbourne, Victoria, 1996, pp. 82-84.

[37] Dept of Agriculture and Food, "Skeleton weed program 2009-2010: Report to grain growers," Perth, W.A., 2010.

[38] J. Dodd, "Invited review: The role of ecological studies in assessing weed eradication programmes," in *9th Australian Weeds Conference*, Adelaide, South Australia, 1990, pp. 416-426.

[39] S. Jacquemoud and S. Ustin. (2008). *Modeling Leaf Optical Properties,* [Online]. Available: http://www.photobiology.info/

[40] Natural Phenomena Simulation Group. (2012). *Plant leaf data,* [Online]. Available: http://www.npsg.uwaterloo.ca/data/leaves.php

[41] R. Zwiggelaar, "A review of spectral properties of plants and their potential use for crop/weed discrimination in row-crops," *Crop Protection,* vol. 17, pp. 189-206, May 1998.

[42] R. Wheeler. (2011, April). *Leaf tissue structure,* [Online]. Available: http://en.wikipedia.org/wiki/File:Leaf_Tissue_Structure.svg

[43] S. Jacquemoud, W. Verhoef, F. Baret, P. J. Zarco-Tejada, G. P. Asner, C. Francois*, et al.*, *PROSPECT+SAIL: 15 Years of Use for Land Surface Characterization*, 2006.

[44] K. L. Castro-Esau, G. A. Sanchez-Azofeifa, and T. Caelli, "Discrimination of lianas and trees with leaf-level hyperspectral data," *Remote Sens. Environ.,* vol. 90, pp. 353-372, Apr 2004.

[45] P. S. Thenkabail, E. A. Enclona, M. S. Ashton, C. Legg, and M. J. De Dieu, "Hyperion, IKONOS, ALI, and ETM plus sensors in the study of African rainforests," *Remote Sens. Environ.,* vol. 90, pp. 23-43, Mar 2004.

[46] S. Jacquemoud, C. Bacour, H. Poilve, and J. P. Frangi, "Comparison of four radiative transfer models to simulate plant canopies reflectance: Direct and inverse mode," *Remote Sens. Environ.,* vol. 74, pp. 471-481, Dec 2000.

[47] P. S. Thenkabail, R. B. Smith, and E. De Pauw, "Evaluation of narrowband and broadband vegetation indices for determining optimal hyperspectral wavebands for agricultural crop characterization," *Photogramm. Eng. Remote Sens.,* vol. 68, pp. 607-621, Jun 2002.

[48] G. A. Carter and A. K. Knapp, "Leaf optical properties in higher plants: Linking spectral characteristics to stress and chlorophyll concentration," *Am. J. Botany,* vol. 88, pp. 677-684, Apr 2001.

[49] J. G. Ferwerda, A. K. Skidmore, and O. Mutanga, "Nitrogen detection with hyperspectral normalized ratio indices across multiple plant species," *Int. J. Remote. Sens.,* vol. 26, pp. 4083-4095, Sept 2005.

[50] G. A. Blackburn, "Hyperspectral remote sensing of plant pigments," *J. Exp. Botany,* vol. 58, pp. 855-867, Mar 2007.

[51] D. N. H. Horler, J. Barber, and A. R. Barringer, "Effects of heavy metals on the absorbance and reflectance spectra of plants," *Int. J. Remote. Sens.,* vol. 1, pp. 121-136, Apr-Jun 1980.

[52] P. K. Goel, S. O. Prasher, R. M. Patel, D. L. Smith, and A. DiTommaso, "Use of airborne multi-spectral imagery for weed detection in field crops," *Trans. ASAE,* vol. 45, pp. 443-449, Mar-Apr 2002.

[53] J. L. Hatfield, A. A. Gitelson, J. S. Schepers, and C. L. Walthall, "Application of spectral remote sensing for agronomic decisions," *Agronomy J.,* vol. 100, pp. S117-S131, May-Jun 2008.

[54] D. L. Zhao, K. R. Reddy, V. G. Kakani, J. J. Read, and S. Koti, "Selection of optimum reflectance ratios for estimating leaf nitrogen and chlorophyll concentrations of field-grown cotton," *Agronomy J.,* vol. 97, pp. 89-98, Jan-Feb 2005.

[55] A. A. Gitelson, Y. Zur, O. B. Chivkunova, and M. N. Merzlyak, "Assessing carotenoid content in plant leaves with reflectance spectroscopy," *Photochem. Photobiol.,* vol. 75, pp. 272-281, Mar 2002.

[56] P. S. Thenkabail, E. A. Enclona, M. S. Ashton, and B. Van der Meer, "Accuracy assessments of hyperspectral waveband performance for vegetation analysis applications," *Remote Sens. Environ.,* vol. 91, pp. 354-376, Jun 2004.

[57] E. Vrindts, "Automatic weed detection with optical techniques as a basis for site-specific herbicide application," Ph.D. dissertation, Faculty of Applied Bioscience and Engineering, Katholieke Universiteit Leuven, Leuven, 2000.

[58] N. Wang, N. Zhang, F. E. Dowell, Y. Sun, and D. E. Peterson, "Design of an optical weed sensor using plant spectral characteristics," *Trans. ASAE,* vol. 44, pp. 409-419, Mar-Apr 2001.

[59] H. Okamoto, T. Murata, T. Kataoka, and S. I. Hata, "Plant classification for weed detection using hyperspectral imaging with wavelet analysis," *Weed Biology Manage.,* vol. 7, pp. 31-37, Mar 2007.

[60] E. Vrindts and J. D. Baerdemaeker, "Optical weed detection and evaluation using reflection measurements," in *Precision Agriculture and Biological Quality*, 1999, pp. 279-289.

[61] M. Keränen, E.-M. Aro, E. Tyystjärvi, and O. Nevalainen, "Automatic Plant Identification with Chlorophyll Fluorescence Fingerprinting," *Precision Agriculture,* vol. 4, pp. 53-67, Mar 2003.

[62] W. L. Felton, A. F. Doss, P. G. Nash, K. R. McCloy, and E. Amer Soc Agr, "A microprocessor controlled technology to selectively spot spray weeds," in *Automated Agriculture for the 21st Century: Proceedings of the 1991 Symposium*, 1991, pp. 427-432.

[63] R. E. Blackshaw, L. J. Molnar, D. F. Chevalier, and C. W. Lindwall, "Factors affecting the operation of the weed-sensing Detectspray system," *Weed Science,* vol. 46, pp. 127-131, Jan-Feb 1998.

[64] J. E. Hanks and J. L. Beck, "Sensor-controlled hooded sprayer for row crops," *Weed Technol.,* vol. 12, pp. 308-314, Apr-Jun 1998.

[65] E. Franz, M. R. Gebhardt, and K. B. Unklesbay, "The use of local spectral properties of leaves as an aid for identifying weed seedlings in digital images," *Trans. ASAE,* vol. 34, pp. 682-687, Mar-Apr 1991.

[66] N. Zhang and C. Chaisattapagon, "Effective criteria for weed identification in wheat fields using machine vision," *Trans. ASAE,* vol. 38, pp. 965-974, May-Jun 1995.

[67] L. Tian, "Development of a sensor-based precision herbicide application system," *Comput. Electron. Agriculture,* vol. 36, pp. 133-149, Nov 2002.

[68] B. L. Steward and L. Tian, "Real-time machine vision weed sensing," presented at the 1998 ASAE Annual International Meeting, Orlando, Florida, 1998.

[69] S. D. Noble, R. B. Brown, and T. G. Crowe, "The use of spectral properties for weed detection and identification – a review," presented at the AIC 2002, Saskatoon, Saskatchewan, 2002.

[70] S. G. Raymond, P. J. Hilton, and R. P. Gabric, "Intelligent crop spraying: A prototype development," in *1st International Conf. on Sensing Technology*, Palmerston North, New Zealand, 2005, pp. 488-493.

[71] H. A. Macleod, *Thin-Film Optical Filters*, 3rd ed.: Taylor & Francis, 2001.

[72] National Instruments, (2012). "NI LabVIEW," [Program]. Available: http://www.ni.com/labview

[73] I. Taylor, L. MacKinnon, and B. Inchbold, "Regional weeds of cotton," in *WEEDpak – a guide for integrated management of weeds in cotton*: Australian Cotton CRC, 2002.

[74] M. Widderick and J. Moore, "Profiles of common weeds of cropping," in *Integrated weed management in Australian cropping systems*, T. McGillion and A. Storrie, Eds., Adelaide, SA.: CRC for Australian Weed Management, 2006.

[75] S. Rees, C. McCarthy, X. Artizzu, C. Baillie, and M. Dunn, "Development of a prototype precision spot spray system using image analysis and plant identification technology," in *Proceedings of the 2009 CIGR International Symposium of the Australian Society for Engineering in Agriculture (SEAg 2009)*, Brisbane, Queensland, 2009, pp. 343-349.

[76] M. Hogarth and P. Allsopp, Eds., *Manual of Cane Growing*. Indooroopilly, Qld: Bureau of Sugar Experiment Stations, 2000.

[77] Octave community, (2012). "GNU/Octave," [Program]. Available: http://www.gnu.org/software/octave/

[78] R. O. Duda, P. E. Hart, and D. G. Stork, *Pattern Classification*, 2nd ed. New York: Wiley, 2001.

[79] A. Paap, S. Askraba, K. Alameh, and J. Rowe, "Photonic-based spectral reflectance sensor for ground-based plant detection and weed discrimination," *Opt. Express,* vol. 16, pp. 1051-1055, Jan 21 2008.